# UNIVERSITA' DEGLI STUDI DI TORINO

**Dottorato di ricerca in Scienze Biomediche ed Oncologia Umana**

**Indirizzo in Scienze Cliniche**

# TESI DI DOTTORATO

**EPIGENETIC THERAPY FOR FRIEDREICH'S ATAXIA: A PHASE 1, FIRST IN MAN, ASCENDING DOSE CROSSOVER STUDY TO INVESTIGATE THE SAFETY, PHARMACOKINETICS AND PHARMACODYNAMICS OF RG2833 (A HISTONE DEACETYLASE INHIBITOR) IN ADULTS WITH FRIEDREICH'S ATAXIA**

**Candidata: Dott.ssa Stefania De Mercanti**

**Tutor: Prof.ssa Marinella Clerico**

**Coordinatore: Prof. Emilio Hirsch**

**ANNI ACCADEMICI 2014 - 2017**

# INDEX

# INTRODUCTION

## FRIEDREICH'S ATAXIA

### DEFINITION

The term "ataxia" comes from the Greek word "*a-taxis*", meaning "without order or coordination", and refers to a lack of coordination of voluntary movements, impairing their smooth performance. The rate, range, timing, direction, and force of movement may be affected [1].

Friedreich's ataxia (FRDA; online Mendelian Inheritance in Men database #229300) is the most common hereditary autosomal recessive cerebellar ataxia (ARCA or AR-HCA) in Caucasian population, with a prevalence of approximately 2 to 3 in 100,000 in North America and in Europe [2].

FRDA causes progressive neurological disability characterized by progressive trunk and limb ataxia, dysarthria, instability of fixation, sensory neuropathy, and pyramidal weakness [3]. Skeletal abnormalities such as scoliosis and *pes cavus* are common [3]. Onset usually occurs around the time of puberty and, on average, after 10 to 15 years from onset, progressive gait and limb ataxia eventually results in the need for a wheelchair and for continuous help with all daily activities [3]. Premature death generally occurs in patients who have a very severe cardiomyopathy associated to cardiac insufficiency or arrhythmia [3]. The complications of diabetes may further increase the disease burden and disability [3].

Clinical features in FRDA are due to a genetically determined deficient expression of mitochondrial protein, frataxin (FNX), that leads to deleterious alterations in iron mitochondrial metabolism. In the majority of cases the pathogenic mutation consists of homozygous (GAA)n trinucleotide repeat in the first intron of FNX gene [4]. The reduction of FNX level is presumed to play a crucial role in the oxidative damage that leads to degenerative features [4].

**HISTORY**

In 1863 Nikolaus Friedreich (1825-1882), a German pathologist from Heidelberg, described a new spinal disease for the first time [5,6], but it was accepted as a new disease after his fourth publication in 1877 [7]. Friedreich presented clinical findings in six patients among two families with a severe hereditary disorder of the nervous system and executed full autopsies in four of them [8]. The result of his work allowed to define the fundamental clinical and pathologic characteristics of FRDA: age at onset, typically paediatric age or around puberty, and degenerative atrophy of the posterior column of spinal cord that causes progressive ataxia, sensory loss and muscle weakness [8]. Moreover, he described skeletal abnormalities (scoliosis and pes cavus) and cardiomyopathy [9]. In his 1863 article [5], Friedreich discussed the etiology of the disorder and mentioned hereditary "predisposition", but it was not until 1876 that the term "hereditary" appears in the title of the article [7]. It is interesting that despite this extraordinary insight, he persisted in his original opinion that the disease process in the spinal cord was a chronic spinal leptomeningitis[7]; in fact he thought that the inflammation began on the surface overlying the dorsal columns and progressed deep into the spinal white matter and then across the gray matter of the dorsal horns to the anterolateral columns. Possibly he may have been influenced by the prevalence of *tabes dorsalis* at that time, considering that the gait disorder in Friedreich's ataxia does resemble tabetic gait [8]. Few years later the French school of neurologists recognized the importance of Friedreich's work, and in 1893 the article by Pierre Marie (1893) separated this hereditary disease from other inherited cerebellar ataxias, based on clinical and pathological observations [8]. Throughout the XIX century there was much debate as to whether the condition represented a unique nosological entity [10], but it was not until the 1970s and 1980s that systematic phenotypic descriptions lead to the development of reliable diagnostic clinical criteria [11,12]. These papers also included optic atrophy and deafness as part of FRDA [11,12].

Only in 1988 Chamberlain and colleagues [13], by genetic linkage studies, mapped the mutation causing FRDA on human chromosome 9q13. In 1996 Campuzano et al. [14] identified the X25 gene (now named FNX gene) and the mutation responsible for FRDA. The discovery of the genetic

abnormality responsible for the vast majority of cases of FRDA lead to genotype-phenotype correlations and expanded the previously understood phenotypic spectrum, allowing the confirmation with a genetic diagnosis of the atypical cases presenting with very early or late onset, retained reflexes or limited progression [10].

## EPIDEMIOLOGY

A recent systematic review of prevalence studies [15] reported an AR-HCA global prevalence range of 0,0 to 7,2/105 and underlined that FRDA is the most frequent among them (representing nearly 50% of AR-HCA cases), with the exception of Southeast Norway where it reaches the second place after ataxia-telangiectasia. The estimated prevalence in Caucasic population is 2-4:100,000 with a healthy carrier (heterozygote condition) rate of 1:60-100 individuals and an estimated birth incidence of 1:29,000 [16,17]. FRDA is most common in Europe, in the Middle East, in South Asia (Indian Subcontinent) and in North Africa. Conversely FRDA has not been documented among Southeast Asians, Saharan Africans or native Americans. A lower than average prevalence is reported in Mexico [18]. In a recent research, Pierre Vankan [19], combining data from epidemiological studies in FRDA and patient organization membership list, reported that FRDA prevalence in Europe displayed a southwest to northeast gradient with higher levels observed in northern Spain, southern and central France and Ireland, and lower levels in Scandinavia, eastern Germany, Austria and Russia. He underlined that this peculiar distribution co-localized with the gradient of the chromosomal R1b marker as detected within west Europe. However, FRDA and R1b marker were not genetically linked but they co-existed in a hypothetical founder population. Therefore, Vankan concluded that FRDA distribution in Europe (figure 1) arose from Palaeolithic migration out of the Franco-Cantabrian Ice age refuge [19]

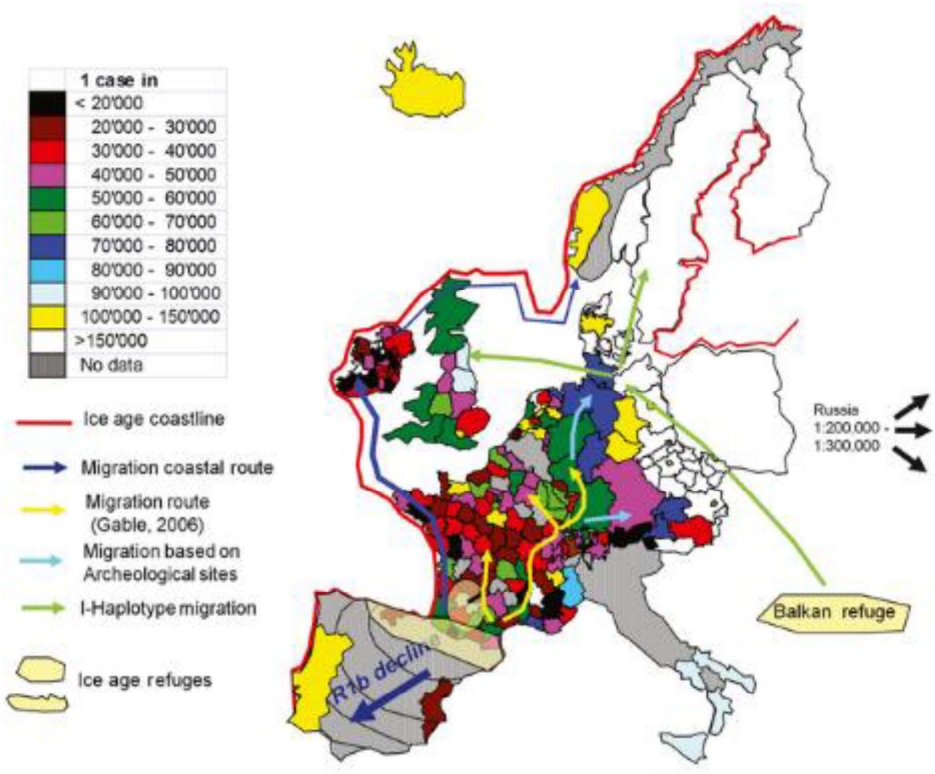


**Figure 1 - Prevalence gradients of Friedreich's ataxia in Europe [19].**

Regarding the Italian situation, two publications have to be cited at least [20,21], based on studies carried out between 1980s and 1990s. In particular, Leone and Colleagues [21] analysed the prevalence on Northern Italy and concluded that point prevalence ratio was 1-2:100,000 population and birth incidence rate was 1:36,000 live births. Romeo et al. [20], studying consanguineous marriage, estimated an Italian whole incidence between 1:22,000-1:24,000, concluding that the incidence in southern Italy appeared lower than in the north. Ruano and Colleagues [15] concluded that, especially concerning AR-HCA, prevalence could be underestimated because, in spite of the advances in molecular research, many patients and familiars remain without genetic diagnosis.

## ETIOLOGY AND PHYSIOPATHOLOGY

### *The Friedreich's ataxia gene*

FRDA is inherited in an autosomal recessive disease; the mutated gene, called FNX, in localized in the proximal long arm of chromosome 9 [3] and contains five axons and four introns (figure 2) [22]. The main messenger RNA (mRNA) has a size of 1.3 kilobases and corresponds to 5 exons (numbered 1-5a). Minor splice variants containing an alternative exon 5b and a sixth noncoding exon exist, but their functional significance is unknown [14].

Within the first intron there are polymorphic (GAA)n repeats in the centre of AluSq element (a short interspersed element, SINE) approximately 1,3 kb downstream of the major FNX transcription start site (TTS).

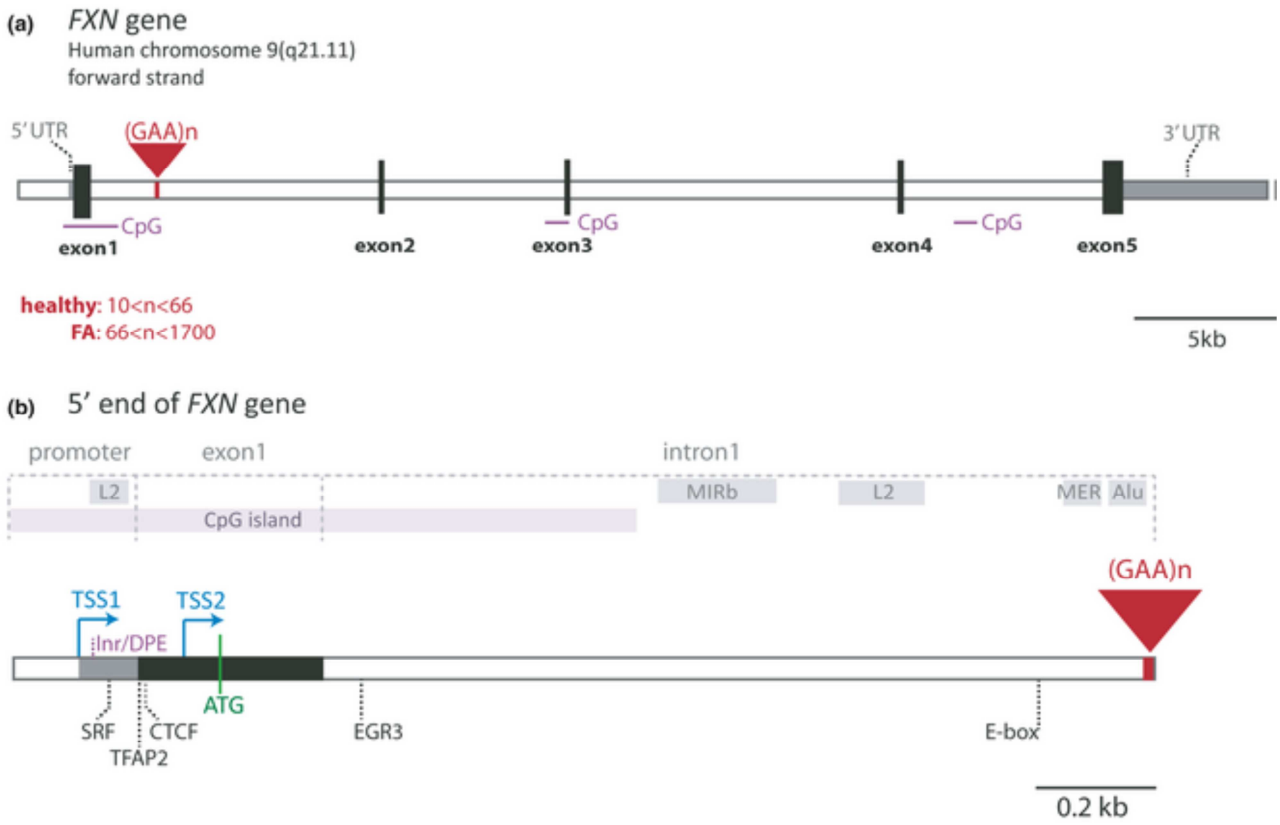


**Figure 2 - The human Frataxin (FXN) gene and its regulatory components**

Description provided by the authors. (a) Full body of FXN. The FXN gene consists of five exons and four introns. Three putative cytosine–phosphoguanine (CpG) islands were identified on FXN. (b) Regulatory elements at the 5′ end of FXN. FXN is known to be transcribed from two main TSS. TSS1 is 221 bp upstream of the translation start site (ATG), whereas TSS2 is only 62 bp upstream. The region between TSS1 and the first exon is thought to be a TATA-less downstream promoter, which contains Inr/downstream promoter element-like elements. Moreover, binding sequences were identified for transcription factors serum response factor, TFAP2 and EGR3 as well as for

the insulator protein CCCTC-binding factor. An E-box is present in the vicinity of (GAA)n repeats [22].

The encoded protein, called frataxin, contains 210 amino acids [3]; frataxin has an N-terminal leader peptide that directs its subcellular localisation to mitochondria matrix [3,23]. It is highly conserved in evolution, with homologues in all eukaryotes and in many prokaryotes [2]. Simple unicellular organisms as yeast can survive without frataxin, but frataxin is lethal for higher organisms, including mice, [24] which die early during embryonic development. In conditional frataxin knockout mice, total lack of frataxin results in the eventual demise of the targeted cells [2]. Frataxin function and its essentiality for survival, particularly during embryonic development, are still unknown [2].

The FXN gene is expressed ubiquitary, but at variable levels, which can be accounted for only in part by differences in mitochondrial content [3]. In adult humans, FXN mRNA is most abundant in the heart and spinal cord, followed by liver, skeletal muscle, and pancreas [14]. In mouse embryos, FXN mRNA expression starts in the neuroepithelium at embryonic day 10.5 (E10.5), and it reaches its highest level at E14.5 and into the postnatal period. At E16.5, the highest levels of FXN mRNA are found in the spinal cord, particularly at the thoracolumbar level, in the dorsal root ganglia, in proliferating neural cells in the periventricular zone, in the cortical plates, and in the ganglionic eminence. FXN mRNA expression is high in heart, liver, and brown fat [25,26].

### *Mutations causing Friedreich's ataxia*

The hyperexpansion of a GAA-triplet repeat in the first intron of FXN gene is the mutation found in all individuals with FRDA [14]. Almost all patients are homozygous for this mutation; whereas only a few, estimated between 2% and 5% in different countries, are compound heterozygous for the GAA expansion and a different mutation that leads to FXN loss of function [14,27].

In normal chromosomes there are up to approximately 38 triplets, whereas disease-associated repeats contain from 70 to more than 1000 triplets, most commonly 600 to 900 [2,28]. Heterozygous carriers are clinically healthy[2]. This is the most common disease-causing triplet-repeat expansion identified so far, about 1 in 100 Europeans being a carrier[2]; a study in France revealed a prevalence

of carriers of 1 in 90 [27]. No other disease has been recognized to date to be caused by an expansion of GAA triplets [2]. The GAA-expansion mutation determines partial silencing of FXN and therefore low levels of frataxin [2]. The other rare mutations are either missense changes that cause the encoded protein to be nonfunctional or only partially functional or are null alleles [27]. As demonstrated in knockout animals, complete lack of frataxin leads to early embryonic death. Homozygosity for expanded GAA repeats allows the synthesis of some structurally and functionally normal frataxin, at least around 5% of normal levels [2]. The FRDA-associated expansion is characterized by instability when transmitted from parent to child [14]: expansions and contractions can both be observed and are equally likely after maternal transmission, while contractions are most common after paternal transmission [29]. For this feature, FRDA resembles the other diseases associated with very large expansions in noncoding regions, such as fragile X syndrome and myotonic dystrophy, and differs from the diseases that are caused by CAG repeats in coding regions, such as dominant ataxias and Huntington disease, in which size increases generally occur after paternal transmission [2]. The GAA expansion is also unstable mitotically and even in postmitotic cells [2]. It is open to discussion whether one of the factors contributing to the specific vulnerability of some cell types in FRDA, such as dorsal root ganglia sensory neurons, is the inherent tendency of the GAA repeat in these cells to undergo further expansion [30]. The level of (GAA)n instability which determine expansion mutations is known to start when repetitions reach a threshold of about 35, therefore, repeat numbers between 35 and 66 are referred to as permutation [22]. Within this range, a meiotic instability has been shown that can result in disease in offspring.

The FRDA-associated GAA repeat lies in the middle of a repetitive Alu sequence of the Alu-Sx subfamily [2]. It is preceded by an average stretch of 16 A nucleotides, apparently derived from an expansion of the canonical (A)5(TACA)6 sequence linking the 2 halves of Alu sequences [2]. Alleles at the GAA-repeat site can be subdivided into 3 classes depending on their length: short normal (SN) alleles of fewer than 12 GAA triplets (approximately 82% in Western Europeans), long normal (LN) alleles of 12 or more GAA triplets (approximately 17% in Western Europeans), and

pathologic expanded (E) alleles (approximately 1% in Western Europeans). The length polymorphism of the GAA repeat in normal alleles suggests that it was generated by 2 types of events [2]. Small changes, plus or minus 1 trinucleotide, were likely the consequence of occasional events of polymerase slippage during DNA replication followed by misrealignment of the newly synthesized strand by 1 or a few repeat units (stuttering). Conversely, the passage from the SN to the LN group was probably an exceptional event. Linkage disequilibrium studies indicate that E and LN alleles appear genetically homogeneous, while SN represents a heterogeneous class of alleles [31]. It is possible that the event that created LN alleles was the sudden duplication of an SN allele containing 8 or 9 GAA triplets, creating an LN allele with 16 or 18 GAA triplets. The passage from LN to E alleles probably involved a second similar genetic event, which generated very long LN alleles containing 30 to 34 GAA triplets still on the same haplotype background as the shorter LN alleles from which they were derived. By reaching the instability threshold, estimated as 32 GAA triplets, they form a reservoir for expansions. This length is close to the instability threshold for other triplet repeat–associated disorders, such as those involving CGG and CAG repeats [2]. One of the mechanisms underlying the instability of E alleles may be strand displacement during DNA replication. For this phenomenon to occur, the displaced strand has to form some kind of secondary structure, in fact a single DNA strand containing a GAA repeat is able to form different types of secondary structures, which may be involved in instability. The triplex-forming ability of long GAA repeats may be involved in repeat instability by causing DNA-polymerase stalling and by forming a target for protein binding [2]. The (GAA)n repeat is a tract of DNA that contains only purine (R) in one strand and only pyrimidine (Y) in the other; R-Y sequences can adopt a special three-stranded non-B DNA structure: R-R-Y triplex. Under the influence of negative supercoiling, these triplexes are likely to adopt secondary structures, known as ‘sticky DNA’, that were suggested to impair transcription creating a physical blockage effect (figure 3) [32,33]. This block, in fact, makes more difficult for the elongating RNA Polymerase II (RNAPII) complex to unwind the DNA template

and move forward; thus it pauses at the end of the repeats. Furthermore, triplex structures allow the formation or stable RNA-DNA hybrids that are thought to stall RNAPII.

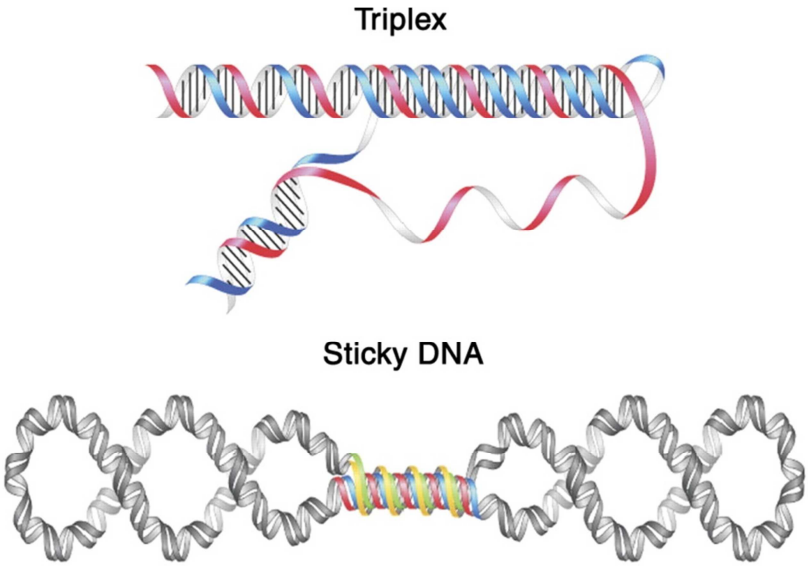


Figure 3 - Models of an intramolecular DNA triplex and sticky DNA structures [32].

Moreover, FNX transcriptional deficiency is due to an epigenetic mechanism that is considered predominant in FRDA pathogenesis [34]. Indeed, the epigenetic silencing of FNX gene, due to heterochromatization, causes a deficient transcriptional initiation (figure 4) [35]. Several studies reported an increased methylation on specific CpG islands of the promoter and intron regions flanking the (GAA)n-repeat expansion [9], respectively in lymphoblast [36], peripheral blood [37] and brain and heart tissue [38] of FRDA patients. Moreover, the classical heterochromatin marks histone h3 lysine 9 di-methylation (H3K9me2), H3K9me3 and H3K27me are enriched particularly in the immediate flanking region of expanded (GAA)n repeats [22], whereas acetylation marks are reduced.

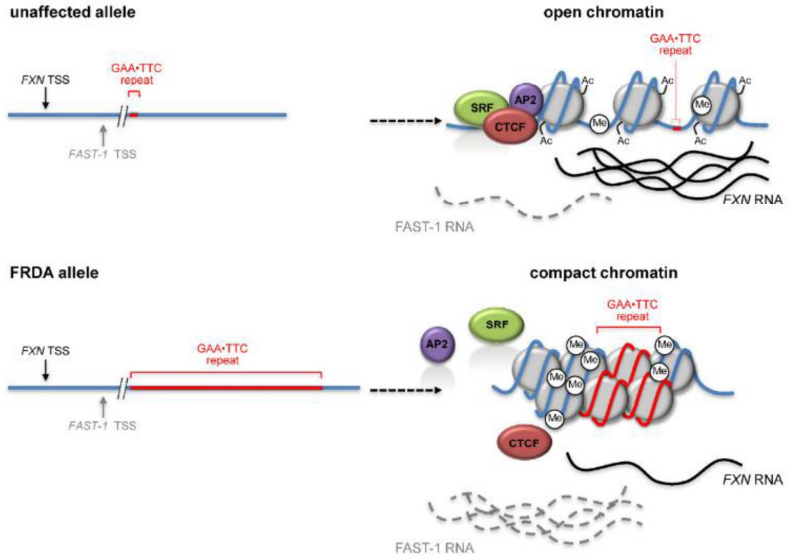


**Figure 4 - Diagrammatic representation of an epigenetic model for FRDA**

Description provided by the authors. Unaffected alleles are aberrantly methylated in the region flanking the repeat. Nonetheless, the 5' end of the gene is associated with histones that are enriched for marks of active chromatin. In particular, acetylation of histone H3 and H4 is high. The net result is that the chromatin is open and permissive for transcription. Transcription factors including serum response factor (SRF), activator protein 2 (AP2) and CCCTC-binding factor (CTCF) associate with the 5' end of the gene. Under these conditions transcription initiation and elongation takes place normally. In contrast, FRDA alleles become associated with histones that are hypoacetylated and show more extensive DNA methylation in the region flanking the repeat. The final effect of these histone changes is the formation of a compact chromatin configuration. This reduces binding of transcription factors and both frataxin (FXN) transcription initiation and elongation are reduced. Loss of CTCF binding is correlated with an increase in the amount of FXN antisense transcript-1 (FAST-1) RNA that is transcribed antisense to FXN. TSS: transcription start site [35].

Other important elements to understand (GAA)n induced heterochromatin are CTCF binding site within the 5'UTR of the FNX gene and antisense transcription. CTCF or CCCTC-binding factor is a chromatin insulator protein known to prevent the spreading of heterochromatin from the expanded (GAA)n repeat toward the promoter. The depletion in CTCF binding in FRDA patient fibroblast and the association of this with increased antisense transcription were also described by De Biase et al. [39]. In the same study the authors hypothesized the presence of a link between heterochromatin and antisense transcription by the identification of higher level of 'FNX antisense transcript 1' (FAST1) in the fibroblast obtained from FRDA patients compared to healthy patients [39]. It is noteworthy that the degree of methylation and hence FNX gene silencing is proportional to the extent of (GAA)n expansion [34,37,38]. This evidence underlines that the genetic and epigenetic models to explain FNX gene silencing might not be mutually exclusive. The epigenetic silencing mechanism will be explored in the experimental part of the thesis.

### *Frataxin function and FRDA pathogenesis*

The silenced FNX gene transcription determines the reduced expression of the encoded mitochondrial protein, frataxin [2,14,40]. Frataxin is an evolutionarily conserved small acid protein (with isoelectric point on average around 4.9 [40]) present from gram-negative bacteria to eukaryotes [14], that showed to bind iron ions in vitro [41,42]. A frataxin homolog was also identified in the human parasite Trichomonas vaginalis [43]. This last finding is interesting since these unicellular eukaryote organisms do not have mitochondria, but hydrogenosomes which share common ancestry with mitochondria [40]. In the last years extensive structural and biochemical studies have been carried out for human (HsFtx), yeast (Yfh1) and bacterial frataxin orthologues (CyaY) [44] (figure 5). Bacterial frataxin contains only conserved sequence of 100 to 130 residues, whereas eukaryotic form has an additional N-terminal tail, which contains the mitochondrial import signal [45].

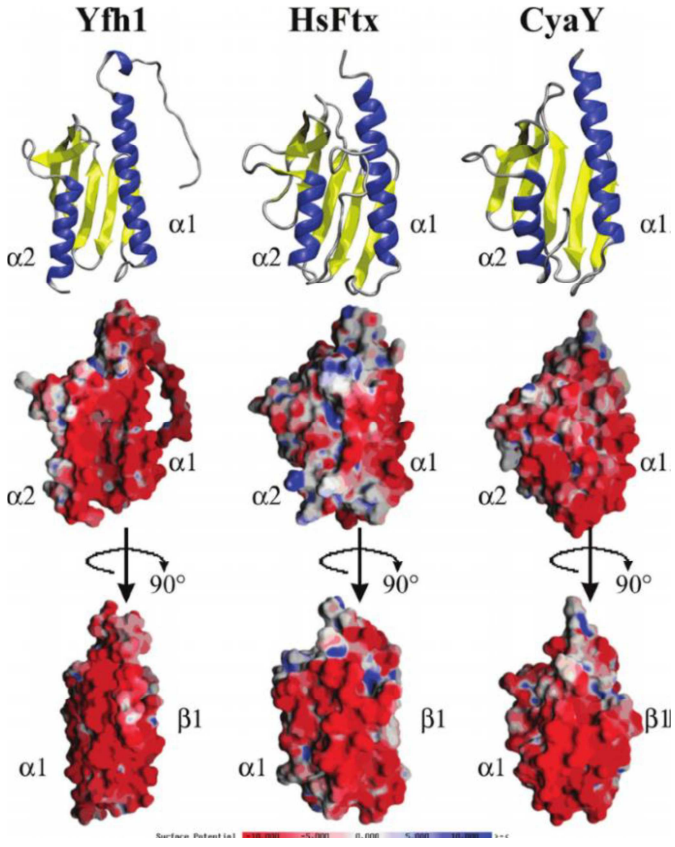


Figure 5

Top: ribbon diagram for yeast, human and bacterial frataxin. Description provided by the authors. Middle: electropotential plots for proteins in same orientation. Bottom: electropotential plots for proteins rotated -90 degrees around the y-axis compared to top display [44].

The C-terminal region is highly conserved from bacteria to humans, indicating that it is functionally important; this region is reported to contain an exposed tryptophan residue (Trp155 in human FNX) [46]. Significantly, it was noticed that all missense mutations found in FRDA compound heterozygotes affect conserved residues, and the mutation of conserved exposed tryptophan (W155R) leads to a particular severe FRDA phenotype [47,48]. In eukaryotes, frataxin is encoded in the nucleus as a 210 amino acid protein, the precursor form of the protein [40]. Later, it is translated in the cytoplasm and then imported into mitochondria, where a two-step, proteolytic processing removes the transit sequences to produce the mature protein [49]. Structurally, mature frataxin is a compact, globular protein that contains an N-terminal α helix, a middle β-sheet region composed of 7 β strands, a second α helix, and a C-terminus in an extended conformation [50]. The α helices are folded upon the β sheet, with the C-terminus filling a groove between the 2 α helices. On the outside, a ridge of negatively charged residues and a patch of hydrophobic residues are highly conserved. The acidic ridge is essential for function, as shown by structural and functional in vitro studies and by complementation experiments in frataxin-deficient yeast using specific missense mutants, and is likely to be involved in iron-mediated protein-protein interactions [51].

Although FNX gene expression and production of frataxin are ubiquitous, the levels of mRNA and protein show tissue specificity that partially correlate with the main sites of the disease [9]. In humans the highest levels of FNX expression were observed in the heart and spinal cord, with intermediate levels observed in cerebellum, liver, skeletal muscle and pancreas and very low levels in cerebral cortex [14]. Probably, the reason why only certain tissues are affected in FRDA may be that neurons, cardiomyocytes and pancreatic β-cells are highly dependent on mitochondrial metabolism and, being non-dividing cells, are not replaced when they die [52]. Alternatively, this tissue specificity could be due to somatic instability and accumulation of larger (GAA)n repeat expansions in these cell types [30].

Frataxin was initially found to be associated with the inner mitochondrial membrane and crests [53]; however, it has no apparent structural characteristics that would enable its anchorage at the mitochondrial membrane. Hence, it is possible that FNX is linked with mitochondrial membrane bounding mitochondrial proteins to form a complex [54].

Frataxin functions are still not completely clear [40], but many studies have indicated an important function in different aspects of iron metabolism. The first functional hypothesis on frataxin was focused on iron binding and aggregate formation [40]. Frataxin was put forward as a ferritin-like scavenger that keeps iron in a bio-available form [55,56]. This hypothesis was supported by the evidence that ferritin can partially complement absence of frataxin [57]. However, other studies suggest that this could not be the major function of frataxin [40]:

- the effect of other ions on oligomerization is such that physiological concentrations of magnesium or calcium salts within the mitochondria would stabilize CyaY and Yfh1 in an iron bound monomeric state and destabilize oligomerization [58].
- It was independently shown that oligomerization is unessential when the protein functions as an iron chaperone during heme and Fe-S cluster assembly [59].
- In higher organisms, mitochondria contain a specialized ferritin [60], that, when expressed in yeast, can prevent iron accumulation caused by Yfh1 deletion, suggesting that iron storage is a redundant function, at least in mammals [61].

Iron is an essential element for the organism and plays a crucial role in growth. However, its chemical proprieties that allow its versatility also create a paradoxical situation, making acquisition by the organism very difficult. Indeed, at physiological PH (7,4) and oxygen tension the relatively soluble ferric form iron (Fe II) is rapidly oxidized to ferrous iron (Fe III), which upon hydrolyses form insoluble ferric hydroxides. The result of this insolubility is the potential toxicity because of its strong redox activity; for this reason, iron must be constantly chaperoned with specialized molecules that maintain it in soluble non-toxic form [54].

To understand the role of frataxin deficiency in FRDA, it is important to develop an overview of mitochondrial iron uptake and metabolism, and about their role in iron homeostasis. Indeed, the mitochondrion is a critical organelle for intracellular iron process and it is also the major site of cellular iron utilization [4]. For this respect, it is the reversible oxidation states of iron, from Fe II to Fe III, that enable the mitochondrion to catalyse electron transport and use this process in energy transduction [54]. Concerning mitochondrial iron uptake, even if this process is not well understood, it has been suggested that cytosolic iron may be taken up directly by this organelle as "free" Fe II, which is dependent on the mitochondrial membrane potential [62]. The mitochondrial-specific iron transport protein, mitoferrin (MFRN), facilitates the transport of iron across the inner mitochondrial membrane. Interestingly, MFRN exists in two homologues MFRN1 and MFRN2, respectively in erythroid and non-erythroid cells [63]. Once in mitochondrion, iron is utilized in three major metabolic pathways: (1) mitochondrial ISCs (iron-sulfur clusters) biogenesis (2) heme biosynthesis (3) mitochondrial iron storage. All these processes are crucial for cell life [4].

(1) ISCs are ubiquitous protein cofactors, consisting of iron and sulphide anions (S2-) assembled to form [2Fe-2S] or [4Fe-4S] clusters in which iron ions are coordinated with cysteine residues. Mammalian ISCs biogenesis occurs in two different but functionally connected compartments: the ISC assembly apparatus in mitochondria and the cytosolic assembly (CIA) system. The biogenesis of ISC seems to occur in two phases: the first consists in the transient synthesis of the ISC on a scaffold assembly protein. In the mitochondrial ISC system, the ISC core is assembled with the NFS1 which abstracts sulfur from cysteine residues. In the eukaryotes, the accessory protein ISD11 and two monomers of the dedicated scaffold protein ISCU bind NFS1. While ISD11 stabilizes the NFS1, ISCU provides the backbone structure for the formation of new cluster containing covalently bound iron and inorganic sulfur58.The second phase concerns the transfer of these ISCs to target apo-proteins by the concerted action of cluster-transfer

proteins [4]. The formed ISCs have a critical cellular function such as electronic transport, redox reactions and metabolic catalysis and sensing of ambient conditions [64].

(2) The mitochondrion can also utilize iron for the synthesis of heme, which is an essential cofactor of important proteins such as haemoglobin and myoglobin. Heme is synthesises by a pathway of eight sequential reactions in the mitochondrion and cytoplasm and it occurs in all cells, particularly hepatocytes and erythroid cells. The first and last three steps in heme biosynthesis pathway take place in mitochondria [54]. The final enzyme of this pathway is ferrochelatase (FECH) that inserts iron into protoporphyrin IX (PPIX), a heme precursor, to generate heme [54]. Importantly, in erythroid cells the rate of heme biosynthesis is regulated by cytosolic iron though cytosolic iron regulated proteins (IRP1 and 2). IRPs are RNA binding proteins that bind to iron responsive elements (IREs), specific sequences in the 5' or 3' UTR of mRNA that encode iron homeostatic protein. Their control activity aims to prevent both iron deficiency and iron toxicity. Under high cellular iron levels IRP1's IRE binding capacity is inactivated by the conversion in a cytosolic aconitase by the assembly of Fe-S cluster; concerning IRP2 it is degradated by iron-dependent ubiquitination [65].

(3) Iron can be stored in the mitochondrion via its sequestration in mitochondrial ferritin (FTMT). This protein prevents redox reaction and hence, mitochondrial oxidative damage, thanks to both its ferroxidase activity, that inhibits the production of free radical, and its capacity to storage iron [66]. FTMT is expressed in cells with high-energy requirements and consumption such as brain, heart, thymus, testis and smooth muscle; conversely, it is not expressed in cells with iron storage function (liver and spleen). This suggests that the level of FTMT expression is associated with oxidative metabolic activity [67].

All of these mitochondrial pathways are supposed to be affected following frataxin deficiency.

Concerning mitochondrial iron storage, the hypothesis that frataxin is able to stow iron was proposed observing that yeast frataxin formed oligomers that have ferroxidase activity. The iron-binding capacity of yeast frataxin appeared to be high in aggregates, which are able to maintain iron in a redox inactive state [68,69]. However, human frataxin has a lower iron-binding capacity that yeast one, even under condition of mitochondria iron accumulation [56]. This condition could be due to the fact that yeast does not express ferritin. Besides, with the discovery of FTMT in human tissue the idea of frataxin as iron store became improbable [66]. On the contrary, the frataxin is involved in ISCs formation; in fact, patients with FRDA, and know-out animal models have deficiency in Fe-S cluster proteins [70–72]. Furthermore, multiple lines of evidence in yeast and human cells have shown that frataxin interacts with the core ISC assembly protein (NFS1, ISD11 and ISCU) [73,74]; indeed the interaction with human ISCU-1 (the cytosolic form of ISCU) appears to be iron dependent. Hence, frataxin has been proposed as an iron chaperone that interacts with and donates iron to proteins involved in ISC biosynthesis [75]. The same function of iron-chaperone has been attributed to frataxin in heme biosynthesis, in which this protein seems to interact with FECH in the final step of heme generation [76]. It has also been hypothesized that frataxin may act as an iron sensor, particularly in regulating ISCs synthesis. Indeed, studies under the bacterial orthologe of frataxin have shown that it negatively regulates ISCs synthesis in case of iron excess relative to the amount of available ISC apo-acceptors proteins [77].

Frataxin has also been suggested to manage iron metabolism by functioning as a metabolic switch. A previous study has demonstrated this role of FNX in differentiating erythroid cells; here, FNX was able to distribute iron between major mitochondrial metabolic pathways. This hypothesis is supported by the observation that an increased level of the heme intermediate, PPIX, leads to the down-regulation of FNX expression and potentially a diversion of iron from metabolic pathways, such as ISCs synthesis, toward heme biogenesis [78].

The illustrated possible functions of human FNX are summarized in figure 6.

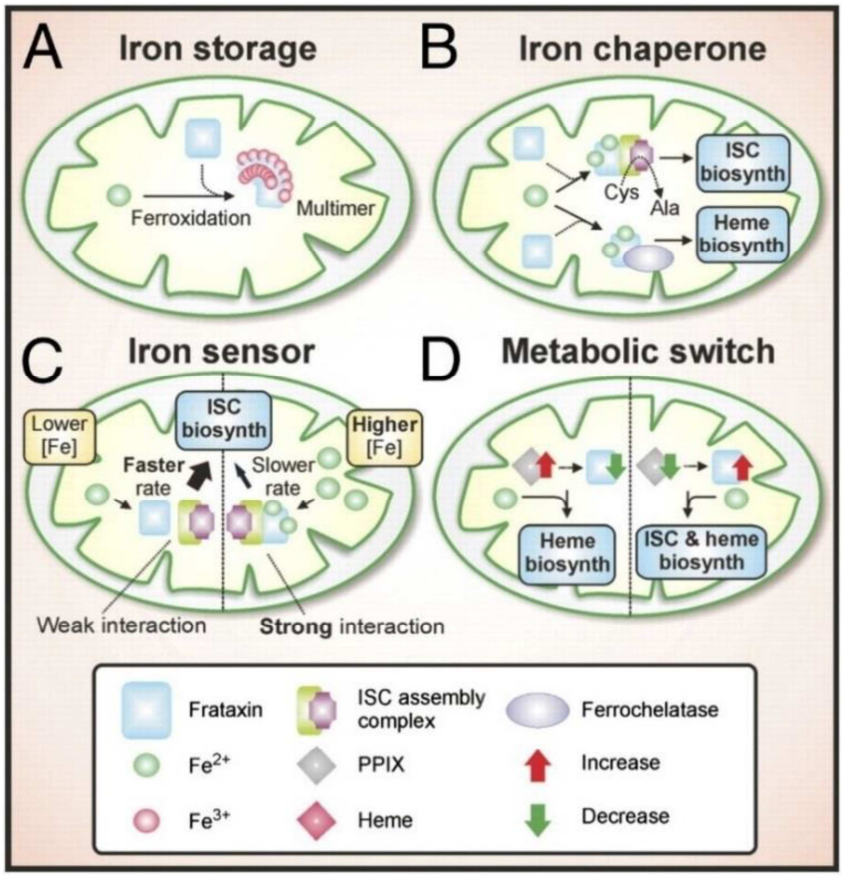


Figure 6 - Graphical summary of the principal possible functions of frataxin [54]

It is therefore clear that frataxin deficiency determines an increased cellular iron uptake: iron is targeted away from cytoplasm and ferritin toward the mitochondrion, possibly as a consequence of suppressed utilization of mitochondrial iron in metabolic process. Indeed, It was hypothesized that a signal was sent from mitochondrion to cytoplasm to up-regulate iron up-take [70]. This "rescue response" led to a relatively cytosolic iron deficiency and mitochondrial iron overload [54] (figure 7).

Previous studies in FRDA mice model, which exhibited targeted FNX-deletion in the heart and skeletal muscle, have shown that TfR1 (transferrin receptor 1) expression is up-regulated, whereas FPN1 (ferroportin 1) and ferritin expression are down-regulated. These changes are due to the increase of IRP1 activity that cannot be converted in aconitase because its Fe-s cluster is partially or fully disassembled. This results in a marked influx of iron in cardiomyocytes with an increase in its mitochondrial uptake via an up-regulation of mitochondrial transporter, MFRN2. Indeed, the

absence of FNX causes a decrease of three principal mitochondrial pathways: ISCs, heme biosynthesis and iron storage [70].

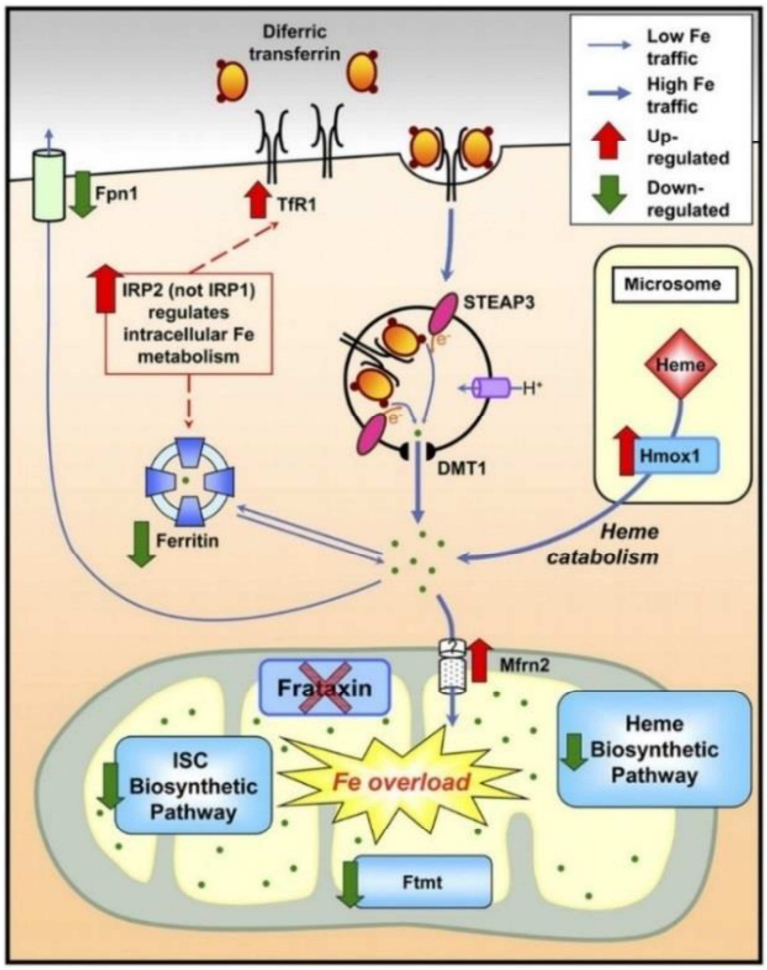


Figure 7 - Model of alteration in iron uptake in Friedreich's ataxia [54]

Interestingly, decreased frataxin expression in FRDA subject does not result in marked defects in heme synthesis in erythroid cells; indeed, it has been demonstrated that erythroid differentiation leads to a reduction of FNX expression. Thus in these cells FNX deficiency appears coupled to the marked increase of heme synthesis, with iron export from mitochondria and prevention of iron toxicity. Indeed, while in non-erythroid cells the rate of heme synthesis is dependent on the rate of mitochondrial enzyme ALAS, in erythroid cells the limiting factor is iron assimilation [79].

Conversely, in non-erythroid cells such as myocardiocytes, given that they have a minimal heme production rate [79], iron accumulates within mitochondria rather than being effectively assimilated by rapid heme synthesis [4].

In addition to the deleterious effect on iron metabolism, the ensuing oxidative stress is a feature in FRDA. In fact, frataxin deficiency leads to dysfunctional respiratory chain (particularly complexes I, II and III) by decreased ISCs biosynthesis [75]. This alteration, together with mitochondrial iron accumulation in form of inorganic iron crystallite without a protective protein [71], could increase the generation of reactive oxygen species (ROS).

Furthermore, frataxin deficiency has also been associated with a decrease in antioxidant response. In FRDA patients' cells and in yeast model, the antioxidant glutathione (GSH), markedly decreased [80,81]; the loss of aconitase activity-an iron-sulfur mitochondrial protein involved in oxidative demage repair-was also found [82]. Besides, frataxin deficiency has been linked with the impaired activity of the nuclear factor erythroid 2 related factor 2 (Nrf2), which is crucial in the regulation of genes that are involved in antioxidant defence [83,84].

Even if, at present an appropriate biomarker does not exist to measure oxidative stress in FRDA tissue, several studies underlined it is a crucial role in progressive cell death in FRDA patients [4]. The increase in oxidative stress in FRDA cells can cause lipid peroxidation [84] and protein and nucleic acid damage, particularly in mitochondrial DNA [85,86], that leads cells to death.

As anticipated, the cells which are particularly sensible to mitochondrial impairment and oxidative damage in FRDA are neurons, particularly in the dorsal root ganglia [87], the dorsal root of spinal cord [8], the dentate nucleus of cerebellum [88], cardiomyocytes [89] and pancreatic β cells.

Cardiac muscle is a high energy demanding tissue, for this reason the decrease in mitochondrial bioenergetics caused by respiratory chain disfunction, with insufficient synthesis of high energy phosphate, is the supposed main mechanism involved in the development of cardiomyopathy [90].

Furthermore, a detailed analysis of the neuron-specific enolase (NSE) and muscle creatine-kinase (MCK) mouse models of FRDA demonstrated that cardiac hypertrophy and mitochondrial iron-sulfur cluster protein defects precede any evidence of myocardial iron deposition, suggesting that iron accumulation may be a secondary disease phenotype [71]. A more recent study [91] also hypothesized that frataxin deficiency may determine improper assembly of intercalated disk early in life, with an alteration of end-to-end adhesion of cardiomyocytes of the growing heart making this organ more vulnerable to mechanical stress in childhood and adolescence. On the other hand other studies have shown that in the MCK mouse models the use of a mitochondrial permeable iron chelator, deferiprone, seems to limit cardiac iron-loading and hypertrophy. Besides, another study of iron chelation therapy in a frataxin-knockdown cell line found an increase in aconitase activity and improvements in mitochondrial membrane potential and ATP production [91]. In conclusion, even if Fe-mediated oxidative damage may not be the only mechanism underlying cardiomyocyte necrosis, increase sensitivity to oxidative stress is also likely to contribute to cardiac disease progression in FRDA [90].

In addition, it was also suggested that frataxin may play a role in controlling cell survival, in fact Cossée and Colleagues, studying mice model with inactivation of the FNX gene product, noticed that the lack of this protein causes embryonic lethality a few days after implantation, demonstrating that its absence is incompatible with life [24].

**PHENOTYPE**

In nineteenth century Friedreich described the essential clinical and pathological features of the disease as a “degenerative atrophy of the posterior columns of the spinal cord”, leading to progressive ataxia, sensory loss, and muscle weakness, often associated with scoliosis, foot deformity, and heart disease [3,5]. Almost 100 years later, in the late 1970s and early 1980s, a renewed interest in FRDA and the availability of modern biochemical and molecular genetic

approaches led to the establishment of rigorous diagnostic criteria for use in the selection of families for research [12]. Finally, in 1996, the discovery of the mutated FXN gene, responsible of FRDA, resulted in a direct molecular diagnostic test [14], whose availability allowed neurologists to characterise the full clinical spectrum of the disease.

FRDA typical age of onset is late in the first decade or early in the second decade of life, but this may vary substantially even between siblings [92]. About 25 percent of people with FRDA have an atypical form in which signs and symptoms begin after age 25 [93]; more in detail, affected individuals who develop Friedreich ataxia between ages 26 and 39 are considered to have late-onset FRDA (LOFA) [92]. When the clinical picture manifests after age 40 the condition is called very late-onset FRDA (VLOFA) [93]. In LOFA and VLOFA the clinical picture usually develops more slowly than in typical FRDA [93,94].

FRDA is now considered a spectrum of different phenotypes due to the same genetic defect. Typical phenotype, described by Harding, is observed in about 75% of affected individuals and atypical presentations can be seen in about 25% of them [95].

### *Correlation between genotype and phenotype*

An interesting aspect of FRDA is the relation between genotype and phenotype; indeed the GAA triplet expansion size determines the level of residual frataxin expression and hence has an influence on the severity of the phenotype [3]. Particularly, an inverse correlation has been found between the number of (GAA)n repeats of the smaller allele (allele 1) both with age at onset [96–98] and more rapid disease progression, measured as time passed until necessity of wheelchair [97,99,100].

The inverse correlation between the expansion of (GAA)n repeat on allele 1 and several clinical features might be explained by the evidence that residual levels of frataxin vary according to the size of the smaller allele [53,101]. Nevertheless, the amount of residual frataxin has been reported to vary in different types of cells, underlining a tissue-specific somatic instability; in fact, the evidence

of mosaicism of the (GAA)n expansion might explain the discordance between neurological and cardiologic phenotype, mentioned above. Concerning neurological features, Santoro et al. [100] noticed that central somatosensory pathway involvement in FRDA is mainly determined by the (GAA)n repeat length on the smaller allele of the FNX gene; conversely degeneration of pyramidal tracts, auditory and visual pathways seems to be a continuing process during the life of FRDA patients. Also the possibility to develop diabetes has been correlated with the size of the (GAA)n trinucleotide expansion in the FRDA gene in some studies [97,102], but not in others [98]. Conversely, cardiomyopathy frequently arises in patients with large expansion on the smaller allele and is independent of the duration of the disease according to most of the studies [96,97,103]. In detail, Bit-Avragim and Colleagues [103] highlighted that the extent of left ventricular hypertrophy is inversely related with (GAA)n repeats on the smaller allele but not with those on the larger one. However, a recent long term longitudinal study noticed that also the length of (GAA)n repeats on the larger allele correlate inversely with septum thickness [104]; the Authors reported that the length of (GAA)n repeats on both alleles is the best predictor of mortality in FRDA.

Different studies reported that only 37% to 50% of the variation in age at onset is accounted for by the size of the smaller allele [95,97,102]. Variability among individuals is very high, and it might be very difficult to predict the clinical severity basing only on the (GAA)n mutation [9]. A good example of this variability is the existence of phenotypic variants in FRDA, hence in about 25% of presentations individuals with FRDA fall outside the diagnostic criteria as described by Harding [11].

## *Neurological signs and symptoms*

### Gait and limb ataxia

Individuals with typical FRDA phenotype develop progressive ataxia with onset around or before puberty, on average late in the first or early in the second decade of life (mean 10 ± 7,4 years [12]); anyway, the age of onset can vary highly even between siblings [105].

Gate ataxia and general clumsiness are the most common symptoms at onset [3,106]. Many patients in retrospect describe a long history of clumsiness, trips or inability to participate in sports [10]. Ataxia is the result of both spinocerebellar degeneration, peripheral sensory neuropathy, cerebellar and vestibular pathology [107]. Truncal ataxia results in swaying on sitting and broad based gait with frequent loss of balance requiring at first intermittent then constant support [3]. Patients typically show as early sign problematic walking on uneven terrain or in feeble light and dependence on aid to move [3,107]. Patients develop an increasing dependence on aids to walking, initially furniture, walls and other people, and ultimately sticks, crutches and wheeled walkers [10]. On average, 10 to 15 years after onset, patients lose the ability to walk, stand, and eventually sit without support [12,92]. However, disease progression is considerably variable, thus patients with mild disease may still be ambulatory decades after onset, while those with severe disease may become wheelchair-bound within a few years [3]. Romberg's test is usually early positive and there may be difficulty in tandem position [10]. Limb ataxia determines increasing difficult in daily activities which need fine manual dexterity like washing, dressing, use of cutlery, carrying drinks or food and handwriting [10]. Harding in 1981 [12] found that 99% of cases showed finger-nose ataxia and 97% had upper limb dysdiadocokinesia. In lower limbs 72% of cases had heel-shin ataxia, but all the remaining 28% could not be tested because of profound muscle weakness [12]. Although ataxia is unremitting, periods of stability are frequent at the beginning of the illness [3].

**Weakness and wasting**

Central origin limb weakness, due to pyramidal tract degeneration, appears and then worsens with the progression of FRDA [3], being a relatively late sign. It initially affects proximal muscles, then becomes generalised and significantly contributes to disability [3]. It is much more prominent in the lower limbs compared to the upper limbs: indeed, patients often have very well preserved upper limbs power even when wheelchair-bound and profoundly disabled, and may only ever develop mild distal upper limbs weakness [10]. However, this can contribute significantly to difficulties with

fine manual dexterity. Harding found mild weakness of the upper limbs in 45% of cases and severe weakness in only 2% [12]. By contrast in the lower limbs, 30% of cases had mild weakness and 28% of cases, severe weakness [12]. Filla et al. noted 46% weakness of the upper limbs and 80% weakness in the lower limbs [108]. In advanced stages of FRDA weakness could confound the evaluation of ataxia eliminating some ataxic features, such as intention tremor [3].

Amyotrophy, particularly in the hands [3] and in the lower limbs, are very common. Harding [12] noted mild distal upper limbs wasting in 39% of cases, but severe wasting in only 3%; in the lower limbs, distal wasting was present in 39% of cases with generalized wasting in 25%. Filla found upper limbs wasting in 49% of cases and lower limbs wasting in 61% [108].

**Reflexes, tone and sensory loss**

Extensor plantar reaction (i.e. Babinsky's sign) reflects pyramidal pathology and it is present in most of patients [88]; present in 73-89% of cases according to Harding studies [12].

Areflexia, particularly of lower limbs, is an early sign present in almost all cases and reflects the underlying peripheral sensory axonal neuropathy [107]. The peripheral sensory neuropathy typically leads to a reduction or loss of vibration sense and proprioception, and results from degeneration of the posterior columns of the spinal cord [107]. Harding [12] found all reflexes were absent in 74% of cases with the biceps reflexes present in 25% and the patellar reflexes in just 1%. McCabe et al. [109] found upper limbs reflexes absent in 89% of typical cases and 45% of atypical cases, whereas lower limbs reflexes were absent in 100% of typical cases and 27% of atypical cases. Neurophysiological studies of peripheral nervous system show a severe reduction or complete loss of sensory nerve action potentials [107]. These abnormalities generally do not worsen over time but correlate with the size of the (GAA)n triplet repeat expansion in FNX gene underlining that pathology is established early and strictly depend of genetic alteration [100].

Muscle tone is typically normal or reduced, especially in the early stages of the disease [10]. Harding [12] found decreased upper limbs tone in 24% of cases and increased upper limbs tone in no cases. Tone was decreased in the lower limbs in 16% of cases and increased in 12%. Spasticity, particularly in the lower limbs can cause pain, discomfort, positioning problems and ultimately contractures if left untreated [10]. It can be associated with muscle cramps and spasms [10]. Geoffroy and Colleagues [11] found spasticity in 15% of the typical cases they described; they proposed that spasticity should be included as anancillary feature when describing the signs and symptoms of FRDA. Harding [12] found finger contractures 11% of cases, only in the later stages of the disease. Equinovarus deformity is commonly seen and may result in contractures and significant morbidity [18].

**Ophthalmic features**

Eye movements abnormalities are a common early sign in FRDA [10]. One of the commonest feature is fixation instability interrupted by involuntary saccades, or square wave jerks (SWJs), which can occur in primary position, horizontal or vertical fixation [10]. These were found in all patients by Furman and Colleagues [110]; they also found evidence of an oblique component to SWJs and some rare vertical SWJs [110]. The amplitude of refixation abnormality can vary up to 15° with latency up to 500 ms [10]. Some patients have a clear leftward or rightward predominance in movement, but most are equally bidirectional [110]. SWJs can also interrupt smooth pursuit movements and be so prominent that they inhibit assessment of smooth pursuit and nystagmus [10]. Nystagmus is less common but still frequent. It is typically horizontal gaze-evoked nystagmus on lateral gaze, and less commonly on vertical gaze. Furman et al. [110] found the former in 33% of cases with 13% having rebound nystagmus on returning to primary position. Harding [12] found nystagmus in 20% of cases. FRDA patients usually experience only transient 'focusing' difficulties on gaze deviation [10]. Fahey and Colleagues [111] found that only 20% of patients had symptomatic oscillopsia. Smooth pursuit movements typically have normal or only slightly reduced velocity, but are commonly interrupted

by saccadic intrusions [10]. These were found in 12–30% of cases [12,95] although are more common in our experience. Slow-phase velocity is slightly reduced under optokinetic stimulation and saccadic velocities are often normal but dysmetria is very common, often with a mix of hypo- and hypermetria [110]. A study of saccadic movements [111] estimated that 54% of saccades were accurate to within 10% of the saccadic amplitude, 37% were hypermetric and 9% were hypometric. Ptosis is found in a small but significant proportion of cases, perhaps 5–10% [108]. Decreased visual acuity is less common [10], accounting approximately 20% of patients [12,95]. Some patient have sudden bilateral loss of vision, mimicking Leber's hereditary optic atrophy [10]. On fundoscopy 30% of patients have disc pallor visible [12]. In symptomatic patients, field loss may show generalized concentric field loss, concentric superior-inferior arcuate defects or isolated paracentral field loss [112]. Regardless of the lack of symptoms, all patients show reduced retinal nerve fibre layer thickness throughout all four quadrants on optical coherence tomography [10]. Visual-evoked potentials show increased latency in 34–70% of patients [95,112]. Diffusion coefficients on diffusion-weighted magnetic resonance imaging (MRI) of the optic radiations were significantly higher than controls [112].

**Speech and swallowing**

Dysarthria is quite universal, affecting 90% of FRDA patients [10], and consists of slow, jerky speech that usually begins within two years after disease onset and progresses until speech becomes almost unintelligible [3]. A study of 38 individuals with FRDA showed that 68% had mild dysarthria characterized by consonant imprecision, decreased pitch variation, impaired loudness maintenance, reduced phrase length, hypernasality and impaired breath support for speech [113]. Moreover, cluster analysis revealed two further subgroups with increased laryngeal dysfunction (13%) and increased velopharyngeal involvement (11%) [114].

Dysphagia is another common symptom and can evolve in advanced disease phases, becoming problematic [10], in some patient percutaneous endoscopic gastroesophageal tube insertion is required [3,10]. Patients may cough or choke on solids or liquids including saliva; dry dusty and small

particulate foods such as peanuts or fruits which produce large amounts of juice on chewing are particularly difficult [10]. Chewing may also be compromised requiring avoidance of tough foods or cutting into small pieces [10]. Dysphagia prevalence vary between 27 and 74% [95,108]. Although no systematic studied have been carried out, aspiration pneumonia is a recognized as a cause of death, thus, rutinary dysphagia assessment is advised [10].

**Hearing**

Hearing alteration due to auditory neuropathy are a common and understated problem which can be very socially disabling even in the early stages of disease [10]. Prevalence of hearing loss in case series vary widely from 8 to 39% [11,12,95]. Harding [12] found mild deafness in 5.2%, moderate in 1.7% and severe in 0.9% of patients. Sound perception, as measured by hearing thresholds across audiometric frequencies (250–8000 Hz) in a quiet room, is typically normal in FRDA [115] or there may be minor deficiencies at different frequencies [116,117]. Almost all patients show disordered neural conduction in the central auditory pathways which functionally results in impaired speech understanding in conditions of background noise typical of everyday listening conditions, which can lead patients to be able to access only 50% of information available compared to unaffected individuals [118]. Peripheral auditory (outer and middle ear) function is generally unaffected, as shownby normal tympanometry and equal air and bone conduction in pure tone audiometry [116]. Preneural cochlear responses, such as otoacoustic emissions, are also normal [117]. Retrocochlear and brainstem responses, such as acoustic reflexes, synthetic sentence identification with ipsilateral competing message and brainstem-evoked auditory potentials, are abnormal [116,117]. In particular, there appears to be impairment of temporal resolution of complex acoustic signals as shown by temporal discrepancies between oto-acoustic emissions, cochlear microphonics and brainstem-evoked auditory potentials [115]. Such auditory neuropathy dys-synchrony grossly impairs the ability to perceive rapidly changing auditory signals which is vital for phoneme discrimination and so speech perception. In more recent times, it has been shown that in FRDA patients with

electrophysiological evidence of auditory neuropathy, binaural speech processing is impaired. The authors identified a significant correlation between disease duration and functional hearing [119].

**Bladder**

Sphincter alterations are poorly analysed in FRDA; disturbances in this district range from 7 to 41% in case series [95,108]. Urinary urgency with secondary urinary incontinence is the commonest complication encountered with urodynamic studies showing uninhibited contractions and altered bladder capacity [120,121]. Bladder hyperactivity symptoms are common in FRDA and are probably functionally exacerbated by mobility and transfer problems; however, suprapubic or transurethral catheterization is rarely required [10]. Bowel complications have not been systematically studied in FRDA, but they seem less frequent and disabling [10].

**Cognition and psychologic aspects**

Although 'decrease in intelligent quotient' was specifically mentioned in the first clinical criteria for FRDA [11], more recent studies show that cognitive functions are generally well preserved, even though subtle abnormalities, particularly of executive functions and information processing, have been detected [122]. Causing severe physical disability, FRDA may have a substantial impact on academic, professional, and personal development [3]. However clinicians' general experience is that cognitive deficits do not preclude participation in education, employment or social activities. Assessment of cognitive function can be significantly hampered by motor, speech and auditory impairments influencing reaction times, fluency and comprehension [10]. More recently, Mantovan and Colleagues [123] showed impairments in tasks related to visuoconstructive and visuoperceptual capacity, verbal fluency and motor and mental reaction times. The intelligence profile of FRDA patients was characterized by concrete thinking and poor capacity in concept formation and visuospatial reasoning [123]. Another study showed that FRDA patients perform significantly worse in tests of phonemic and action fluency but not in semantic fluency, when compared to controls [124].

The Authors postulated that this might represent primary prefrontal or cerebello-prefrontal dysfunction. Psychomotor function in FRDA was analysed with a variety of tests [125,126], it results that FRDA patients have difficulty in accommodating unexpected movements, are disadvantaged by conditions requiring initiation of movement without a direct visual cue, and are differentially affected in reaction time to incongruent, compared with congruent stimuli. These deficits could be the consequence of cerebellar impairment disrupting cerebro-ponto-cerebellothalamo-cerebral loops [125,126]. Klopper and Colleagues [127] found deficits in sustained volitional attention and working memory in FRDA. Nieto and Colleagues [124] examined performance in tasks measuring information processing speed, attention, working memory, executive function, verbal and visual memory, language, visuo-perceptive, visuospatial and visuo-constructive functions in 36 FRDA patients compared to controls. They found deficits in motor and mental speed, conceptual thinking, verbal fluency, acquisition of verbal information, use of semantic strategies in retrieval, action naming, visuo-perceptive and visuo-constructive problems. They suggested that these deficits could indicated parieto-temporal dysfunction [124]. In conclusion, taken together, these studies provide evidence in the growing field of cerebellar cognitive function and suggest that interruptions of the cerebro-cerebellar circuits may be functionally important in FRDA.

As in other chronic diseases, depression is more prevalent than in the unaffected population; Flood and Perlman [128]found that 92% of patients with FRDA develop an affective disorder ranging from mild mood disturbances to major depression (8%).

## *Non Neurological signs and symptoms*

### Skeletal abnormalities

Scoliosis, often at first diagnosed as idiopathic, is present at onset in two thirds of patients, in which neurological signs may or may not be observed [3]. When radiographically assessed, scoliosis is present in almost all patients: Labelle and Colleagues [129] found scoliosis of more than 10 degrees in

100% of patients and hyperkyphosis in 66%. Most cases show double thoracic and lumbar curves. Of those that were followed up long term, roughly equal numbers progressed or were non-progressive [129]. Milbrandt and Colleagues [130] found in a series of 77 patients that 63% had scoliosis and 24.5% hyperkyphosis; 33% had a double major curve and 20% were treated with braces and 33% underwent spinal fusion. In other case series, 33 to 94% of patients had scolioisis, most series finding a prevalence of more than 75% [11,12,95,108].

Also foot abnormalities are common; case series show foot deformities in 55 to 90% of cases [11,12,95,102,108,109]. Also Friedreich in his original analysis observed that both *pes cavus* and *talipes equinovarus* occur, either singly or in combination [5,131]. In classical cases *talipes equinovarus*, which is a progressive condition found in advanced disease and very disabling, is more common than *pes cavus* [10]. in classical cases. *Pes planus* is sometimes also seen [12]. If the patient is still ambulant, it can prevent proper placement of the foot on the floor and so contribute to instability and requirement for walking aids or orthotic devices. If the patient is wheelchairbound, it can impede positioning and transfers [132]. A study [132] analysed equinovarus deformities in 32 Australian individuals with FRDA and found absent or mild deformities in 15%, moderate but reducible (dynamic) deformities in 25% and severe and irreducible (static) deformities in 28%. Severity of deformity correlated with current age, duration of disease and duration of wheelchair dependence, but not GAA size or age at onset.

**Diabetes mellitus**

The association between FRDA and diabetes mellitus, although suspected for many years, was only confirmed relatively late [133]. About 10% of FRDA patients develop diabetes mellitus, and about 20% have carbohydrate intolerance. The underlying mechanisms are complex, with both β-cells dysfunction and insulin resistance [3] in peripheral tissues such as muscle [133,134]. These abnormalities in turn are likely to result from mitochondrial dysfunction [133]. There is not probably an underlying immune pathology driving these changes [135]. There is some evidence that heterozygous carriers of

the GAA expansion in the frataxin gene may have increased incidence of insulin resistance [133]. In case series, diabetes mellitus was found in 6–19% of cases [12,102,108,109]. Diabetes is typically a later feature of FRDA [133].

**Cardiac involvement**

Although FRDA patients are often asymptomatic, evidence of cardiac complications is found in the majority of cases of FRDA [136]. Patients sometimes report palpitations, but overt symptoms of heart failure are uncommon [10]. The most common cardiologic feature is progressive hypertrophic cardiomyopathy, which is a common cause of death in FRDA patients, leading to arrhythmias or cardiac failure [136]. It is quite rare for cardiomyopathy to develop before neurological features, and even if the patient is initially referred to a cardiologist, on detailed history collection or examination, neurological features will be found, preceding the cardiac complications [10]. Ischaemic heart disease is also rare [10]. In large cases series, hypertrophic cardiomyopathy or evidence of left ventricular hypertrophy (LVH) was found in 28 - 100% [11,95,102,108,109], although definitions vary greatly between studies. Asymmetric septal hypertrophy or dilated cardiomyopathy are less commonly seen and may represent progression from hypertrophic cardiomyopathy [137]. Blood pressure is typically normal or low, and hypertension is a problem in few cases [138]. An interesting feature is the absence of a clear correlation between the presence of cardiac complications and severity of neurological involvement [138]; this highlights the importance of cardiac monitoring in all patients. The disjunction between cardiac and neurological feature could be a consequence of tissue specific somatic instability and mosaicism of the GAA expansion [10]. Electrocardiographic alterations are present in almost all cases, the commonest anomalies are inferolateral or widespread Twave inversion [10,136,138]. Other non-specific alterations consist in ST segment and T-wave abnormalities, including ST-segment depression or elevation and flattening of T waves, are also seen [139,140]. Electrocardiogram evidence of LVH is seen less frequently and if present is usually accompanied by echocardiographic evidence of LVH [10]. QRS axis deviation is variable but most

commonly to the right [138–140]. Conduction abnormalities are very rare [138,141]. Sinus rhythm or sinus tachycardia is usually present, although patients may be troubled with paroxysmal or sustained arrhythmias, particularly atrial fibrillation, and only rarely require pacemaker or defibrillator insertion [142]. Echocardiographic studies show very variable findings among patients; LVH is usually seen. It is most commonly concentric but can show asymmetric septal hypertrophy [139]. There is commonly impaired systolic function but with relatively preserved ejection fraction [10]. In a longitudinal study including 113 echocardiograms in FRDA children, median ejection fraction was 61% [143]. Systolic function shows a slow non-linear decline with ejection fraction decreasing more rapidly with increasing age [143]. It is noteworthy that diastolic function frequently is only mildly impaired, less than might be expected. Only in advanced stages a diastolic pattern of impaired relaxation and pseudonormalization can be detected [143]. An explanation may be that the increase in LV wall thickness develops quite rapidly; thus, many patients with hypertrophy have a normal diastolic function [141]. Disease progress is characterised by initial concentric remodelling in early stage, followed by concentric hypertrophy in the advanced stage. At that time, myocardial fibrosis gradually develops, impacting heavily on morphology and function.

The cardiac valves are generally normal but hypertrophied papillary muscle may be seen [139]. In a large study of 204 FRDA patients, 140 (69%) had evidence of cardiomyopathy, of which 58.5% were classified as mild, 23.5% intermediate and 18% severe. The mean interventricular septal thickness at diastole across these groups was 12.0 mm, whilst left ventricular posterior wall thickness at diastole was 10.8 mm and ejection fraction 63.2% [138].

Cardiac MRI studies have broadly confirmed the echocardiographicstudies [136,138] with increased left ventricular mass seen in FRDA, especially with short disease duration and longer GAA size. There seems to be a tendency to left ventricular thinning with longer disease duration [144].

### *Progression and mortality*

There is no accepted measure of FRDA progression, although a variety of rating scales and performance measures have been employed, including a combinations of neurological and other parameters, or more specific measures of particular signs or symptoms [10]. Harding found that 72% of patients were wheelchaired [12]. The mean duration from age at onset to age at wheelchair-bound was 15.5 years (range 3–44) which represented a mean age of 25 (range 11–58); the distribution of age at wheelchair-bound was not parametric with a prolonged upper tail [12]. Half of cases were wheelchair-bound 16 years after onset of symptoms (age 26 years) and 95% 23 years after onset (age 44) [12]. Various clinical parameters progress at different rates, with dysarthria present in 100% of cases by 10–15 years since onset, lower limbs pyramidal weakness by 25–30 years since onset and distal upper limbs wasting and loss of vibrational and joint position sense by 45–50 years since onset [12]. Another more recent study [145] found that the mean time from onset to wheelchair-bound is 11 years (range 5–26), with a mean age of 24 (range 15–44). Mean age at onset of dysarthria is 20.8 years in a group whose mean age at onset of any symptom was 14.2 years [145]. These measures correlated with the length of the shorter GAA expansion [145]. De Michele and Colleagues [146] found the median time to loss of independent gait was 8 years (range 2–25), and to wheelchair-bound 15 years (range 6–29). Symptom onset before 20 years of age and the presence of LVH predicted increased rate of progression; 17% developed diabetes with a median time from symptom onset of 16 years (range 4–27) corresponding to a median age of 29 (range 9–42) [146].

A study [147]compared different rating scales to determine which best captured disease progression in FRDA. The Authors found that a mean change of 9.5 points in the Friedreich's Ataxia Rating Scale (FARS) and 5 points in the International Co-operative Ataxia Rating Scale (ICARS) over 12 months. They suggested the FARS required fewer patients for an equivalently powered study, although the ICARS requires less time to administer [147,148]. Friedman and Colleagues [149] studied 236 patients with FRDA, 159 of whom returned for follow-up after 1 year and 124 after 2 years. They used a variety of clinical rating scales and performance measures to monitor disease

progression including those relating to specific symptoms (9-hole board test, timed 25-foot walk, PATA speech test, low-contrast letter acuity vision charts) and more general scales (FARS, functional disability scale, activities of daily living). These measures and various composite versions captured disease progression although with differing sensitivities, linearity and subjection to bias, ceiling and floor effects. The same group in an expanded cohort of 259 patients found the annual rate of change of the FARS to be 2.66 points over the first year and 6.20 points over the first two years of follow-up. Burk and Colleagues [148] rated 96 patients using three different clinical scales, the FARS, ICARS and the Scale for the Assessment and Rating of Ataxia (SARA). Although these rating scales have very different structures from each other, SARA total scores were significantly correlated with ICARS and FARS making the SARA, which is shorter and quicker, suited for trials. However, a ceiling effect is also seen in the use of the SARA in patients in a late stage of the disease.

Cardiac complications are the commonest cause of death in FRDA [10]. Most of the studies report a mean age around the third decade; Andermann and Colleagues [150] found mean age at death of 30.6 years (range 4.5 to 40), Leone and Colleagues [151] found a median age at death of 34.5 (range 19–54) amongst the 14 patients who died in their cohort of 59 North-West Italian patients; in this study females had better prognosis than males. In a further Italian study, De Michele and Colleagues [146] found median age at death of 41 (range 10–65). The largest study of mortality in FRDA looked retrospectively at the notes of 61 individuals who had died. Mean age at death was 36.5 years (range 12–87) with cardiac or probable cardiac dysfunction accounting for 62% of cases [152]. Of these, the majority resulted from congestive cardiac failure or arrhythmia; other causes of death included stroke, ischemic heart disease and pneumonia. Increased GAA expansion size, presence of arrhythmia and dilated cardiomyopathy were greater in deceased compared to live patients, but there was no difference in hypertrophic cardiomyopathy [152].

**DIAGNOSIS AND FOLLOW UP**

An individual, especially a child, with a chronic progressive ataxia presents a diagnostic challenge. Given that the differential diagnosis is broad and some of the clinical features overlap, determining the mode of inheritance is the first important step. As said above, FRDA is the main autosomal recessive ataxia, especially among the paediatric onset cerebellar ataxias [16]. Molecular diagnosis can be performed by long-range PCR (Polymerase chain reaction) using primer that flaks the (GAA)n triplet expansion region, but this method cannot distinguish carriers from compound heterozygous FRDA patients. In this situation, further molecular tests are needed, such as analysis of FXN axons (1-5a and 5b) for point mutations and for axonic deletions [153].

It is fundamental to provide genetic counselling (including discussion of potential risk to offspring and reproductive option) to young adult who are affected, are carrier, or are at risk of being carriers [18]. To establish the extent of disease and the needs in individuals diagnosed with FRDA, some evaluations are recommended. A full neurological examination to assess gait and standing capacities, muscle weakness and wasting, hypoacusis, sphincter disturbance, swallowing difficulties, tendon reflexes and visual complaints is performed at the first visit to the clinic. To monitor disease progression, three appropriate and sensitive scales – the ICARS, the FARS and the SARA can be used for neurological evaluations.

Brain and spine MRI scan and electrophysiological study may be useful in the first assessment phase. MRI normally shows thinning in the cervical spinal cord, and might also highlight signal abnormalities in the posterior and lateral columns [154]. Brain MRI can be useful to differentiate FRDA, in which in most cases there is not cerebellar atrophy except occasionally in sever advanced cases, from other forms of hereditary recessive ataxias. Neurophysiological studies highlight sensory axonal neuropathy [154]. The peripheral motor system is often less severely affected and shows normal or mildly impaired compound muscle action potential and motor nerve conduction velocities [154].

Considering the complex clinical picture, FRDA's management should be multidisciplinary with a collaboration between neurologist, cardiologist, orthopedist, physiatrist, diabetologist and nutritionist [155]. A 2014 consensus statement for the care of patients with FRDA recommended to perform an ECG and echocardiogram [156] at the time of initial diagnosis, and the patients should be referred to a cardiologist if there are cardiac symptoms or abnormal findings on these exams [156]. Patients with an abnormal ECG should undergo annual electrocardiograms, even in asymptomatic patients [156]. Based on the overall low prevalence of arrhythmias, baseline ambulatory ECG Holter monitoring is warranted in asymptomatic patients; however, annual Holter monitors are not recommended unless the patient is symptomatic and/or is having no atrial arrhythmias [156]. Given the high prevalence of LV hypertrophy, as well as the progression to a dilated cardiomyopathy, annual cardiac imaging studies are reasonable [155,156].

The evaluation of blood glucose concentration is necessary to highlight glucose intolerance or diabetes mellitus, and it should be repeated on a yearly basis [18].

## TREATMENTS

At present there is no proven treatment that can slow the progression or eventual outcome of this life-shortening condition [156]. Many researches led to the development of numerous drugs in various phases of development and testing (figure 8) [157]. Therapeutic development options can be grouped into 6 groups [158]:

(1) Mitochondrial functioning related drugs

(2) Iron modulation and mitochondrial protective pathways

(3) Frataxin raising therapies

(4) Symptomatic treatment options

(5) Genetic modulation

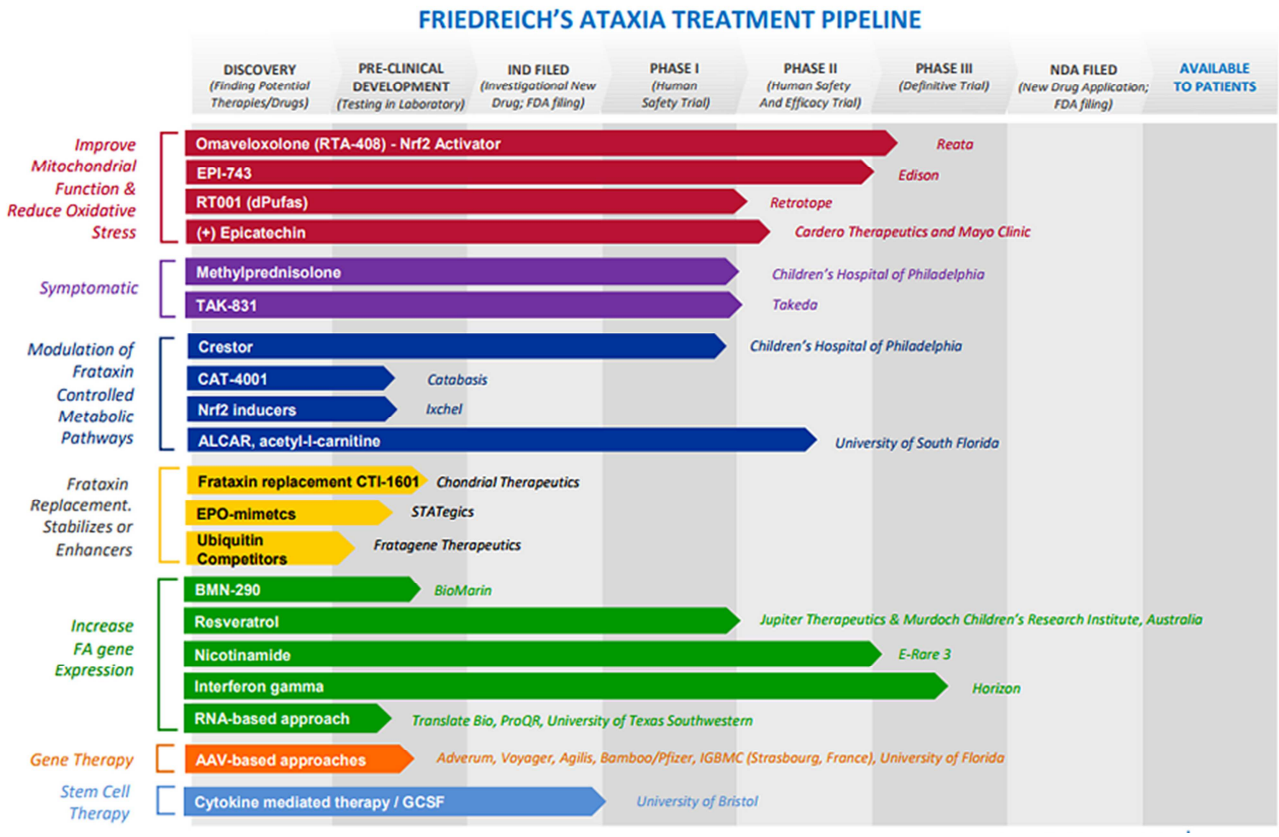


Figure 8 - FRDA treatment pipeline [157]

### *(1) Mitochondrial functioning related drugs*

**Idebenone and coenzyme Q10**

Idebenone and coenzyme Q10 are small antioxidant molecules with similar structures characterized by cell-protective properties in vitro [159,160]. Several clinical trials have been conducted on both idebenone and coenzyme Q10 assessing outcomes in cardiac and neurological function, but no statistically significant therapeutic benefit has been demonstrated [161]. Although the lack of a clear efficacy, these drugs continue to be used by many FRDA patients, considering that these agents have few side effects, are relatively inexpensive, and may have a small therapeutic benefit [158,162].

Early open-label studies of idebenone suggested some improvement in cardiac measures, including a decrease in left ventricular mass index, a reduction in left ventricular mass, and a significant decrease in cardiac hypertrophy [163,164]. A further larger placebo-controlled study of 70 subjects did not find significant cardiac improvements in the treatment group compared with the placebo group [165]. Regarding possible neurological improvements, early open-label trials found a correlation between serum idebenone levels and ICARS scores as well as a stabilization in neurological progression in paediatric patients [166,167]. A 6-month placebo-controlled trial examining differences in ICARS and FARS scores found modest improvements in the treatment group as compared to the placebo group, although these results failed to reach significance, as well as improvement in the open-label phase [168].

Early open-label studies on coenzyme Q10 found improvements in energy metabolism in heart and skeletal muscle as well as an increase in ATP synthesis, but these were not associated with any neurological changes [169,170]. Although the results from these studies did not reach statistical significance, about half of all patients with FRDA continue using coenzyme Q10 and vitamin E as supplements [162].

**EPI-743/A0001**

The first enhanced version of idebenone/coenzyme Q tried in FRDA patients was A0001 (alpha tocopheryl quinone), a molecule having structural features of both vitamin E and coenzyme Q [161]. In a single study of FRDA subjects, neurological exam scores on the FARS improved significantly in a 1-month period, although the primary outcome measure (diabetic disposition index) and blood glucose-related measures were unchanged [171]. Rather than moving forward in clinical trials, EPI-743 (Alpha-tocotrienol quinone), another agent similar in structure to A0001, was pursued in further studies. In addition to FRDA, EPI-743 has been tested in other mitochondrial diseases, including Leigh syndrome and Leber's hereditary optic neuropathy [161]. The ongoing clinical trials

## *(2) Iron modulation and mitochondrial protective pathways*

**Deferiprone**

As anticipated, FRDA can be considered as a disease of abnormal intracellular iron distribution. Excess mitochondrial iron can determine oxidative stress and cellular damage, ultimately leading to increased morbidity and mortality [161]. It has been supposed that removing surplus iron by way of chelation, it may reduce oxidative stress. Early trials of desferioxamine failed, as this chelating agent does not cross cell membranes well [172]. Only chelators capable of penetrating the mitochondria are likely to be useful in FRDA, although in cardiac tissue it is increased throughout the cell [173,174]. Deferiprone is an oral iron chelator presently approved for the treatment of thalassemia major [175]. Its ability to cross cellular barriers and the blood–brain barrier (BBB) to redistribute intramitochondrial iron suggest that it might be useful in FRDA [174]. Combination therapy of deferiprone and idebenone demonstrated neurological stabilization, reduction in iron on MRI of the dentate nucleus, and decreased intraventricular septum thickness and left ventricular mass index; side effects

included reversible neutropenia in two subjects [176]. A study using 20, 40, and 60 mg/kg/day of deferiprone demonstrated worsening ataxia with intermediate and high doses; all groups exhibited decreased cardiac hypertrophy [174]. In contrast, triple therapy with deferiprone, idebenone, and riboflavin demonstrated no clear neurologic or cardiac benefit [177]. While deferiprone appears to be relatively safe at lower doses and there is some evidence to support therapeutic benefit, there have been no systematic, large-scale, placebo-controlled studies to further evaluate its utility [161]. One question is whether chelation of mitochondrial iron is a true potential therapy: its role in FRDA has not been proven to be causal; instead, it could simply represent an epiphenomenon [161]. In addition, while iron accumulates in the mitochondria, the cytosol (except for cardiac tissue) is iron deficient and the body behaves as if it is iron deficient, consequently, only extremely selective iron removal from the mitochondria with a parallel increase in cytosolic iron increase should theoretically be beneficial in FRDA [161].

**PGC-1α modulation**

PGC-1α is a transcription factor that promotes mitochondrial biogenesis and controls specific metabolic pathways within the cell. PGC-1α is paradoxically reduced in some frataxin-deficient FRDA cells and in some tissues from patients with FRDA [178,179]. Theoretically, increasing PGC-1α levels may raise frataxin levels by promoting mitochondrial biogenesis, thereby producing therapeutic benefit [161]. In addition, a failure of mitochondrial biogenesis might prevent mitophagy, the process by which mitochondria are renewed. Pioglitazone, traditionally used as a treatment for type II diabetes, is an agonist of PPAR-γ which acts in concert with PGC-1α to increase mitochondrial function [179]. A 2-year proof of concept trial of pioglitazone was initiated in 2012 in order to examine the effect of this drug on the neurological function of FRDA patients [157].

**RTA-408**

RTA-408 (also known as omaveloxolone) is a semi-synthetic triterpenoid which has anti-inflammatory and antioxidant properties [161]. It is part of a class of compounds which slow the degradation of nuclear factor erythroid-derived 2-related factor 2 (Nrf2). Nrf2 is a transcription factor that targets genes including a large network of antioxidant enzymes by binding to the antioxidant response element on deoxyribonucleic acid (DNA), and thus impacts mitochondrial function by defending against ROS production. Nrf2 is involved in several other areas of mitochondrial function, including fatty acid oxidation, ATP production, and regulation of mitophagy [180,181]. Nrf2 activation is protective in both in vitro and in vivo models of several neurologic diseases such as PD, Alzheimer's disease, and Huntington's disease [182]. FRDA, in which decreased expression of FXN gene and production of frataxin protein is linked to decreased expression of Nrf2, is another promising target for Nrf2-activating compounds [83]. A multisite Phase II clinical trial of RTA 408 capsules in a population of FRDA patients recently concluded; this study was designed as a double-blind placebo-controlled trial with sequential dose cohorts and escalating doses. Results from the study demonstrated induction of Nrf2 with associated improvements in mitochondrial and neurological function, with time- and dose-dependent effects on modified FARS scores [183].

**Resveratrol**

Resveratrol, a potential mitochondrial enhancing agent perhaps through its activating effect on SIRT1 (NAD-dependent deacetylase sirtuin-1), has shown some success in early trials in FRDA. An open-label trial suggested some benefit at high doses, but this was confounded by the presence of side effects [184]. In addition, the delivery of resveratrol is complicated by its complex bioavailability [161]. New delivery methods may be beneficial in this regard [185].

### *(3) Frataxin-raising therapies*

**Erythropoietin (EPO)**

EPO is an endogenous hormone, currently approved for increasing red blood cell production in chronic anaemia, produced in the kidneys that increases frataxin expression in lymphocytes, cardiomyocytes, and cardiofibroblasts in vitro [186]. Peripheral blood mononuclear cell frataxin levels also increase in vivo in patients with renal disease when given EPO [186]. A 6-month open-label trial in individuals with FRDA demonstrated therapeutic benefit, with significant improvements in scores on ataxia rating scales and frataxin levels [187]. However, half of the patients in the trial showed elevated hemoglobin levels that required phlebotomy at the conclusion of the trial. Two other open-label studies of EPO in patients with FRDA also found prolonged increases in frataxin but no clinical improvements in disease symptoms [188,189]. Finally, two double-blind placebo-controlled trials of EPO in FRDA patients did not demonstrate differences in clinical outcomes between the placebo and drug treatment groups [190,191]. Considering that increases in frataxin levels and clinical improvements have been inconsistent across studies, it is difficult to make conclusions about the potential benefits of EPO in patients with FRDA [161].

**Interferon gamma**

Interferon gamma is an endogenous cytokine involved in the immune response to viral infection. Interferon gamma-1b is currently FDA-approved as an orphan drug for the treatment of chronic granulomatous disease and severe malignant osteopetrosis [161]. In cell and mouse models of FRDA, interferon gamma-1b can increase frataxin mRNA and protein levels. In addition, in one mouse model it also led to improvements in coordination and locomotion [192]. Such evidence justified pilot studies in FRDA in the United States and Italy. In a small 12-week open-label trial in the United States, frataxin protein levels were not significantly changed from baseline in whole blood or buccal swab samples; however, the

average improvement in the FARS was 5 points, a statistically significant effect representing approximately 18 months reversal of symptom progression [193,194]. In contrast, in an exploratory dose-escalation study in Italy of nine individuals with FRDA for 35 days, there were no changes observed in neurologic function as measured by the SARA scale, or in frataxin levels [195]. In both studies, interferon gamma-1b was well tolerated with surprisingly few adverse events beyond those known to occur with this agent, such as injection site reactions and flu-like symptoms. These small pilot studies have led to a phase III multicenter study of interferon gamma treatment in 90 individuals with FRDA in the United States [196]. This trial was divided into three parts: a 6-month placebo-controlled trial, a 6-month open-label period, and an open extension phase. In a press release, there was no statistically significant difference in the modified FARS exam scores in individuals taking interferon gamma-1b versus placebo. Secondary endpoints also did not meet statistical significance. As such results would not lead to a regulatory submission, the trial was discontinued in spite of the absence of new risks and of full results [197]. It is unclear whether the use of interferon gamma in FRDA will be further explored [161].

## *(4) Symptomatic treatment options*

### Methylprednisolone

Iron build-up in the mitochondria of FRDA patients may lead to an increase in sensitivity to oxidative stress, which can potentially trigger a global secondary inflammatory response [161]. Microarray analyses of autopsy specimens indicate altered immune response pathways and changes in the expression of inflammatory and satellite cells in FRDA specimens compared to control specimens [198]. Such findings may have major implications in the pathogenesis of cardiomyopathy in FRDA [199]. Some patients with FRDA have shown significant neurologic improvement following steroid administration [200]. These findings identify the anti-

inflammatory properties of steroids as potential source of benefit for FRDA patients, particularly those in the early stages of disease. To evaluate the safety and efficacy of steroid treatment in FRDA, a small, open-label pilot study of methylprednisolone is currently underway [201].

### *(5) Genetic modulation*

Perhaps the most promising potential therapy to replace the loss of frataxin in FRDA is gene therapy. The epigenetic silencing mechanism and the emerging epigenetic therapies will be explored in the experimental part of the thesis.

# EXPERIMENTAL PART

# A PHASE 1, FIRST IN MAN, ASCENDING DOSE CROSSOVER STUDY TO INVESTIGATE THE SAFETY, PHARMACOKINETICS AND PHARMACODYNAMICS OF RG2833 (A HISTONE DEACETYLASE INHIBITOR) IN ADULTS WITH FRDA

## EPIGENTIC SILENCING AND INHIBITION OF HISTONE DEACETYLASES

As mentioned above, FRDA is caused by severely reduced levels of frataxin [53], that result from a large GAA triplet repeat expansion within the first intron of the frataxin gene (FXN) [14]. In vitro and in vivo in bacterial plasmids the expanded repeat can adopt a triple helical structure that directly interferes with transcriptional elongation [202]. The discovery that long GAA repeats suppress the expression of a nearby reporter gene in transgenic mice in a manner similar to position effect variegation (PEV) observed in Drosophila pointed to a role of epigenetic mechanisms in the pathogenesis of FRDA [38,203,204]. PEV results in the silencing of a gene located near a heterochromatic region because of the spreading of heterochromatin into the gene itself [205]. This phenomenon does not occur in all cells, hence the term “variegation”, but nevertheless leads to an overall downregulation of the involved gene at the tissue and organ level [205]. In agreement with this hypothesis, the typical marks of heterochromatin, such as DNA methylation and histone deacetylation, are found near the expanded GAA repeat both in FRDA patients’ cells and in mouse models [38,204,206,207]. The dynamic interplay between histone acetylation, performed by histone acetyltransferases (HATs) and deacetylation, catalyzed by HDACs, is indeed a central mechanism to regulate gene expression, with increased acetylation associated with an open chromatin conformation and active genes [208]. Inhibition of histone deacetylases (HDACs) might be able to cause reactivation of FXN transcription [209].

Heterozygous carriers of the repeat allele have approximately 50 – 60% of the frataxin levels found in unaffected individuals and are themselves healthy. Thus, increasing frataxin levels to those found in carriers is predicted to be therapeutically useful [209]. Eighteen HDACs have been identified in the human genome, including the zinc-dependent HDACs (class I, class II, and class IV), and the NAD+-dependent enzymes (class III or sirtuins) [210,211] (figure 9 [212]). HDACs 1, 2, 3, and 8 belong to class I, showing homology to the yeast enzyme RPD3. Class II is further divided into class IIa (HDACs 4, 5, 7, and 9) and IIb (HDAC 6 and 10), according to their sequence homology and domain organization. HDAC11 is the lone member of class IV (9, 11). The sirtuins (class III) are related to the yeast Sir2 protein and are involved in regulation of metabolism and aging [210].

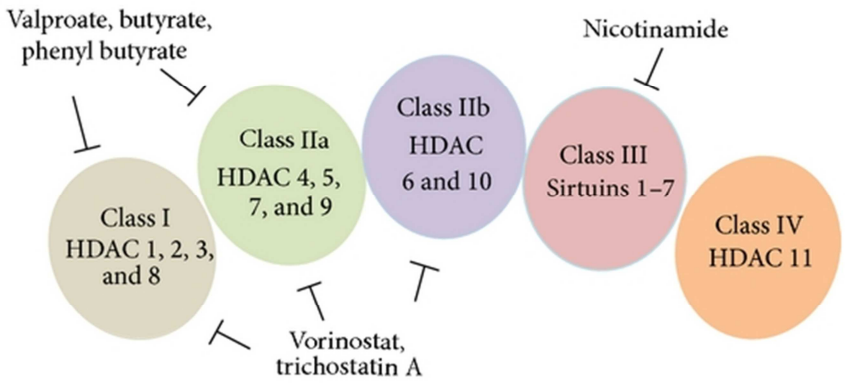


Figure 9 - Classification of histone deacetylase families [212]

A study [205] speculated that HDAC inhibitors (HDACIs) might reverse FXN silencing by directly increasing histone acetylation on the FXN gene, leading to chromatin decondensation and active transcription. A diverse class of compounds that inhibit HDACs has been developed; many of these molecules are well tolerated in humans and some of them show therapeutic promise in a wide range of diseases, including cancer, metabolic and neurological diseases [213,214].

**DEVELOPMENT OF HDAC INHIBITORS IN FRDA**

A commercially available HDACI (BML-210), and derivatives (pimelic diphenylamides), relieve repression of the FXN gene in lymphoid cell lines derived from FRDA patients, in primary lymphocytes from donor FRDA patient blood, and in the brain and heart of a mouse model for

FRDA [206,207]. Only members of the pimelic diphenylamide family of HDAC inhibitors increase FXN gene expression, and many common and highly active HDAC inhibitors, including the hydroxamates trichostatin A (TSA) and suberoylanilide hydroxamic acid (SAHA), are inactive [205]. Pimelic diphenylamide HDACIs specifically target class I HDACs, with the highest inhibitory effect on HDAC3 [215]. They are further characterized by a slow-on slow-off kinetics, leading to a more persistent histone hyperacetylation than induced by other HDACIs, including very potent molecules like SAHA [205].

In order to further improve the pharmacological profile of pimelic diphenylamide HDACIs as potential therapeutics for FRDA, Rai and Colleagues [207] treated KIKI mice with a novel histone deacetylase inhibitor, named compound 106, which increased frataxin mRNA levels in cells from Friedreich ataxia individuals. Treatment increased histone H3 and H4 acetylation in chromatin near the GAA repeat and restored wild-type frataxin levels in the nervous system and heart, as determined by quantitative RT-PCR and semiquantitative western blot analysis. No toxicity was observed and, furthermore, most of the differentially expressed genes in KIKI mice reverted towards wild-type levels. In conclusion, the lack of acute toxicity, normalization of frataxin levels and of the transcription profile changes resulting from frataxin deficiency provide strong support to a possible efficacy of this or related compounds in reverting the pathological process in FRDA. Considering these positive results, Rai and colleagues [205] synthesized additional compounds, similar in structure to each other and to compound 106, and they named them compounds 136 and 109, that differ for overall potency and degree of specificity for HDAC3, both being higher for compound 109. The Authors tested their ability to upregulate frataxin at a range of concentrations in order to determine a minimal effective dose in FRDA patients' peripheral blood lymphocytes and in the KIKI mouse model. In FRDA patients' peripheral blood mononuclear cell (PBMC), compound 109 was much more potent than compound 136 in upregulating frataxin, supporting the concept that HDAC3 selectivity correlates with this property. A good dose-response correlation could be detected for compound 109, with a 4- to 9-fold upregulation of frataxin mRNA at the highest tested

concentration of 10 µM. Compound 136 turned out to be effective at a threefold lower dose and more consistently in the KIKI mouse model, both in the FRDA target tissues after sub-cutaneous treatment and in in vitro treated splenocytes. The similar response of mouse splenocytes (closely related to the PBMCs tested in human patients) and of mouse nervous and cardiac tissue supports the hypothesis of a species difference rather than a cell type difference. It is possible that the mouse and human enzymes have differences in the response to the inhibitor, the inhibition kinetics having been determined with the human enzyme. It is also possible that the compounds differ in pharmacokinetic or metabolic properties in the mouse. The species differences have to be taken into account in the preclinical development of these drugs [205]. An important conclusion of this study comes from the analysis of the time course of the effects of these compounds in patients' PBMC and in mice, that long exceeds the time of direct exposure to the drugs. Frataxin mRNA remained elevated in PBMC for at least 12 hours after drug removal and in mice for at least 24 hours after a single subcutaneous injection. In both systems, the time course of frataxin mRNA upregulation paralleled the increase in total and local histone acetylation. These data confirm that HDAC inhibition is a more persistent phenomenon after transient exposure to this category of compounds than to other HDACIs like SAHA [15]. Most importantly, the increase in frataxin protein was the most sustained effect, lasting more than 48 hours after drug dosing in the mouse. It is of note that frataxin protein levels sharply increased in PBMC immediately after drug washout, reaching much higher levels compared to those obtained with continued exposure to the compounds. This finding may be due to inhibition of translation or of some post-transcription RNA processing step by the HDACI [17]. Taken together, these data suggest that intermittent administration of the drug, i.e. less than once daily and possibly as spaced as once or twice a week, may be the dosing regime of choice for the future clinical testing of these drugs. Such regimen would minimize toxic side effects by reducing drug exposure, at the same time allowing sustained upregulation of frataxin protein. Even in this series of experiments, neither in cell culture, nor in the animal studies, this class of HDACIs has not shown any apparent toxicity. Together with the previous studies [206,207], these results support

the pre-clinical development of pimelic diphenylamide HDACIs as potential therapeutics for FRDA.

## RATIONALE

The encouraging results from previous studies [205–207], led to the development of a phase 1 study with compound 109 (here under the development name of RG2833 for the formulated drug product, produced by Repligen Corporation, Boston, MA, USA) in FRDA patients. Moreover, although in vivo treatment using transgenic animal models that carry expanded GAA repeats has corroborated the findings in human blood cells, showing increased FXN mRNA and protein in target tissues [205,207,216] and reduced disease-related pathology [216], the question remains whether the human target tissue in FRDA, the neuron, would demonstrate the same molecular pathology and response to treatment with a disease-modifying agent as the surrogate tissue, the PBMC. Derivation of neurons from patient-derived induced pluripotent stem cells (iPSCs) is an important new tool to address this question [217,218].

## OBJECTIVES

### PRIMARY OBJECTIVES

1. To evaluate the safety of a single dose of RG2833 in comparison to placebo in patients FRDA
2. To evaluate the plasma pharmacokinetics (PK) of a single dose of RG2833 in patients with FRDA
3. To evaluate the pharmacodynamic (PD) response to a single dose of RG2833 on cellular and molecular biomarkers in patients with Friedreich's Ataxia

**SECONDARY OBJECTIVE**

1. To investigate whether RG2833 would be effective in an in vitro model for FRDA

## MATERIALS AND METHODS

***STUDY DESIGN:***

This was a phase I, first-in-man, single ascending dose, intermittent crossover design study in adult FRDA patients. The study consisted of 4 cohorts of 5 FRDA patients: Cohort 1 and 2 were open label, with single 30 to 120mg doses; Cohorts 3 and 4 were randomized, double-blind, placebo-controlled crossover studies. Cohort 3 received a single 180mg or placebo dose; Cohort 4 received two 120mg or placebo doses, 4 hours apart. All patients gave written informed consent according to the principles of Good Clinical Practice. The study protocol and consent forms were approved by the Italian Superior Health Institute (protocol No. 31637[11]PRE21–1101; EudraCT No. 2011-000248-12) and by the Ethical Committee of San Luigi Gonzaga University Hospital (protocol No. 10090-25/05/12; file No. 172/2011).

An independent Data Safety Monitoring Board (DSMB) reviewed major safety assessments and periodically assessed safety and efficacy.

There was a period of time between enrolment (i.e. initial study drug administration) of the previous cohort and the subsequent cohort in order to collect the safety and PK data, analyse the applicable PK samples, and have the applicable data reviewed by the DSMB. The period of time between cohorts was as follows:

- Five weeks between enrolment of the last patient in Cohort 1 and the first patient in Cohort 2.
- Five weeks between enrolment of the last patient in Cohort 2 and the first patient in Cohort 3.

- Nine weeks between enrolment of the last patient in Cohort 3 and the first patient in Cohort 4.

Data collection and monitoring, and safety reporting management were performed by independent expert contractors.

Adult patients with FRDA were admitted to the hospital on Day 0, and fasting started 8 hours prior to planned study drug dosing on Day 1. The patients remained in the hospital until 48 hours after study drug administration to monitor cardiac status via telemetry and to collect other safety data, PK and biomarkers. The patients were discharged after the Day 3 assessments were performed and then returned for outpatient visits on Day 7 and Day 14 so additional safety data, PK and biomarkers were collected.

Patients in Cohorts 3 and 4 were re-admitted to the hospital on Day 29, and fasting started 8 hours prior to planned study drug dosing on Day 30. The patients remained in the hospital until 48 hours after the second dose of study drug to monitor cardiac status via telemetry and to collect other safety data, PK and biomarkers. The patients in these cohorts were discharged after the Day 32 assessments and then returned for outpatient visits on Day 36 and Day 43 so additional safety data, PK and biomarkers were collected.

A follow-up visit for all patients in each cohort will occurred 28 days (+ 2 days) after the final study drug administration: this occurred on Day 29 (+ 2 days) for patients in Cohorts 1 and 2 and Day 58 (+ 2 days) for patients in Cohorts 3 and 4. Finally, the patients were contacted by telephone for this visit to assess adverse events and concomitant medications.

***INCLUSION CRITERIA***

1. Males and females, aged 18 to 55 inclusive
2. Genotype confirmed for homozygous GAA expansion at FXN locus, with at least 100 repeats at the shortest allele

3. Ejection fraction 50% documented by echocardiogram or equivalent study within 12 months prior to Visit 2 (Day 0)
4. Medically stable
5. Willing and able to give informed consent

***EXCLUSION CRITERIA***

1. Chronic or intermittent clinically significant cardiac arrhythmias at any time in the past 12 months prior to Visit 1 (screening)
2. Clinically significant findings (including clinically significant cardiac arrhythmias) on the Visit 1 or Visit 2 ECGs or on cardiac telemetry prior to study drug administration at Visit 3 (Day 1)
3. Total body weight less than 60 kg for patients in Cohorts 1 and 2 or total body weight less than 40 kg for patients in all other cohorts
4. History of allergic reaction or sensitivity to any of the ingredients in the study drugs (including lactose intolerance)
5. History of significant allergic reactions or anaphylaxis
6. History of any significant cardiac, endocrine, hematologic, hepatic, immunologic, metabolic, urologic, pulmonary, neurologic (excluding FRDA), dermatologic, psychiatric, renal and/or other major disease in the past 12 months prior to Visit 1 which, in the opinion of the investigator, precludes study participation
7. Current anaemia, low haemoglobin (defined as < 11 g/dL for females and < 13 g/dL for males) or low haematocrit (defined as < 36% for females and < 39% for males) at Visit 1 or Visit 2
8. Seropositive for Hepatitis B or C, or HIV, types I or II
9. Clinically significant abnormality in the Visit 1 or Visit 2 laboratory results which, in the opinion of the investigator, precludes study participation

10. Use of any medication, dietary aids or supplements within 24 hours prior to study drug administration at Visit 3, excluding paracetamol and contraceptive medication
11. Treatment with an investigational drug, device or biological agent within 30 days prior to Visit 1
12. Any blood donation within 30 days prior to Visit 1
13. History of substance or alcohol abuse or dependence within 12 months prior to Visit 1 or a positive urine drug screen at Visit 1 or Visit 2
14. Smoker (defined as three or more cigarettes or tobacco products per day for the past 30 days)
15. Unable or unwilling to fast from food or drink for 10 hours
16. Patients who are not willing to use effective contraception, and whose partners are not willing to use effective contraception, during the study and for a period of 2 months afterward (excluding female patients or female partners of non-childbearing potential)
17. Females who are pregnant or breastfeeding
18. Not suitable to participate in the study in the opinion of the investigator

***PATIENTS***

Patients' demographic and clinical characteristics are reported in Table 1.

Table 1- Demographic and Clinical Characteristics of study subjects

| Characteristic | Value |
|---|---|
| Demographics | |
| Age, yr[a] | 30.0 ± 8.1 |
| Sex, No. (%) | |
| M | 9 (40.9) |
| F | 13 (59.1) |
| Disease data | |
| GAA•TTC triplet expansion on shortest allele[a] | 1,084.8 ± 784.5 |
| Age of onset, yr[a] | 10.7 ± 4.6 |
| FARS[b] score at screening[a] | 59.7 ± 23.2 |
| Cardiac function, ejection fraction %[a] | 63.0 ± 6.9 |

[a]Data are shown as the mean ± standard deviation.
[b]See Beconi et al.[45]
F = female; FARS = Friedreich Ataxia Rating Scale; M = male.

***CELL CULTURE AND IN VITRO DIFFERENTIATION***

Induced pluripotent stem cells (also known as iPSCs) are a type of pluripotent stem cell that can be generated directly from adult cells [219]. The iPSC technology was pioneered by Shinya Yamanaka's lab in Kyoto, Japan, who showed in 2006 that the introduction of four specific genes encoding transcription factors could convert adult cells into pluripotent stem cells [219].

Fibroblasts from FRDA patients were grown at 37 °C and 5% CO2. Fibroblasts were cultured with 10% FBS in minimal essential medium, 2 mm glutamine, 1% nonessential amino acids, 20 mm HEPES, and 1% antibiotic/antimycotic (Invitrogen).

Derivation of iPSCs followed previous methods with minor deviations [220]. These normal and FRDA iPSCs have been characterized by standard methods [221].

In vitro differentiation of FRDA iPSCs to neurospheres and neurons was performed as follows: iPSC colonies were passaged onto high-density γ-irradiated mouse embryonic fibroblasts (at 60 × 103 cells/cm2) with ROCK inhibitor (10 μm; Stemgent). Induction was performed with either noggin (0.5 μg/ml; PeproTech Inc., Rocky Hill, NJ) or dorsomorphin (5 μm; P5499, Sigma-Aldrich) and SB431542 (10 μm; 040010, Stemgent) in ESC medium. During induction, FRDA iPSCs were maintained for 2 weeks without passage. Subsequently, induced colonies were dissected and transferred to suspension culture as neurospheres in Neurobasal-A medium with EGF (20 ng/ml) and basic FGF (20 ng/ml). Neurospheres were maintained as a suspension culture and passaged manually every 4–5 days. Neural differentiation was performed by dissociating neurospheres with Accutase (Invitrogen) and replating onto polylysine/laminin-coated plates at 50 × 103 cells/cm2. Neurons were maintained in Neurobasal-A medium without EGF or FGF for 7 or 8 days after replating. Generally, experiments were done with neurons at 8-days post-differentiation, except for the electrophysiology experiments, where the neurons were matured for 7 to 8 weeks.

***IMMUNOCYTOCHEMISTRY***

Cells were fixed in 4% paraformaldehyde for 10 minutes at ambient temperature and permeabilized/blocked with 10% goat serum/0.1% Triton X-100 detergent for 1 hour at ambient temperature (all in phosphate-buffered saline [PBS]). Primary antibodies were incubated at 4C overnight or at ambient temperature. After three 5-minute washes, secondary antibodies were incubated at ambient temperature for 1 hour. After 3 more washes, nuclei were stained with DAPI (10lg/ml) at ambient temperature for 15 minutes. All washes and incubations were performed in blocking buffer. Cells were imaged using an Olympus (Tokyo, Japan) IX-70 inverted fluorescent microscope. Primary antibodies included b-III tubulin (Tuj1; Covance, Princeton, NJ; 1:400), microtubule associated protein 2 (MAP2; Millipore, Billerica, MA; 1:500), and neuronal nuclei/FOX3 (NeuN; Millipore, 1:10), and secondary antibodies included antimouse Alexa 488 and antirabbit Alexa 488 (Invitrogen, Carlsbad, CA; both at 1:1,000).

### *CONVENTIONAL POLYMERASE CHAIN REACTION, QUANTITATIVE REVERSE RANSCRIPTASE POLYMERASE CHAIN REACTION AND MICROARRAY ANALYSIS*

For GAA·TTC triplet-repeat length conventional Polymerase Chain Reaction (PCR), Phusion polymerase (New England Biolabs, Ipswich, MA) was used according to the manufacturer. Twenty ng of genomic DNA (~6600 genomic equivalents) and 0.1 μm primers GAA-104F and GAA-629R were used (12) in 20-μl reactions cycled through the following conditions: denaturation at 98 °C for 5 s, annealing at 70 °C for 15 s, and extension at 72 °C for 90 s for 40 cycles with a 5-min initial denaturation and a 5-min final extension. Quantitation of PCR band size was performed using an inverse power function directly correlating gel migration of a molecular weight ladder to its known sizes (ImageJ software) [222]. PCR products from the FXN locus contain 499 bp of non-repeat sequences, so GAA·TTC triplet-repeat number estimations were adjusted accordingly.

Quantitative reverse transcriptase PCR (qRT-PCR) was performed using the qScript One-Step SYBR Green qRT-PCR kit from Quanta Biosciences (Gaithersburg, MD) according to the manufacturer's instructions. qRT-PCR reactions were detected on a PTC-200 thermal cycler with the Chromo4 real-time module (MJ Research, Waltham, MA). Primers to detect FXN mRNA were previously described.6 Primers for neuronal characterization were as follows: MAP2-R1 (50-CAGGAGTGATGGCAGTAGAC-30), MAP2-F2 (50-TTTGGAGAGCATGGGTCAC-30) for the MAP2 gene, HUC-F1 (50-GGTTCGGGACAAGATCACAG-30), and HUC-R1 (50-CTGAACTGGGTCTGGCATAG-30) for the ELAVL3 gene. Neuronal cell gene expression profiling was performed on Illumina(San Diego, CA) HT12 arrays.

### *FLOW CYTOMETRY AND QUANTITATIVE WESTERN ANALYSIS*

Whole cell extracts (in 50 mM Tris pH 7.4, 150 mM NaCl, 10% glycerol, 0.5% Triton X-100, protease inhibitor; Roche) were electrophoresed in polyacrylamide gels and transferred onto

nitrocellulose membranes. Primary antibodies were incubated overnight, and secondary antibodies were incubated one hour at room temperature. Signals were detected using HRP-conjugated secondary antibodies and enhanced chemiluminescence (SuperSignal West Pico, Thermo Scientific). Antibodies used in flow cytometry were the following: Tuj1 (Covance, 1:2500), MAP2 (BD Biosciences, Franklin Lakes, NJ; 1:40), glial fibrillary acidic protein (GFAP; Millipore, 1:20), Tra1–81 (Millipore, 1:500), and SSEA3 (Millipore, 1:500). Secondary antibodies were antimouse Alexa 488 (1:1,000), antirat Alexa 488 (1:1,000), or antirabbit Alexa 647 (1:1,000). The following antibodies were used in quantitative Western analysis: frataxin (MitoSciences, Eugene, OR; 1:1,000), RPL13a (Cell Signaling Technology, Danvers, MA; 1:2,000), and RNA polymerase II (Millipore; 1:2,000). Antibodies against acetylated residues of histone H3 and H4 have been described.22 The following secondary antibodies were all obtained from LI-COR Biosciences (Lincoln, NE) and used at the same dilution (1:5,000): antimouse IR680, antimouse IR800, antirabbit IR680, and antirabbit IR800.

***CHROMATIN IMMUNOPRECIPITATION***

Native chromatin immunoprecipitation was performed as follow: PBMCs were resuspended at 8 3 106 cells/ml in ice-cold buffer N (15mM Tris pH 8, 15mM NaCl, 60mM KCl, 250mM sucrose, 5mM MgCl2, 1mM CaCl2, and protease inhibitors); 0.5% NP-40 was added, and cells were incubated on ice for 10 minutes to complete cell lysis. Nuclei were collected by centrifugation at 524 3 g for 5 minutes and resuspended in ice-cold buffer N. After determining the nucleic acid content by spectrophotometry, 1U of micrococcal nuclease was added per microgram of DNA and samples were incubated for 10 minutes at 37C. The reaction was stopped by addition of 10mM ethylenediaminetetraacetic acid (EDTA) and 10mM ethyleneglycoltetraacetic acid. Samples were centrifuged for 5 minutes at 10,000rpm, and supernatant was collected and visualized on an agarose gel to determine the average DNA length. Chromatin (4–5lg) was diluted in chromatin

immunoprecipitation (ChIP) low salt buffer (20mM Tris-Cl, pH 8, 140mM NaCl, 2mM EDTA, 0.1% NP-40), 1lg of antibody against acetylated histone H3K9 (Millipore) was added, and samples were incubated at 4C overnight. The next day, 60ll of protein A agarose bead suspension (Millipore) was added, and samples were incubated for 2 hours at 4C. Beads were then washed 3 times with ChIP low salt buffer and once with ChIP high salt buffer (same as ChIP low salt buffer but with 0.5 M NaCl). Chelex 100 resin (100ll; 10% solution wt/vol in water; Bio-Rad Laboratories, Hercules, CA) was added to the bead–immunoglobulin G complexes, and samples were heated at 100C for 10 minutes. Proteinase K was added (100lg/ml), and samples were incubated at 55C for 30 minutes, followed by heat inactivation at 100C for 10 minutes. Supernatant was collected, and DNA recovery was analyzed by quantitative PCR using primers specific for the FXN region upstream of the GAA•TTC repeat expansion in intron 1 (see Herman et al6 for primer sequences).

***BISULFITE SEQUENCING***

Genomic DNA was extracted using the QIAamp DNA mini kit (QIAGEN, Valencia, CA), and bisulfite treatment of genomic DNA was performed using the EZ DNA methylation-Gold kit (Zymo Research, Orange, CA), following manufacturer instructions. Bisulfite-converted DNA was amplified using the following primers: for the sequence upstream of the GAA•TTC repeats, 50-GTTGTGGGGATGAGGAAGATTTTT-30 and 50-TAATCCACCTTCCTAAACCTCCCA-30; for the sequence downstream of the GAA•TTC repeats, primer sequences were described in Al-Mahdawi et al.8 PCR amplicons were cloned into the pCR-Blunt II-TOPO vector (Life Technologies, Grand Island, NY), and 20 clones per amplicon were sequenced.

***ELECTROPHYSIOLOGY***

Conventional whole cell patch clamp techniques were used for dissociated cells plated on poly-d-lysine and laminin matrigel-coated glass coverslips. Coverslips containing neuronal iPSCs were placed on the stage of a Nikon (Tokyo, Japan) Eclipse Ti inverted stage microscope for patch clamp recordings. Recordings were made using an Axon 700B Multiclamp amplifier (Axon Instruments, Sunnyvale, CA). Signals were sampled at 10kHz and filtered at 1.6kHz. Whole cell capacitance was fully compensated, and series resistance was compensated 60 to 70%. iPSC-derived neurons were identified based on morphology under bright field differential interference contrast. Coverslips of neuronal iPSCs were transferred to a recording chamber constantly perfused with bath solution consisting of (in millimolars): 140 NaCl, 5 KCl, 0.8 MgCl2, 10 N-2-hydroxyethylpiperazine-N0-2-ethanesulfonic acid (HEPES), and 10 glucose (pH 7.4). Recording electrodes (tip resistance of 4-6MX) were filled with solution containing (in millimolars): 20 KCl, 100 K-gluconate, 10 HEPES, 4 Mg21-adenosine triphosphate, 0.3 sodium guanosine triphosphate, and 10 phosphocreatine (pH 7.3). For voltage clamp recordings, cells were clamped at 270mV; Na1 and K1 currents were stimulated by voltage step depolarizations. Command voltages varied from 290 to 150mV in 10mV increments. For current clamp recordings, action potentials (APs) were induced by stimulation steps from 20.2 to 10.5 nA. All recordings were performed at ambient temperature. Offline analysis of data was performed using the Clampfit (pCLAMP 10 software, v10.2 Molecular Devices, Sunnyvale, CA), Excel (Microsoft, Redmond, WA), and Origin (OriginLab, Northampton, MA) programs.

***FLUORESCENCE IN SITU HYBRIDIZATION***

HEKGFP560GAA cells,23 fibroblasts, and FRDA neurons were plated onto coverslips and fixed in 4% paraformaldehyde in PBS for 30 minutes at room temperature. After fixation, cells were washed twice with PBS and stored overnight in 70% ethanol at 4C. Cells were then rehydrated in 50%

formamide, 23 standard saline citrate (SSC) for 5 minutes at room temperature and hybridized overnight at 37C in 100ll of a solution containing 10% dextran sulfate, 2mM vanadyl-ribonucleoside complex, 0.2% bovine serum albumin, 100lg yeast tRNA, 23 SSC, 50% formamide, and 1.2lg Cy3-(TTC)10 probe. After hybridization and washing, nuclei were stained in Hoechst 33342 (1:200 dilution) for 30 minutes at ambient temperature. Coverslips were mounted on slides using Prolong Gold Antifade Reagent. Cells were imaged with a 363 objective on a Zeiss (Oberkochen, Germany) LSM 710 laser scanning confocal microscope.

### *FORMULATION OF RG2833 FOR CLINICAL STUDIES*

Both RG2833 and placebo were produced, packed, and labelled according to Good Manufacturing Practice. RG2833 drug Soragni et al: Epigenetic Therapy for FRDA October 2014 491 product capsules contained 30mg, 60mg, or 150mg of 109 free-base equivalent. Each capsule contained a blend of RG2833 active pharmaceutical ingredient (109) and Ac-Di-Sol (2% croscarmellose sodium). Placebo consisted of capsules matched in size and appearance.

### *RG2833 PLASMA DRUG CONCENTRATION ANALYSIS*

Plasma samples were thawed, and protein was precipitated by addition of 9 volumes of acetonitrile. Supernatant was then transferred to a new tube containing 9 volumes of an ammonium acetate aqueous buffer. Samples were analyzed by ultra performance liquid chromatography/mass spectrometry using a Waters (Milford, MA) Acquity BEH C18 column with a water/acetonitrile gradient containing formic acid. Polarity of the mass spectrometer was set to positive mode, and the transition from 340.3 to 119.1amu was used to quantify RG2833. Pharmacokinetic parameters for RG2833 and metabolites in plasma were calculated using noncompartmental analysis. Only plasma concentrations greater than the respective lower limit of quantification (LOQ) were used in the pharmacokinetic analysis. The maximum plasma concentration (Cmax) and time to Cmax were

taken directly from the data. The elimination rate constant, lz, was calculated as the negative of the slope of the terminal log-linear segment of the plasma concentration-time curve. The slope was determined from a linear regression of the natural logarithm of the terminal plasma concentrations against time; at least 3 terminal plasma concentration time points, beginning with the final concentration greater than LOQ, were selected for the determination of lz, and the regression had to have a coefficient of determination ($r^2$) $\geq$ 0.9000. The range of data used for each patient was determined by visual inspection of a semilogarithmic plot of concentration versus time. Elimination half-life (t1=2) was calculated according to the following equation:

$$t_{½} = \frac{0{,}693}{\lambda k}$$

Area under the curve (AUC) to the final sample with a concentration greater than LOQ [AUC(0-t)] was calculated using the linear trapezoidal method and extrapolated to infinity [AUC(inf)] using:

$$AUC(inf) = AUC(0 - t) + \frac{Crf}{\lambda z}$$

where Ctf and tf are the final concentration $\geq$ LOQ and the time at which it occurred.

Clearance (CL/F) and volume of distribution (Vz/F), uncorrected for bioavailability (F), were calculated for RG2833 according to

$$CL / F = \frac{Dose}{AUC(inf)} \text{ and } Vz / F = \frac{Dose}{AUC(inf) \times \lambda z}$$

respectively.

### *WHOLE BLOOD AND PBMC FXN qRT-PCR*

The levels of FXN transcript were measured with a SYBR green-based qRT-PCR assay. For whole blood analysis, total RNA was isolated from blood collected with PAXgene Blood RNA tubes and processed using PAXgene Blood RNA Kit IVD (QIAGEN). For RG2833 in vitro treated PBMC analysis, PBMCs were isolated from predose patient blood with Ficoll gradient and treated with RG2833 in culture for 24 hours.

Cells were then pelleted, and RNA was isolated from the cell pellets using the RNeasy Mini Kit (QIAGEN). cDNA was then synthesized using the RT2 HT First Strand Kit (SABiosciences, Valencia, CA). Twenty-five nanograms of cDNA was combined with RT2 FAST SYBR Green/ROX qPCR master mix, RT2 qPCR primer assay for FXN (PPH05744B, SABiosciences), and RT2 qPCR primer assay for TBP (PPH01091G, SABiosciences) in a 25ll reaction volume. Assays were performed in duplicate using an Mx3005 or Mx3000 instrument and analysed using MxPro Software (Agilent Technologies, Santa Clara, CA). The amount of FXN mRNA in each sample was determined relative to the pre-dose sample and normalized to the levels of TBP mRNA.

### *PBMC ISOLATION, FRATAXIN PROTEIN, AND DEACETYLASE ASSAY*

PBMCs were isolated from whole blood using BD (Franklin Lakes, NJ) Vacutainer CPT tubes, following manufacturer instructions. Erythrocytes were lysed by treatment with buffer EL (QIAGEN). PBMCs isolated at the clinical site were lysed with lysis buffer (25mM Tris-HCl, pH 8.0, 137mM NaCl, 2.7mM KCl, 1mM MgCl2, 1% IGEPAL CA-630) on ice for 20 minutes. Supernatant was collected after centrifugation, and cell lysate protein concentration was measured with bicinchoninic acid protein assay reagent (Thermo Scientific, Waltham, MA). Frataxin protein was determined with a dipstick assay, as described.15 HDAC deacetylase assay was performed using a 96-well microplate assay by incubating cell lysate containing 0.5mg/ml of protein with 50mM of Fluor de Lys substrate (Enzo Life Sciences, Plymouth Meeting, PA) at ambient temperature for 30 minutes. At the end of the incubation, equal volume of stop solution (10mg/ml

trypsin with 2mM trichostatin A) was added, and the mixture was incubated at room temperature for 15 minutes. Fluorescence was then measured at excitation wavelength 360nm and emission wavelength 460nm. The level of deacetylase activity in each dosed PBMC sample was determined as a percentage of the pre-dose sample fluorescence.

## RESULTS

### *PHASE I CLINICAL TRIAL IN FRDA WITH RG2833*

HDACi 109 was evaluated in preclinical toxicology, pharmacology, and safety studies consistent with supporting the use of this compound in FRDA patients [205]. Approval was obtained from the Italian Health Ministry after review by the European Medicines Agency for an ascending dose crossover study in adults with FRDA. A phase I clinical study to evaluate the safety, pharmacokinetics, and pharmacodynamics of orally administered RG2833 (solid dose form of 109) was conducted with appropriate informed consent and ethical committee approval as described in the Materials and Methods section. The study consisted of 4 cohorts with 5 FRDA patients in each cohort (patient characteristics are summarized in Table 1). Cohort 1 and 2 were open label, wherein Cohort 1, 2 patients received a single 30mg dose and 3 patients received a single 60mg dose. In Cohort 2, all 5 patients received a single 120mg dose. Cohorts 3 and 4 were randomized, double-blind, placebo-controlled crossover studies. Based on the pharmacokinetics and safety data from the first 2 cohorts, each patient in Cohort 3 was administered a single dose of 180mg RG2833 and a single dose of placebo. Each patient in Cohort 4 received 2 doses of 120mg RG2833, administered 4 hours apart, and 2 doses of placebo, administered 4 hours apart. The 2 treatments of drug or placebo for a given patient in Cohort 3 or 4 were separated by 29 days and administered in random order. All 20 enrolled patients completed the study. RG2833 was well tolerated with no limiting toxicities reported. One patient suffered from 2 asymptomatic episodes of sinus tachycardia, which occurred >8 hours after dosing, neither of which was considered to be drug related because the Cmax of RG2833 is ≤ 2 hours. All the other side effects have been considered unrelated to the study drug. The independent DSMB identified no safety signals after reviewing the safety, clinical

laboratory, vital signs, physical and neurological examinations, and cardiology data from both 72-hour telemetry and 12-lead ECGs.

Pharmacokinetics of RG2833 was evaluated by analysing drug levels in the plasma of treated patients. An elimination half-life of 6 to 10 hours among the dose groups was observed (Fig 10A and Table 2). Metabolites of RG2833 were identified in patient serum. The major metabolite was a benzimidazole, which showed AUC exposure ratio between 160 and 250% of the parent compound in all dose groups. The benzimidazole had considerably longer elimination half-life than the parent compound, with t1=2 ranging from 35 to 42 hours. Other metabolites were products of amide hydrolysis, including o-phenylenediamine (OPD), acetylated OPD, and acids, as well as the glucuronide of RG2833. Based on in vitro efficacy data for FXN mRNA induction in primary lymphocytes [205,223] and neuronal cells, we estimate that a 5lM plasma concentration of RG2833, sustained for at least 6 to 8 hours, would result in similar increases of FXN expression in circulating PBMCs, and such levels were obtained in Cohorts 3 and 4 (Figure 10B). Using a deacetylase assay, up to 50% inhibition of total HDAC activity was detected in PBMCs from subjects of the 3 highest dose groups and an average of 35% inhibition was observed at the 180mg and 240mg doses (Figure 10C). It is important to highlight that this assay reflects inhibition of total deacetylase activity, not just the activity contributed by HDACs 1, 2, and 3.

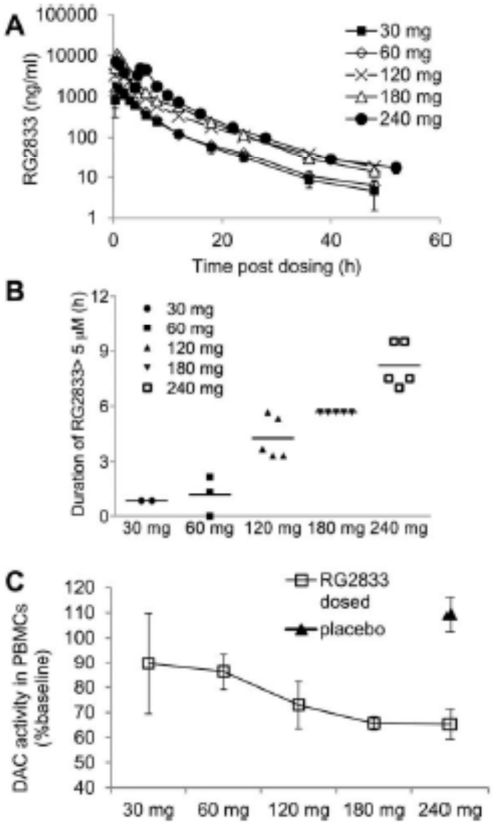


**Figure 10 - A – B – C - Pharmacokinetics of RG2833 in plasma after oral administration and inhibition of deacetylase activity in PBMCs.**

(A) Mean plasma concentrations of RG2833 for each cohort of patients as measured by liquid chromatography coupled with tandem mass spectrometry in the first 48 or 52 hours post-dosing. Error bars = standard error of the mean (SEM). (B) Duration of plasma concentration of RG2833 over 5lM for each patient in each dose group. (C) Mean of maximal suppression of deacetylase activity in PBMC extracts from patients in each dose group. Deacetylase activity in the cell lysate was quantified by deacetylation of the Fluor-de-Lys (Enzo Life Sciences) substrate. Error bars = SEM. Baseline is the deacetylase activity in the pre-dose sample of each patient.

**TABLE 2. Summary of Pharmacokinetic Parameters for RG2833 after Oral Administration of RG2833 to Adult Friedreich Ataxia Patients**

| Parameter | Cohort 1 | | Cohort 2, 120mg | Cohort 3, 180mg | Cohort 4, 240mg |
|---|---|---|---|---|---|
| | 30mg | 60mg | | | |
| Cmax, ng/ml | 1,975 ± 106 (2) | 2,563 ± 1,049 (3) | 6,474 ± 3,711 (5) | 10,930 ± 2,431 (5) | 7,154 ± 2,034 (5) |
| Tmax, h | 0.67 (2) [0.67–0.67] | 0.67 (3) [0.67–2.00] | 1.00 (5) [0.33–1.48] | 0.67 (5) [0.65–1.00] | 0.50 (5) [0.47–0.93] |
| AUC (0−τ), h × ng/ml | 7,695 ± 1,095 (2) | 9,631 ± 2,487 (3) | 21,689 ± 6,624 (5) | 34,903 ± 5,447 (5) | 39,344 ± 9,476 (5) |
| AUC (inf), h × ng/ml | 7,758 ± 1,166 (2) | 9,715 ± 2,470 (3) | 21,973 ± 6,470 (5) | 35,058 ± 5,475 (5) | 39,569 ± 9,576 (5) |
| λz, 1/h | 0.0897 ± 0.0306 (2) | 0.0854 ± 0.0208 (3) | 0.0739 ± 0.0223 (5) | 0.1016 ± 0.0225 (5) | 0.0844 ± 0.0191 (5) |
| $t^1/_2$, h | 8.20 ± 2.80 (2) | 8.43 ± 1.93 (3) | 10.1 ± 3.16 (5) | 7.07 ± 1.43 (5) | 8.56 ± 1.93 (5) |
| CL/F | | | | | |
| l/h | 3.91 ± 0.59 (2) | 6.43 ± 1.51 (3) | 5.80 ± 1.46 (5) | 5.24 ± 0.89 (5) | 6.39 ± 1.71 (5) |
| l/h/kg | 0.061 ± 0.016 (2) | 0.087 ± 0.011 (3) | 0.085 ± 0.026 (5) | 0.099 ± 0.018 (5) | 0.119 ± 0.032 (5) |
| Vz/F | | | | | |
| L | 45.1 ± 8.84 (2) | 79.0 ± 31.3 (3) | 89.7 ± 48.4 (5) | 52.8 ± 10.7 (5) | 75.5 ± 6.1 (5) |
| l/kg | 0.69 ± 0.059 (2) | 1.04 ± 0.164 (3) | 1.32 ± 0.825 (5) | 1.00 ± 0.234 (5) | 1.41 ± 0.143 (5) |

Mean ± standard deviation (No.) except Tmax, for which the median (No.) [range] is reported. All pharmacokinetic calculations were performed using SAS for Windows (SAS Institute, Cary, NC).
λz = elimination rate constant; AUC = area under the curve; Cmax = maximum plasma concentration; inf = extrapolated to infinity; $t^1/_2$ = elimination half-life; Tmax = time to maximum; CL = clearance; Vz = volume of distribution; F = bioavailability.

Table 2 - Summary of pharmacokinetic parameters for RG2833 after oral administration of RG2833 to adult FRDA patients

Next we assessed whether oral administration of RG2833 resulted in an increase in FXN mRNA in blood from patients. qRT-PCR demonstrated an upregulation of FXN mRNA levels in patients from the 3 highest dose groups, with an average induction of 1.5- to 1.6-fold observed within 24 hours post-dosing, and a correlation ($R^2$ = 0.417) was observed between the maximal FXN induction and RG2833 exposure in plasma (represented by AUC[inf ]) for each patient (figure 11). We also find a good correlation between increases in FXN mRNA in individual patients in Cohorts 3 and 4 and maximum inhibition of deacetylase activity measured in the same patient's PBMCs ($R^2$ = 0.636), providing evidence for the mechanism of action of the compounds as HDAC inhibitors. For each patient in Cohort 4, we plotted FXN mRNA levels relative to their pre-dose level (as a function of time after dosing), and compared these results to the placebo response for the same individuals. Four of 5 patients in Cohort 4 showed evident drug-induced FXN upregulation when their response to the drug was compared over time with their placebo response. PBMCs isolated from the pre-dose blood sample from the fifth patient treated with 10lM of RG2833 in vitro for 24 hours failed to show FXN mRNA induction, indicating this subject may be a non-responder at the time of the trial.

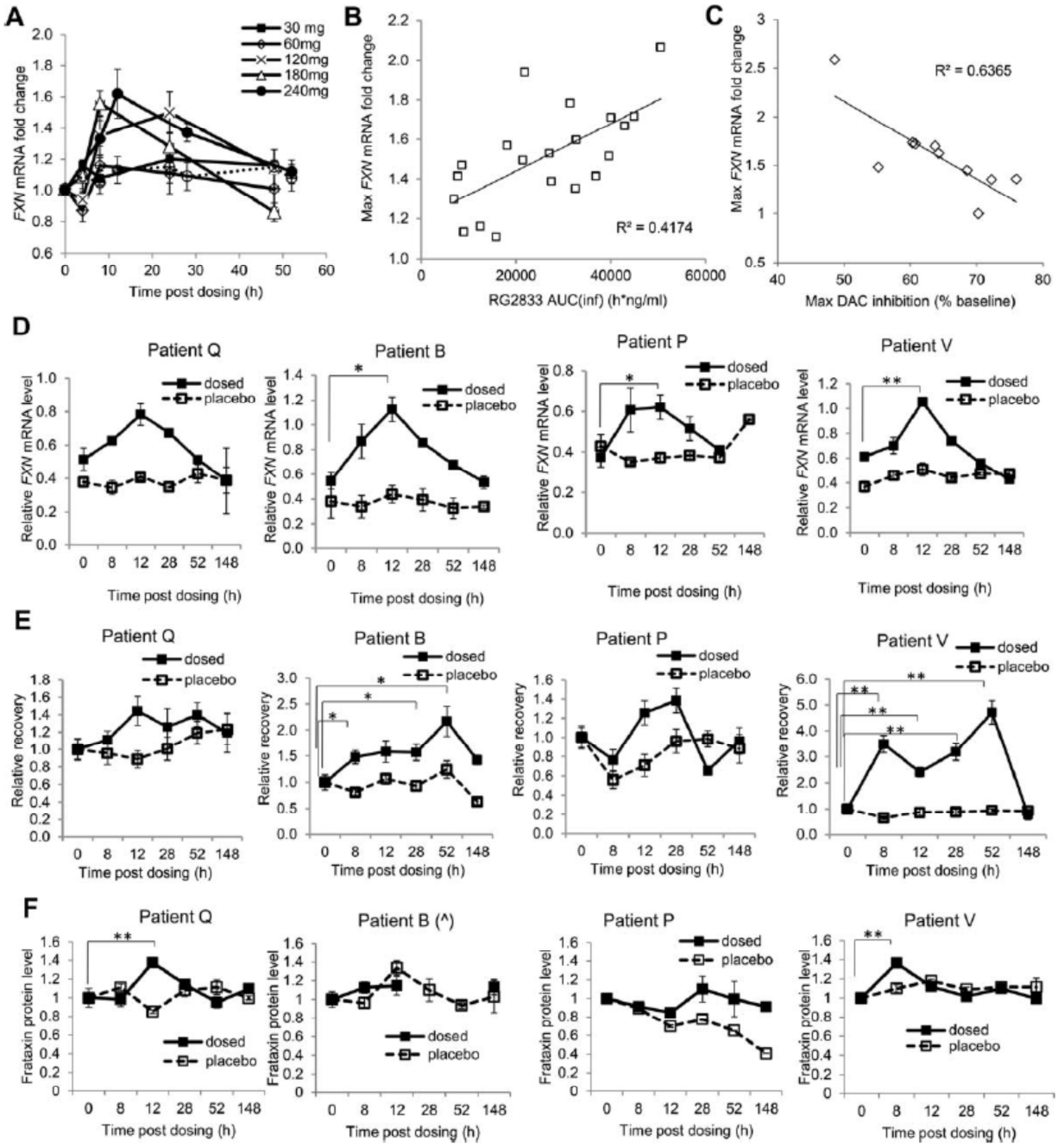


**Figure 11 - FXN mRNA, H3K9 acetylation, and frataxin protein response in adult Friedreich ataxia patients after oral administration**

(A) Mean fold-change of FXN mRNA in whole blood for each cohort upon dosing. FXN mRNA was quantified using quantitative reverse transcriptase polymerase chain reaction on RNA extracted from blood and plotted relative to the pre-dose sample. The expression level of TBP was used to normalize each sample. (B) Relationship between individual patient maximum fold-change of FXN mRNA in whole blood and RG2833 plasma area under the curve extrapolated to infinity (AUC[inf]). (C) Relationship between maximum fold changes in FXN mRNA in individual patients in Cohorts 3 and 4 and maximal deacetylase (DAC) activity in peripheral blood mononuclear cells (PBMCs). (D) FXN mRNA levels in response to dosing in Cohort 4 crossover study. Data for both dosed and placebo samples are plotted for each patient. FXN mRNA levels were normalized by TBP gene expression. Error bars5standard deviation (SD) of duplicate measurements. *p < 0.05, **p < 0.01. (E) Comparison of dosed versus placebo H3K9 acetylation response in Cohort 4 PBMCs. Error bars5standard error of the mean of triplicate measurements. *p < 0.05, **p < 0.01. (F) Frataxin protein levels in PBMCs from Cohort 4 patients were measured with a dipstick assay, as described.15 Data for both dosed and placebo samples are plotted for each patient. Error bars = SD of duplicate measurements. **p < 0.01. For Patient B, the 28-hour and 52-hour data points are missing due to technical problems.

As a downstream signaling event indicating HDAC inhibition, we used native ChIP assays to monitor H3K9 acetylation at the upstream GAA•TTC repeat site of the FXN locus in PBMCs. We observed increased H3K9 acetylation in the same 4 of 5 patients in this cohort (figure 11E). Although the same trends are observed with compound 109 in different patients, the absolute magnitudes of effects of the compounds on histone acetylation differ between patients. Similarly, the quantitative response in terms of increases in FXN mRNA differs between individuals in the patient population. This variability could be due to differences in GAA repeat numbers within the FRDA patients, but the current sample size is too small to draw quantitative conclusions. The effects of drug treatment on both FXN mRNA levels and histone acetylation in PBMCs are transitory (figure 11), as would be expected from the half-life of the compound in serum (figure 10A). We also analysed the frataxin protein levels in the PBMCs. No induction was seen in the first 2 cohorts, whereas 1 patient in the 180mg group and 2 patients in the 240mg group showed ~ 1.4-fold increases at a single time point (between 8 and 12 hours post-dosing; figure 11F). Although encouraging, the transient increase in FXN mRNA would not be expected to significantly add to total frataxin protein in this single dose study. A 50% increase in frataxin protein would require a sustained 2-fold increase in FXN mRNA equivalent to the 50-hour half-life of the protein [224]. Moreover, given the half-life of HDACi 109 in serum (figure 10A), a multiple dosing regimen would be required to see sustained FXN mRNA resulting in a measurable increase in frataxin protein.

***A HUMAN NEURONAL MODEL FOR FRDA***

Immunocytochemical analysis revealed positive staining for the neuronal markers Tuj1, MAP2, and NeuN, and quantitative RT-PCR showed a decrease in the expression levels of pluripotency-associated mRNAs (OCT4, NANOG, GDF3, TERT, and REX1) and an increase in neuron-specific mRNAs (HUC and MAP2) compared to undifferentiated FRDA iPSCs and neural stem cells (figure 12).

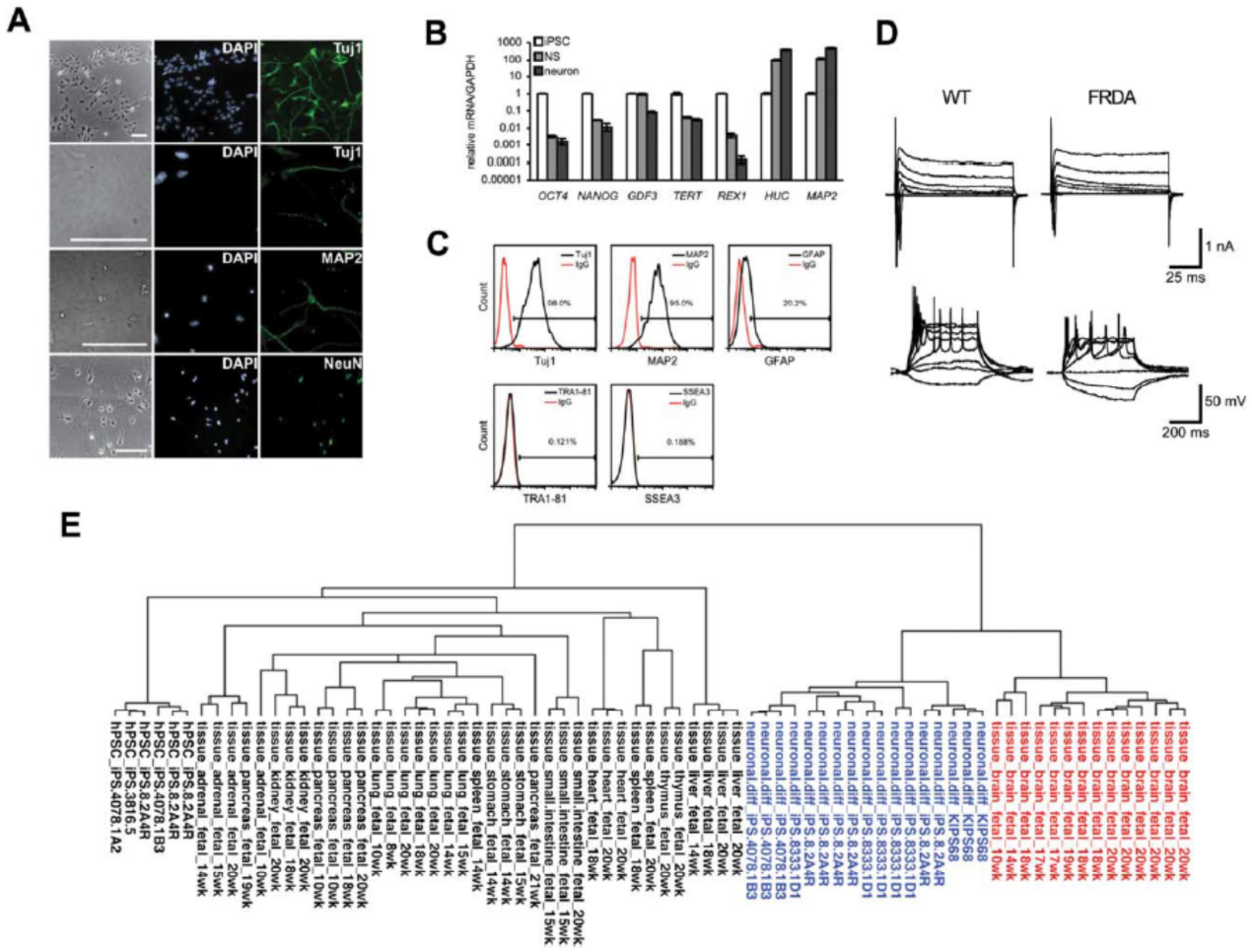


**Figure 12 - Characterization of induced pluripotent stem cell (iPSC)-derived neuronal cells.**

(A) Immunohistochemical staining of neuronal markers in early Friedreich ataxia (FRDA) neurons. Staining of b-III tubulin (Tuj1; top 2 rows), MAP2 (third row), and NeuN (bottom row) is shown. Phase contrast, left column; nuclear staining (DAPI), middle column; neuronal markers (Tuj1, MAP2, NeuN), right column. Scale bars50.1mm. (B) Quantitative reverse transcriptase polymerase chain reaction (qRT-PCR) analysis of mRNA markers of pluripotency (OCT4, NANOG, GDF3, TERT, and REX1) and neuronal differentiation (HUC and MAP2). Samples from iPSCs are shown in white bars, neurospheres (NS) in medium gray bars, and day 8 neurons in dark graybars. Signals are normalized to GAPDH, and iPSC signals were arbitrarily set to 1. Error bars5standard error of the mean of duplicate qRT-PCR measurements. (C) Population analyses of cells expressing the neuronal markers Tuj1 (first row, left column) and MAP2 (first row, middle column), the glial marker GFAP (first row, right column), and pluripotency markers Tra1–81 (second row, left column) and SSEA3 (second row, right column). Immunoglobulin G (IgG) controls are shown for each marker. Unstained background fluorescence channels (FL2-H or FL3-H) were used to gauge autofluorescence and to determine gating parameters. (D) Neuronal cells derived from unaffected (wild type [WT]) and FRDA iPSCs possess functional characteristics typical of neurons. Top, voltage clamp recordings showing inward and outward conductances in response to voltage steps (290 to 150mV). Bottom, current clamp recordings of unaffected and FRDA neurons firing multiple action potentials in response to current injection. (E) Unbiased clustering of iPSC-derived normal and FRDA neurons (blue samples) with human (h) iPSCs (6 left samples) and different fetal tissues, based on all detected autosomal transcripts (21,342 probes). Euclidean distance is displayed.

Flow cytometry indicated the presence of a relatively high percentage of Tuj1+ cell population (98%) and a MAP2+ population (95%) and a low percentage of cells expressing the glial-associated marker GFAP. Next, to determine whether our differentiated neuronal cells possessed the electrophysiological properties of typical neurons, we performed whole cell patch clamp recordings. In voltage clamp mode, a series of voltage steps to iPSC-derived neurons evoked large inward

currents closely followed by outward currents. These currents resembled the voltage-gated inward Na+ and outward K+ conductances that underlie the generation of APs in typical neurons. In current clamp mode, an injection of a depolarizing current triggered single and, in most cases, multiple APs in unaffected and FRDA neurons. Application of tetrodotoxin (1μM), a voltage-gated Na+ channel antagonist, reversibly blocked AP generation, indicating that iPSC derived neurons behaved as typical functional neurons. No significant differences were found between the unaffected and FRDA neurons after 7 to 8 weeks of differentiation in any of these electrophysiological measures, as previously reported [225]. Finally, we performed microarray studies to compare global gene expression of our iPSC-derived neurons to that of unaffected human iPSCs and different fetal tissues. Hierarchical clustering showed that these cells have a transcriptional profile close to that of fetal brain. Together, these data provide evidence that our FRDA iPSCs were differentiated to early Tuj1+/MAP2+ neuronal cells in relatively high purity. PCR analysis of genomic DNA from both neurospheres and neurons indicated that the expanded GAA•TTC triplet repeats are retained in these FRDA cells (figure 13). FRDA neurons also retain characteristically repressed levels of FXN mRNA when compared to non-diseased control neurons (figure14A) and lower levels of FXN protein.

As it has previously been suggested that transcriptional repression is caused by heterochromatin formation along the FXN locus [14,203] we analysed the chromatin state of the FXN gene in FRDA neurons using quantitative ChIP. We interrogated 3 locations along the FXN gene (the promoter, a region directly upstream of the GAA•TTC repeats, and a region directly downstream of the GAA•TTC repeats) for the presence of 11 histone post-translational modifications; 8 of them are associated with actively transcribed genes (“Activating,” in figure 13E) and 3 with repressed chromatin (“Repressing,” in figure 13E). Except for lysine 14 (H3K14ac) and lysine 36 of histone H3 (H3K36me), the activating marks are under-represented in FRDA cells compared to unaffected cells, as shown by an FRDA/unaffected occupancy ratio of <1. Conversely, the repressing histone marks are higher in FRDA cells. ChIP analysisof the same residues in fibroblasts, iPSCs, and iPSC-

derived neurons from the same patient and unaffected individual (figure 14 B, C) reveals that a similar pattern of histone modifications on FXN is present in the 3 cell types, although the histone mark differences between FRDA and unaffected cells seem to be less pronounced in neuronal cells. The same level of FXN repression is observed in each cell type. Together, these ChIP results indicate heterochromatin formation on the FXN gene near the GAA•TTC repeat expansion in FRDA neurons compared to unaffected neurons. Analysis of DNA methylation on 22 CpG sites upstream and downstream of the GAA•TTC repeats in fibroblasts, iPSCs, and neuronal cells revealed interesting differences among the 3 cell types and between unaffected and FRDA cells, but failed to show any indication that DNA methylation is the determinant of FXN gene silencing (figure 15).

### *2-AMINOBENZAMIDE HDAC INHIBITORS REVERSE FXN GENE SILENCING IN FRDA NEURONAL CELLS*

To demonstrate whether FRDA neurons respond similarly, we assessed the levels of FXN mRNA expression by qRT-PCR after treatment with the HDAC inhibitor (HDACi) 109 (N-[6-(2-aminophenylamino) 26-oxohexyl]-4-methylbenzamide), a compound previously shown to upregulate FXN mRNA and protein levels in both patient lymphocytes [205,226] and in the brain in 2 FRDA mouse models [205,216]. HDACi 109, which is moderately (3-fold) selective for HDAC3 over the other class I HDACs 1 and 2,13 upregulates FXN mRNA levels in FRDA neurons in a dose-dependent fashion, with a 2.5-fold increase over vehicle-treated cells at 5lM (figure 13 A), bringing the level of FXN mRNA in these cells to that expected for asymptomatic heterozygous carriers [205,226].

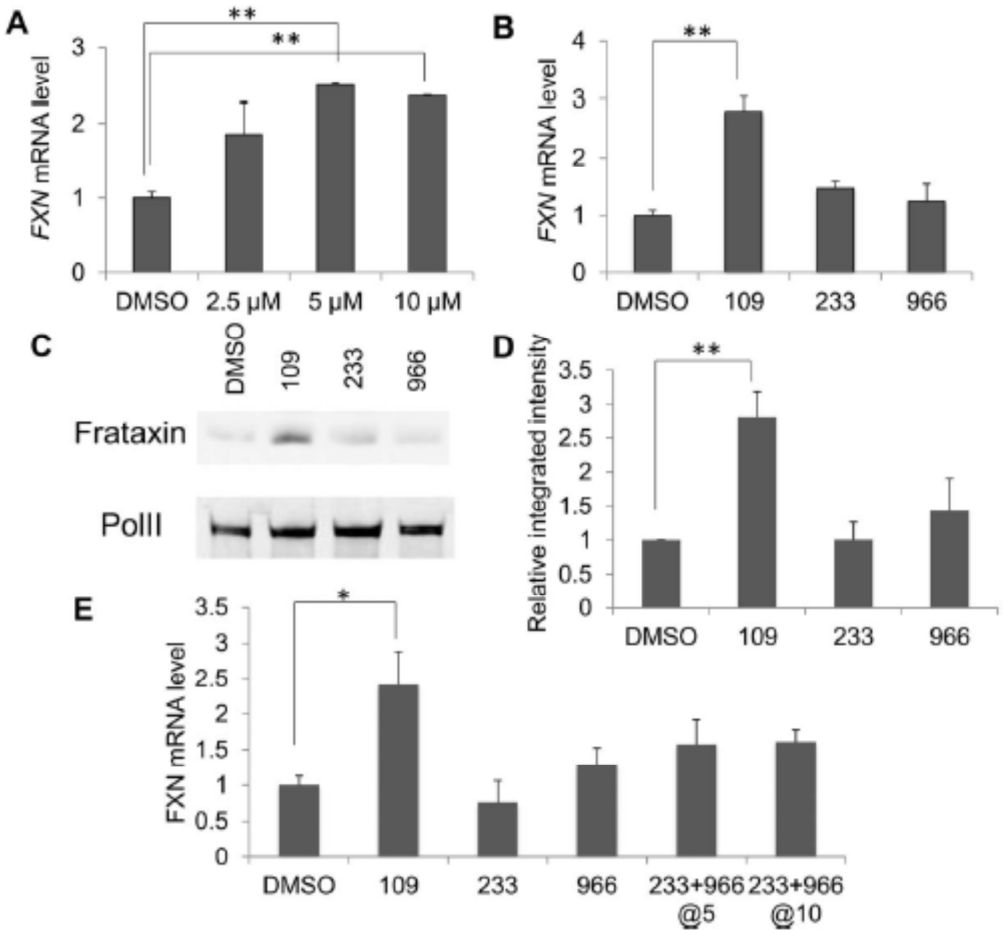


**Figure 13 - Effect of histone deacetylase (HDAC) inhibitors on FXN mRNA levels and frataxin protein in neuronal cells**

(A) Quantitative reverse transcriptase polymerase chain reaction (qRT-PCR) analysis of FXN expression in Friedreich ataxia (FRDA) neurons after 24-hour treatment with HDAC inhibitor 109 at varying concentrations. FXN mRNA levels were normalized to 18S RNA. Signals from dimethylsulfoxide (DMSO)-treated samples were arbitrarily set to 1. Error bars5standard error of the mean (SEM) of duplicate experiments. **p < 0.01. (B) qRT-PCR analysis of FXN expression in FRDA neurons after 24-hour treatment with HDAC inhibitors 109, 233, and 966 at 10lM. FXN mRNA levels were normalized to total RNA. Error bars5SEM of triplicate measurements **p < 0.01. (C) Example of a fluorescence Western blot of FRDA neurons treated with 10lM 109, 233, and 966 for 48 hours. Pol II signal was used as loading control. (D) Average of the quantification of 4 fluorescence Western blots of FRDA neurons (differentiated for 8, 10, and 14 days), treated as in C. Integrated intensity counts for frataxin protein were normalized to counts for Pol II, and the value for DMSO-treated neurons was arbitrarily set to 1.**p < 0.01. (E) qRT-PCR analysis of FXN expression in FRDA neurons after 24-hour treatment with HDAC inhibitors 109, 233, and 966 at 10lM or with a combination of 233 and 966 at 5 or 10lM. FXN mRNA levels were normalized to total RNA. Error bars5SEM of triplicate measurements. *p < 0.05. with human (h) iPSCs (6 left samples) and different fetal tissues, based on all detected autosomal transcripts (21,342 probes). Euclidean distance is displayed.

## *TARGETING HDAC1, 2, AND 3 IS NECESSARY TO REVERSE FXN SILENCING*

To explore the role of HDAC selectivity in FXN gene activation in FRDA neurons, the effects of an HDAC1/2-selective compound (HDACi 233; N-[2-amino-5-(2-thienyl)phenyl]-7-nicotinoylamino-heptanamide; >200-fold selectivity over HDAC3) [227] and a highly HDAC3-selective compound (HDACi 966; [E]-N-[2-amino-4-fluorophenyl]-3-[1-cinnamyl-1H-pyrazol-4-yl]acrylamide; ~ 30-fold selectivity for HDAC3 over HDAC1/2) [228] were examined (figure13 B). Neither of these latter

compounds induced FXN gene expression to the extent observed with HDACi 109. This result was expected for compound 233, as another HDAC1/2-selective compound (N1-[4-aminobiphenyl-3-yl]-N7-phenylheptanediamide) was previously shown to be inactive in terms of FXN upregulation in patient lymphocytes [229]. Moreover, quantitative fluorescence Western blotting showed an upregulation of frataxin protein in 109-treated cells but not in 233- or 966-treated cells (figure 5C, D). In-cell histone deacetylase assays confirm that each of these molecules is a potent inducer of global histone acetylation (at several residues in histones H3 and H4) in human neuroblastoma cells (data not shown), ruling out the possible trivial explanation that these latter compounds are not active HDAC inhibitors in neuronal cells. We also tested the combination of 233 and 966 for effects on FXN mRNA levels in neuronal cells; however, this combination was not as effective as compound 109 in achieving increases in mRNA levels (figure 13 E), suggesting that compound 109 may have a different mechanism of action, such as a longer residence time on its target enzymes (as found for the related compound 106). These results offer insight into the mechanism ofFXN gene reactivation and suggest that only compounds that inhibit the class I HDACs 1, 2, and 3 can induce upregulation of FXN mRNA and frataxin protein.

### *LYSINE 9 OF HISTONE H3 IS A KEY RESIDUE IN THE REGULATION OF FXN TRANSCRIPTION*

To investigate the link between the observed FXN upregulation and HDAC inhibition at pathogenic FXN alleles, we monitored the changes in histone post-translational modifications along the FXN gene in FRDA neurons following compound treatment using quantitative ChIP. Interrogating the same 3 locations along the FXN gene and the same acetylated residues as in Figure 2E, we observed significant changes upon treatment with 109, specifically large increases in occupancy of acetylated H3K9, H4K5, H4K8, and H4K16 (figure 14 A). A similar analysis was conducted in FRDA fibroblasts and iPSCs (figure 15). In these cell types, 109 has no effect in restoring FXN transcription. Whereas in iPSCs, the increase in the level of acetylation upon 109 treatment is 3- to

4-fold for all residues analysed, in fibroblasts the acetylation changes are similar to that of neuronal cells with the exception of H3K9. For this residue, the effect of 109 is higher in neuronal cells versus the other 2 cell types. From these data, it is clear that H3K9 acetylation at the FXN gene is related to whether transcriptional changes occur, and acetylation changes are quantitatively greater in cells that show FXN mRNA increases.

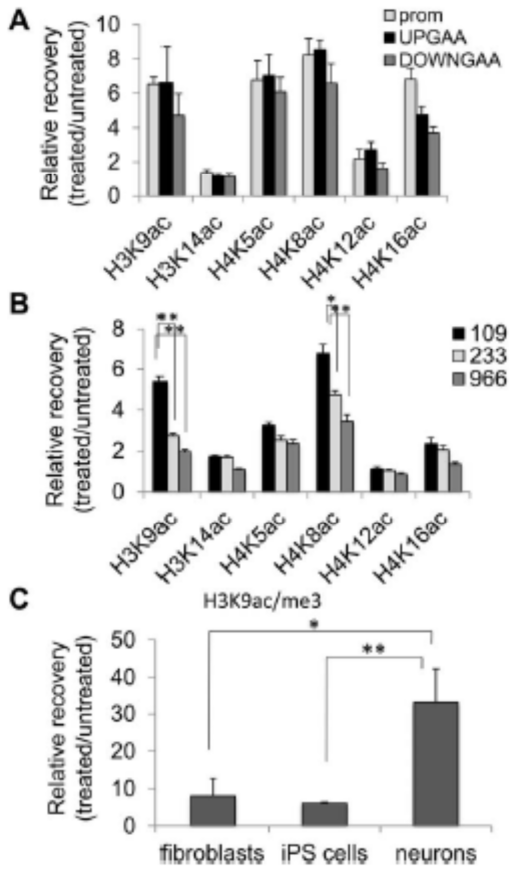


**Figure 14 - Mechanism of action of histone deacetylase**

(A) Quantitative chromatin immunoprecipitation (ChIP) analysis of histone acetylation marks in Friedreich ataxia neurons treated with 10lM 109 for 24 hours. DNA recovery for the FXN promoter (prom), a region upstream of the GAA•TTC repeats (UPGAA), and a region downstream of the GAA•TTC repeats (DOWNGAA)is shown. The ratio of DNA recovery for 109-treated versus dimethylsulfoxide (DMSO)-treated cells is plotted. Error bars = standard error of the mean (SEM) of triplicate measurements. (B) Quantitative ChIP analysis of the same histone acetylation marks as in A upon treatment with 109, 233, or 966 at 10lM. The UPGAA region is probed. The ratio of DNA recovery for 109-treated versus DMSO-treated cells is plotted. Error bars5SEM of triplicate measurements. *p < 0.05, **p < 0.01. (C) Quantitative ChIP analysis of H3K9ac/me3 ratio in fibroblasts, induced pluripotent stem (iPS) cells, and neurons. UPGAA region DNA recovery for the H3K9ac/me3 ratio in 109-treated versus DMSO-treated cells is plotted. Error bars = SEM of 2 independent ChIP assays, both quantified in triplicate. *p < 0.05, **p < 0.01.

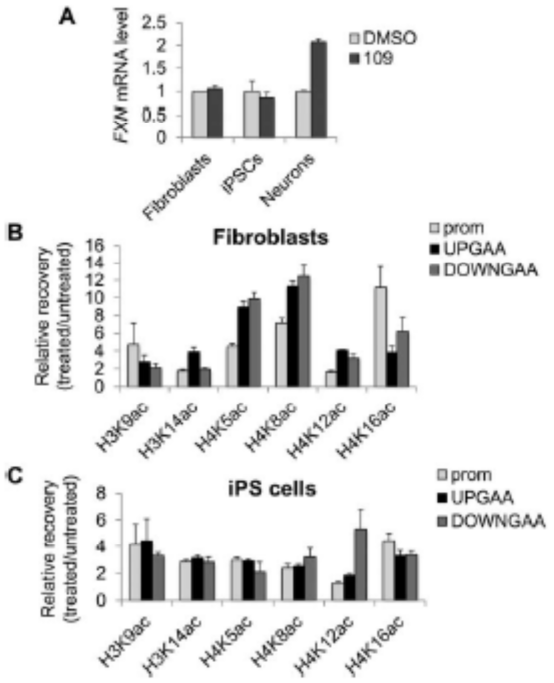


**Figure 15 - Effect of 109 on H3 and H4 acetylated residues in Friedreich ataxia (FRDA) fibroblasts and IPSCs.**

(A) quantitative reverse transcriptase polymerase chain reaction (qRT-PCR) analysis of FXN mRNA expression in fibroblasts, induced pluripotent stem cells (iPSCs), and neurons treated with either 0.1% dimethylsulfoxide (DMSO) or 10lM 109. qRT-PCR signals from FXN mRNA were normalized to total RNA, and the DMSO-treated sample was arbitrarily set to 1. Error bars = standard error of the mean (SEM) of triplicate measurements. (B) Quantitative chromatin immunoprecipitation analysis of histone acetylation marks in FRDA fibroblasts treated with 10lM 109 for 24 hours. DNA recovery for the FXN promoter (prom), a region upstream of the GAA•TTC repeats (UPGAA), and a region downstream of the GAA•TTC repeats (DOWNGAA) is shown. The ratio of DNA recovery for 109-treated versus DMSO-treated cells is plotted. Error bars5SEM of triplicate measurements. (C) Same as in B for FRDA iPSCs.

To address whether this is an indication of the mechanism of action of 2-aminobenzamide HDAC inhibitors in reversing FXN gene silencing, we compared the effect of 109 on histone acetylation upstream of the GAA•TTC repeats with that of compounds 233 and 966 in FRDA neuronal cells (figure 14 B). Based on the observed global activity of each of these compounds in neuroblastoma cells (data not shown), we expect to see global increases in histone acetylation in the neuronal cells; however, the ChIP experiments clearly show differences in the ability of the compounds to induce histone acetylation (figure 14 B) and transcription (figure 13 B) at the FXN locus. Increases in H3K9 and H4K8 acetylation are a signature of HDAC inhibitors that increase FXN mRNA level compared to compounds that are ineffective. These differences between compounds that show differential activity on the FXN gene could be due to specific HDAC complexes at pathogenic FXN alleles, where only compound 109 has the requisite activity for gene activation, or to mechanism of

action. A similar ChIP analysis in PBMCs from blood of 2 FRDA patients also showed the important contribution of H3K9ac and H4K8ac in FXN derepression (figure 16). We note that although the same trends are observed with each compound in different patients, the absolute magnitudes of effects of the compounds on FXN histone acetylation differ between patients. Similarly, the quantitative response to drug for increases in FXN mRNA can differ between individuals in the patient population [226], pointing to epigenetic differences within the human population.

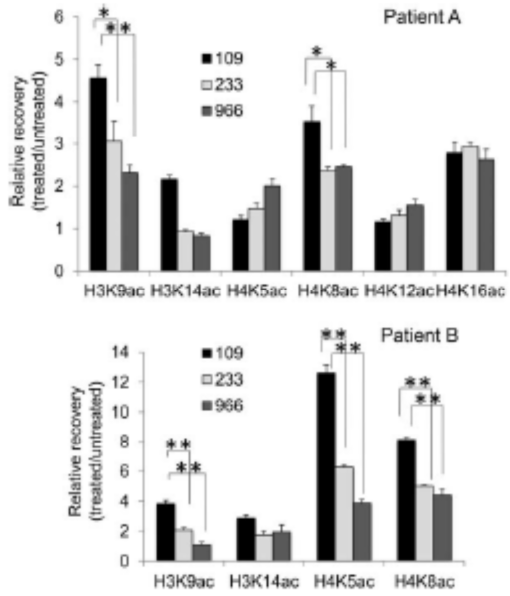


**Figure 16**

Quantitative chromatin immunoprecipitation analysis of H3 and H4 histone acetylation marks in peripheral blood mononuclear cells from 2 FRDA patients upon treatment with 109, 233, or 966 at 10lM. The region upstream of the GAA•TTC repeats is probed. The ratio of DNA recovery for 109-treated versus dimethylsulfoxide-treated cells is plotted. Error bars = standard error of the mean of triplicate measurements. *p < 0.05, **p < 0.01.

To further support the idea that lysine 9 of histone H3 is a key residue in the regulation of FXN transcription, we measured how the ratio of acetylation versus trimethylation for this residue (H3K9ac/me3) changes upon treatment with 109 in fibroblasts, iPSCs, and neurons. Although the ratio of H3K9ac/me3 increases upon treatment with 109 in each of the 3 cell types (figure 14 C), the magnitude of this effect is highest in neuronal cells, the only cell type among the 3 in which HDACi treatment can reverse FXN silencing. We argue that the balance between acetylation and

methylation of H3K9 on FXN determines the transcriptional status of the gene. It is likely that increases in H4K8 acetylation may also contribute to FXN gene activation (figure 14 B).

### *INCREASING FXN TRANSCRIPTION IN IPSC-DERIVED NEURONS DOES NOT PROMOTE GAA REPEAT INSTABILITY AND DOES NOT INDUCE RNA FOCI*

We addressed 2 concerns about the use of therapeutics that increase endogenous FXN transcription and mRNA levels in FRDA. The first is the observation that triplet repeat instability increases with transcriptional activity [230–232]. Higher levels of transcription of the FXN gene could possibly increase GAA•TTC repeat length in affected tissues and worsen the disease. In addressing this issue, we found that the increase in FXN transcription observed upon treatment of FRDA neuronal cells with HDACi 109 had no effect on repeat instability over the course of 12 days, a time frame sufficient to detect repeat instability in FRDA iPS cells (figure 17) [233]. The second concern relates to a possible toxic effect of the expanded triplet-repeat-containing transcript, as in other trinucleotide expansion diseases such as myotonic dystrophy type 1 and fragile X-associated tremor/ataxia syndrome [234]. Two lines of evidence argue against this possibility: (1) we found that expanded intron 1 RNA is present in extremely low levels, in agreement with previous findings [235]; and (2) we failed to detect GAA repeat RNA–containing foci in FRDA fibroblasts and iPSC-derived neurons with fluorescence in situ hybridization, even after FXN upregulation with HDACi. Such foci can be observed with an artificial reporter construct, showing that our methods are capable of detecting GAA-repeat RNA foci. These observations as well as the recent report of prolonged treatment with HDACi in a mouse model of FRDA [207] without negative effects suggest that HDACi treatment should not exacerbate the disease.

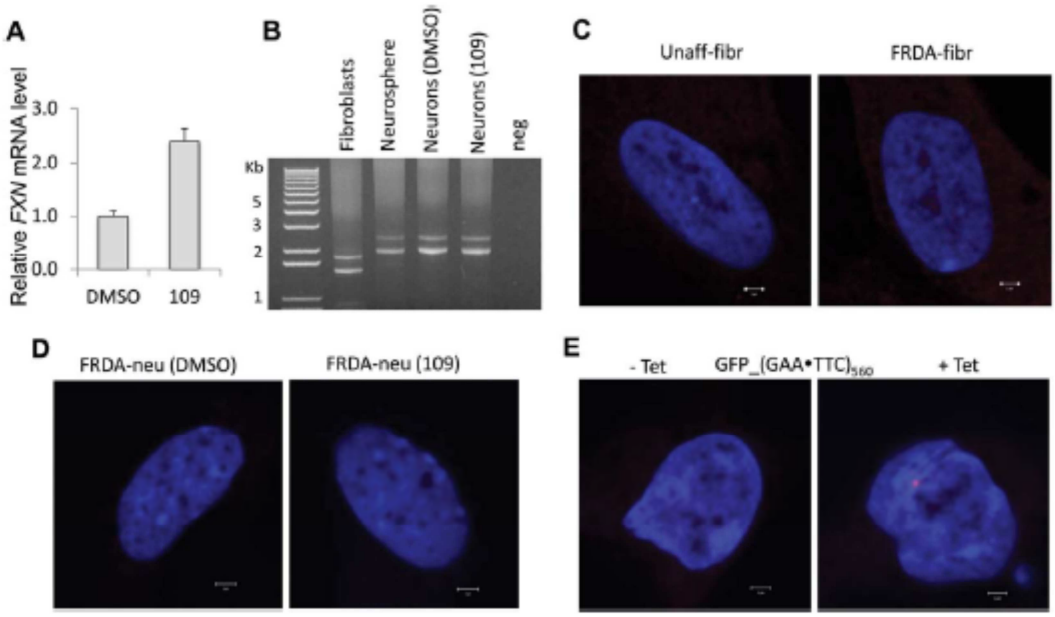


**Figure 17 - Histone deacetylase inhibitor 109 does not induce repeat instability in FRDA neurons, and GAAcontaining**

(A) Quantitative reverse transcriptase polymerase chain reaction analysis of FXN transcript in FRDA neurons treated with either dimethylsulfoxide (DMSO) or 109 at 5lM. Treatment was performed for 24 hours at days 7, 10, 13, and 16 after neuronal induction, and cells were collected for analysis at day 19. FXN mRNA levels were normalized relative to 18S rRNA levels. (B) GAA•TTC repeat length in FRDA fibroblasts, neurospheres, and neurons treated with either DMSO or 5lM 109 as described in A. (C) DAPI-stained nuclei from unaffected (left) and FRDA (right) fibroblasts hybridized with a Cy3-labeled TTC probe. (D) DAPI-stained nuclei from FRDA neurons treated with either DMSO or 10lM 109 and hybridized as in C. (E) DAPI-stained nuclei from cell line GFP_ (GAA•TTC)560 in the absence (2Tet, left panel) and presence (1Tet, right panel) of tetracycline. This cell line expresses green fluorescent protein with an artificial intron that contains 560 GAA•TTC repeats, under the control of a tetracycline-inducible cytomegalovirus promoter. One bright spot is visible in the presence of tetracycline, demonstrating that our Cy3-(TTC)10 probe can detect RNA foci. Scale bars = 2 µM.

## DISCUSSION

In this clinical trial we evaluated the effect of an HDACi, RG2833, on frataxin expression in PBMCs and we correlated the effect within a disease-relevant cell type using iPSC-derived neurons. This study could be very significative, because this approach can potentially be applied to test other therapeutics for FRDA, a disease still without an effective treatment, and for other genetic neurological disorders.

Furthermore, as we assayed cellular responses at a relatively early stage of neuronal differentiation, we are able to exploit the mitotically active nature of differentiated neural stem cells and scale our model system as needed to accommodate pilot studies (or potentially larger throughput screening studies) while maintaining relative population homogeneity. Although protocols for the derivation of sensory neurons from iPSCs have been already published [236–238] , previous studies do not yield sufficiently pure populations of cells for biochemical analyses.

We demonstrated that neurons of FRDA patient genetic background respond to treatment with the HDACi 109, effecting significant changes in histone acetylation near the FXN locus. In turn, this chromatin remodeling coincides with the upregulation of FXN mRNA and protein. Analysis of iPSC-derived neurons also provided insight on the mechanism by which FXN upregulation is achieved. We demonstrated that combined HDAC1, 2, and 3 inhibition is required to counteract the epigenetic changes induced by the GAA•TTC repeat expansion and that H3K9 is a key histone residue whose acetylation/methylation regulates FXN expression. We previously reported that 2-aminobenzamides differed from HDAC inhibitors that failed to activate FXN gene expression in terms of their inhibitory mechanism, where the active molecules inhibit their target enzymes through a slow-on/slow-off mechanism [239]. It is likely that the 4- and 5-substituted 2-aminobenzamides have this property only for their selected HDAC target enzyme and this can account for their lack of effectiveness in reactivating the FXN gene. HDAC inhibitors that fail to activate FXN gene expression, such as SAHA, also target the class I HDACs but differ from the

active molecules in that they exhibit rapid-on/rapidoff inhibition mechanisms [239]. Alternatively, reversal of epigenetic silencing could be achieved only by the unique action of 109 on the specific complexes residing at the FXN locus. In addition, iPSC-derived neurons allowed us to evaluate potential liabilities [240,241] of upregulating FXN transcription in cells bearing expanded repeats by demonstrating repeat stability and lack of RNA nuclear foci in 109 treated cells. All the previous studies with 2-aminobenzamide HDACi were in patient PBMCs or lymphoblast cell lines [242], which are cell types that are not affected in the human disease. The current study examines the efficacy of this HDACi in a cell type that is actually affected in the human disease, namely neuronal cells. The important and unprecedented finding from these studies is that drug exposure inducing epigenetic changes in neurons in vitro is comparable to the exposure required to see epigenetic changes and increases in gene expression in circulating lymphoid cells in FRDA patients. These findings provide a proof of concept that patient-derived neuronal cells can be a quantitative screening tool for the development of an epigenetic therapy for this fatal neurological disease. In line with the results from the iPSC-derived neuronal cells, we detected dose-dependent suppression of deacetylase activity in the PBMCs from drug-treated subjects, along with induction of histone acetylation and FXN mRNA upregulation. Maximal deacetylase inhibition and FXN upregulation were achieved when plasma RG2833 concentration exceeded target exposure of 5lM, an efficacious drug level predicted by the iPSC-derived neuronal cell model. Importantly, we detected a good correlation between increase in FXN transcript and inhibition of deacetylase activity, providing evidence that the mechanism of action of RG2833/109 is through deacetylation. Although only a small and inconstant frataxin protein modulation was observed in the clinical trial, the single dose treatment only allowed a transient increase in mRNA expression, so it is reasonable to predict that protein upregulation will follow the more sustained gene expression increase that can be expected in a repeat dose study.

Although our results are encouraging, 109/RG2833 suffers from liabilities for chronic use as FRDA therapeutics:

1) Suboptimal brain penetration (0.15 brain to blood ratio)
2) Conversion of the active molecule into inactive, potentially toxic metabolic products as benzimidazole and products of amidolysis, that are poorly eliminated in vivo [243,244]. Benzimidazole can inhibit the human ether-a-go-go related gene (hERG) with an IC50 of 0.92lM in the automated patch clamp assay, which puts RG2833 in the high-risk category for inducing QTc prolongation [245]. It is likely the risk factor would increase in a multiple dose regime because of benzimidazole accumulation due to the slow elimination of this metabolite. This risk could be higher in FRDA patients that generally suffer of cardiomyopathy.

For the above reasons, it is unlikely that RG2833 will be taken forward to later phase clinical trials.

Other compounds related to 109/RG2833 from subsequent medicinal chemistry campaigns have eliminated these metabolic liabilities and have favorable brain penetration (>0.7 brain/plasma ratio) [243]. These molecules are candidates for future clinical studies in FRDA.

A recent study [246] evaluated the potential benefits of the use of epigenetic modulation to treat FRDA. The Authors assessed the epigenetic and neurological effects and safety of high-dose nicotinamide, sirtuin inhibitor, in patients with FRDA. Nicotinamide was associated with a sustained improvement in frataxin concentrations towards those seen in asymptomatic carriers during 8 weeks of daily dosing. Although the drug tested seems to have only minor side effects, the doses used in this trial were considerably higher than the suggested daily dose for this supplement, and this is a concrete concern for the long-term use of such drug [247].

After this trial, further investigation of the long-term clinical benefits of nicotinamide and its ability to ameliorate frataxin deficiency in Friedreich's ataxia is warranted.

In contrast, benzamide HDAC inhibitors are effective in the low micromolar range, and the next generation of compounds holds the promise of efficacy in the high nanomolar range, with possibly fewer liabilities for long-term use.

The neuronal cell model developed in our trial can also be used to identify and investigate new biomarkers common to the neuronal cell lineage and lymphocytes that can aid future clinical trials. Long-term studies on large cohorts of FRDA patients are identifying clinical, functional, and quality of life measures, as well as biomarkers of FRDA progression that can be used as outcome measures in phase 2/3 clinical trials [248].

In conclusion, this study provides proof of principle that an orally dosed class I HDACi can increase both FXN mRNA and acetylation of a key residue in the blood of FRDA patients. The correlation of drug exposure response in iPSC-derived neuronal cells and PBMC of treated patients confirms the relevance of the neuronal cells as a model of the neurodegenerative disease FRDA and establishes a general path for drug development in neurological disorders. Although other potential treatments for neurodegenerative diseases have been tested in human iPSC-derived neurons [249–251], and iPSC-derived cells have also been used in high-throughput screens [252,253], this work for the first time bridges treatment evaluation in disease-specific patient neurons and drug exposure in a clinical trial.

# REFERENCES


1. Larner, A. J. *A dictionary of neurological signs.* (2011).

2. Pandolfo, M. Friedreich ataxia. *Arch. Neurol.* **65,** 1296–1303 (2008).

3. Pandolfo, M. Friedreich ataxia: The clinical picture. *Journal of Neurology* **256,** 3–8 (2009).

4. Chiang, S., Kovacevic, Z., Sahni, S., Lane, D. J. R., Merlot, A. M., Kalinowski, D. S., *et al.* Frataxin and the molecular mechanism of mitochondrial iron-loading in Friedreich's ataxia. *Clin. Sci.* **130,** 853–870 (2016).

5. Friedreich, N. Ueber degenerative Atrophie der spinalen Hinterstr??nge. *Arch. f??r Pathol. Anat. und Physiol. und f??r Klin. Med.* **26,** 433–459 (1863).

6. Schulz, J. B. & Pandolfo, M. 150 years of Friedreich Ataxia: from its discovery to therapy. *J. Neurochem.* **126,** 1–3 (2013).

7. Friedreich, N. Ueber Ataxie mit besonderer Ber??cksichtigung der heredit??ren Formen. *Arch. f??r Pathol. Anat. und Physiol. und f??r Klin. Med.* **68,** 145–245 (1876).

8. Koeppen, A. H. Nikolaus Friedreich and degenerative atrophy of the dorsal columns of the spinal cord. *Journal of Neurochemistry* **126,** 4–10 (2013).

9. Santos, R., Lefevre, S., Sliwa, D., Seguin, A., Camadro, J.-M. & Lesuisse, E. Friedreich Ataxia: Molecular Mechanisms, Redox Considerations, and Therapeutic Opportunities. *Antioxid. Redox Signal.* **13,** 651–690 (2010).

10. Parkinson, M. H., Boesch, S., Nachbauer, W., Mariotti, C. & Giunti, P. Clinical features of Friedreich's ataxia: Classical and atypical phenotypes. *Journal of Neurochemistry* **126,** 103–117 (2013).

11. Geoffroy, G., Barbeau, A., Breton, G., Lemieux, B., Aube, M., Leger, C., *et al.* Clinical description and roentgenologic evaluation of patients with Friedreich's ataxia. *The Canadian journal of neurological sciences. Le journal canadien des sciences neurologiques* **3,** 279–286 (1976).

12. Harding, A. E. Friedreich's ataxia: A clinical and genetic study of 90 families with an analysis of early diagnostic criteria and intrafamilial clustering of clinical features. *Brain* **104,** 589–620 (1981).

13. Chamberlain, S., Shaw, J., Rowland, A., Wallis, J., South, S., Nakamura, Y., *et al.* Mapping of mutation causing Friedreich's ataxia to human chromosome 9. *Nature* **334,** 248–250 (1988).

14. Campuzano, V., Montermini, L., Molto, M. D., Pianese, L., Cossee, M., Cavalcanti, F., *et al.* Friedreich's Ataxia: Autosomal Recessive Disease Caused by an Intronic GAA Triplet Repeat Expansion. *Science (80-. ).* **271,** 1423–1427 (1996).

15. Ruano, L., Melo, C., Silva, M. C. & Coutinho, P. The global epidemiology of hereditary ataxia and spastic paraplegia: A systematic review of prevalence studies. *Neuroepidemiology* **42,** 174–183 (2014).

16. Palau, F. & Espinós, C. Autosomal recessive cerebellar ataxias. *Orphanet J. Rare Dis.* **1,** 47 (2006).

17. Sequeiros, J., Martins, S. & Silveira, I. Epidemiology and population genetics of degenerative ataxias. *Handb. Clin. Neurol.* **103,** 227–251 (2011).

18. Bidichandani, S. I. & Delatycki, M. B. *Friedreich Ataxia*. *GeneReviews*® (1993).

19. Vankan, P. Prevalence gradients of Friedreich's Ataxia and R1b haplotype in Europe co-localize, suggesting a common Palaeolithic origin in the Franco-Cantabrian ice age refuge. *J. Neurochem.* **126,** 11–20 (2013).

20. Romeo, G., Menozzi, P., Ferlini, A., Fadda, S., Di Donato, S., Uziel, G., *et al.* Incidence of Friedreich ataxia in Italy estimated from consanguineous marriages. *Am. J. Hum. Genet.* **35,** 523–9 (1983).

21. Leone, M., Brignolio, F., Rosso, M. G., Curtoni, E. S., Moroni, A., Tribolo, A., *et al.* Friedreich's ataxia: a descriptive epidemiological study in an Italian population. *Clinical genetics* **38,** 161–169 (1990).

22. Yandim, C., Natisvili, T. & Festenstein, R. Gene regulation and epigenetics in Friedreich's ataxia. *Journal of Neurochemistry* **126,** 21–42 (2013).

23. Babcock, M. Regulation of Mitochondrial Iron Accumulation by Yfh1p, a Putative Homolog of Frataxin. *Science (80-. ).* **276,** 1709–1712 (1997).

24. Cossée, M., Puccio, H., Gansmuller, a, Koutnikova, H., Dierich, a, LeMeur, M., *et al.* Inactivation of the Friedreich ataxia mouse gene leads to early embryonic lethality without iron accumulation. *Hum. Mol. Genet.* **9,** 1219–1226 (2000).

25. Koutnikova, H., Campuzano, V., Foury, F., Dollé, P., Cazzalini, O. & Koenig, M. Studies of human, mouse and yeast homologues indicate a mitochondrial function for frataxin. *Nat. Genet.* **16,** 345–351 (1997).

26. Cossee, M., Schmitt, M., Campuzano, V., Reutenauer, L., Moutou, C., Mandel, J.-L., *et al.* Evolution of the Friedreich's ataxia trinucleotide repeat expansion: Founder effect and premutations. *Proc. Natl. Acad. Sci.* **94,** 7452–7457 (1997).

27. Cossée, M., Dürr, A., Schmitt, M., Dahl, N., Trouillas, P., Allinson, P., *et al.* Friedreich's ataxia: Point mutations and clinical presentation of compound heterozygotes. *Ann. Neurol.* **45,** 200–206 (1999).

28. Kim, E., Napierala, M. & Dent, S. Y. R. Hyperexpansion of GAA repeats affects post-initiation steps of FXN transcription in Friedreich's ataxia. *Nucleic Acids Res.* **39,** 8366–8377 (2011).

29. Pianese, L., Cavalcanti, F., De Michele, G., Filla, A., Campanella, G., Calabrese, O., *et al.* The effect of parental gender on the GAA dynamic mutation in the FRDA gene. *Am. J. Hum. Genet.* **60,** 460–3 (1997).

30. De Biase, I., Rasmussen, A., Endres, D., Al-Mahdawi, S., Monticelli, A., Cocozza, S., *et al.* Progressive GAA expansions in dorsal root ganglia of Friedreich's ataxia patients. *Ann. Neurol.* **61,** 55–60 (2007).

31. Monticelli, A., Giacchetti, M., De Biase, I., Pianese, L., Turano, M., Pandolfo, M., *et al.* New clues on the

origin of the Friedreich ataxia expanded alleles from the analysis of new polymorphisms closely linked to the mutation. *Hum. Genet.* **114,** 458–463 (2004).

32. Son, L. S. & Wells, R. D. in *Genetic Instabilities and Neurological Diseases, Second Edition* 327–335 (2006). doi:10.1016/B978-012369462-1/50022-3

33. Wells, R. D. DNA triplexes and Friedreich ataxia. *FASEB J.* **22,** 1625–1634 (2008).

34. Chutake, Y. K., Lam, C., Costello, W. N., Anderson, M. & Bidichandani, S. I. Epigenetic promoter silencing in friedreich ataxia is dependent on repeat length. *Ann. Neurol.* **76,** 522–528 (2014).

35. Kumari, D. & Usdin, K. Is Friedreich ataxia an epigenetic disorder? *Clin. Epigenetics* **4,** 2 (2012).

36. Greene, E., Mahishi, L., Entezam, A., Kumari, D. & Usdin, K. Repeat-induced epigenetic changes in intron 1 of the frataxin gene and its consequences in Friedreich ataxia. *Nucleic Acids Res.* **35,** 3383–3390 (2007).

37. Castaldo, I., Pinelli, M., Monticelli, A., Acquaviva, F., Giacchetti, M., Filla, A., *et al.* DNA methylation in intron 1 of the frataxin gene is related to GAA repeat length and age of onset in Friedreich ataxia patients. *J. Med. Genet.* **45,** 808–812 (2008).

38. Al-Mahdawi, S., Pinto, R. M., Ismail, O., Varshney, D., Lymperi, S., Sandi, C., *et al.* The Friedreich ataxia GAA repeat expansion mutation induces comparable epigenetic changes in human and transgenic mouse brain and heart tissues. *Hum. Mol. Genet.* **17,** 735–746 (2008).

39. De Biase, I., Chutake, Y. K., Rindler, P. M. & Bidichandani, S. I. Epigenetic silencing in Friedreich ataxia is associated with depletion of CTCF (CCCTC-binding factor) and antisense transcription. *PLoS One* **4,** (2009).

40. Pastore, A. & Puccio, H. Frataxin: a protein in search for a function. *J. Neurochem.* **126,** 43–52 (2013).

41. Bencze, K. Z., Yoon, T., Millán-Pacheco, C., Bradley, P. B., Pastor, N., Cowan, J. A., *et al.* Human frataxin: iron and ferrochelatase binding surface. *Chem. Commun.* 1798–1800 (2007). doi:10.1039/B703195E

42. Bou-Abdallah, F., Adinolfi, S., Pastore, A., Laue, T. M. & Dennis Chasteen, N. Iron binding and oxidation kinetics in frataxin CyaY of Escherichia coli. *J. Mol. Biol.* **341,** 605–615 (2004).

43. Dolezal, P., Dancis, A., Lesuisse, E., Sutak, R., Hrdý, I., Embley, T. M., *et al.* Frataxin, a conserved mitochondrial protein, in the hydrogenosome of Trichomonas vaginalis. *Eukaryot. Cell* **6,** 1431–1438 (2007).

44. Bencze, K. Z., Kondapalli, K. C., Cook, J. D., McMahon, S., Millán-Pacheco, C., Pastor, N., *et al.* The structure and function of frataxin. *Critical Reviews in Biochemistry and Molecular Biology* **41,** 269–291 (2006).

45. Gibson, T. J., Koonin, E. V., Musco, G., Pastore, A. & Bork, P. Friedreich's ataxia protein: Phylogenetic evidence for mitochondrial dysfunction. *Trends Neurosci.* **19,** 465–468 (1996).

46. Pandolfo, M. & Pastore, A. The pathogenesis of Friedreich ataxia and the structure and function of frataxin. *Journal of Neurology* **256,** 9–17 (2009).

47. Galea, C. A., Huq, A., Lockhart, P. J., Tai, G., Corben, L. A., Yiu, E. M., *et al.* Compound heterozygous FXN mutations and clinical outcome in friedreich ataxia. *Ann. Neurol.* **79,** 485–495 (2016).

48. Ashley, C. N., Hoang, K. D., Lynch, D. R., Perlman, S. L. & Maria, B. L. Childhood ataxia: Clinical features, pathogenesis, key unanswered questions, and future directions. in *Journal of Child Neurology* **27,** 1095–1120 (2012).

49. Koutnikova, H., Campuzano, V. & Koenig, M. Maturation of wild-type and mutated frataxin by the mitochondrial processing peptidase. *Hum. Mol. Genet.* **7,** 1485–1489 (1998).

50. Musco, G., Stier, G., Kolmerer, B., Adinolfi, S., Martin, S., Frenkiel, T., *et al.* Towards a structural understanding of Friedreich's ataxia: Solution structure of frataxin. *Structure* **8,** 695–707 (2000).

51. Foury, F., Pastore, A. & Trincal, M. Acidic residues of yeast frataxin have an essential role in Fe-S cluster assembly. *EMBO Rep.* **8,** 194–199 (2007).

52. Wells, R. D., Dere, R., Hebert, M. L., Napierala, M. & Son, L. S. Advances in mechanisms of genetic instability related to hereditary neurological diseases. *Nucleic Acids Res.* **33,** 3785–3798 (2005).

53. Campuzano, V., Montermini, L., Lutz, Y., Cova, L., Hindelang, C., Jiralerspong, S., *et al.* Frataxin is reduced in Friedreich ataxia patients and is associated with mitochondrial membranes. *Hum. Mol. Genet.* **6,** 1771–80 (1997).

54. Richardson, D. R., Lane, D. J. R., Becker, E. M., Huang, M. L.-H., Whitnall, M., Rahmanto, Y. S., *et al.* Mitochondrial iron trafficking and the integration of iron metabolism between the mitochondrion and cytosol. *Proc. Natl. Acad. Sci.* **107,** 10775–10782 (2010).

55. Adamec, J., Rusnak, F., Owen, W. G., Naylor, S., Benson, L. M., Gacy, A. M., *et al.* Iron-Dependent Self-Assembly of Recombinant Yeast Frataxin: Implications for Friedreich Ataxia. *Am. J. Hum. Genet.* **67,** 549–562 (2000).

56. Cavadini, P., O'Neill, H. a, Benada, O. & Isaya, G. Assembly and iron-binding properties of human frataxin, the protein deficient in Friedreich ataxia. *Hum. Mol. Genet.* **11,** 217–227 (2002).

57. Zanella, I., Derosas, M., Corrado, M., Cocco, E., Cavadini, P., Biasiotto, G., *et al.* The effects of frataxin silencing in HeLa cells are rescued by the expression of human mitochondrial ferritin. *Biochim. Biophys. Acta - Mol. Basis Dis.* **1782,** 90–98 (2008).

58. Adinolfi, S., Trifuoggi, M., Politou, a S., Martin, S. & Pastore, a. A structural approach to understanding the iron-binding properties of phylogenetically different frataxins. *Hum. Mol. Genet.* **11,** 1865–1877 (2002).

59. Aloria, K., Schilke, B., Andrew, A. & Craig, E. A. Iron-induced oligomerization of yeast frataxin homologue Yfh1 is dispensable in vivo. *EMBO Rep.* **5,** 1096–1101 (2004).

60. Levi, S., Corsi, B., Bosisio, M., Invernizzi, R., Volz, A., Sanford, D., *et al.* A Human Mitochondrial Ferritin Encoded by an Intronless Gene. *J. Biol. Chem.* **276,** 24437–24440 (2001).

61. Campanella, A., Isaya, G., O'Neill, H. A., Santambrogio, P., Cozzi, A., Arosio, P., *et al.* The expression of human mitochondrial ferritin rescues respiratory function in frataxin-deficient yeast. *Hum. Mol. Genet.* **13,** 2279–2288 (2004).

62. Lange, H., Kispal, G. & Lill, R. Mechanism of iron transport to the site of heme synthesis inside yeast mitochondria. *J. Biol. Chem.* **274,** 18989–18996 (1999).

63. Shaw, G. C., Cope, J. J., Li, L., Corson, K., Hersey, C., Ackermann, G. E., *et al.* Mitoferrin is essential for erythroid iron assimilation. *Nature* **440,** 96–100 (2006).

64. Lill, R. Function and biogenesis of iron-sulphur proteins. *Nature* **460,** 831–838 (2009).

65. Gozzelino, R. & Arosio, P. Iron homeostasis in health and disease. *International Journal of Molecular Sciences* **17,** 2–14 (2016).

66. Arosio, P., Ingrassia, R. & Cavadini, P. Ferritins: A family of molecules for iron storage, antioxidation and more. *Biochimica et Biophysica Acta - General Subjects* **1790,** 589–599 (2009).

67. Santambrogio, P., Biasiotto, G., Sanvito, F., Olivieri, S., Arosio, P. & Levi, S. Mitochondrial ferritin expression in adult mouse tissues. *J Histochem Cytochem* **55,** 1129–1137 (2007).

68. Huang, M. L.-H., Lane, D. J. R. & Richardson, D. R. Mitochondrial Mayhem: The Mitochondrion as a Modulator of Iron Metabolism and Its Role in Disease. *Antioxid. Redox Signal.* **15,** 3003–3019 (2011).

69. Park, S., Gakh, O., O'Neill, H. A., Mangravita, A., Nichol, H., Ferreira, G. C., *et al.* Yeast frataxin sequentially chaperones and stores iron by coupling protein assembly with iron oxidation. *J. Biol. Chem.* **278,** 31340–31351 (2003).

70. Huang, M. L.-H., Becker, E. M., Whitnall, M., Rahmanto, Y. S., Ponka, P. & Richardson, D. R. Elucidation of the mechanism of mitochondrial iron loading in Friedreich's ataxia by analysis of a mouse mutant. *Proc. Natl. Acad. Sci.* **106,** 16381–16386 (2009).

71. Puccio, H., Simon, D., Cossée, M., Criqui-Filipe, P., Tiziano, F., Melki, J., *et al.* Mouse models for Friedreich ataxia exhibit cardiomyopathy, sensory nerve defect and Fe-S enzyme deficiency followed by intramitochondrial iron deposits. *Nat. Genet.* **27,** 181–186 (2001).

72. Mühlenhoff, U., Richhardt, N., Ristow, M., Kispal, G. & Lill, R. The yeast frataxin homolog Yfh1p plays a specific role in the maturation of cellular Fe/S proteins. *Hum. Mol. Genet.* **11,** 2025–2036 (2002).

73. Gerber, J., Mühlenhoff, U. & Lill, R. An interaction between frataxin and Isu1/Nfs1 that is crucial for Fe/S cluster synthesis on Isu1. *EMBO Rep.* **4,** 906–911 (2003).

74. Wang, T. & Craig, E. A. Binding of yeast frataxin to the scaffold for Fe-S cluster biogenesis, Isu. *J. Biol. Chem.* **283,** 12674–12679 (2008).

75. Yoon, T. & Cowan, J. A. Iron-sulfur cluster biosynthesis. Characterization of frataxin as an iron donor for

assembly of [2Fe-2S] clusters in ISU-type proteins. *J. Am. Chem. Soc.* **125,** 6078–6084 (2003).

76. Yoon, T. & Cowan, J. A. Frataxin-mediated iron delivery to ferrochelatase in the final step of heme biosynthesis. *J. Biol. Chem.* **279,** 25943–25946 (2004).

77. Abbruzzese, G., Cossu, G., Balocco, M., Marchese, R., Murgia, D., Melis, M., *et al.* A pilot trial of deferiprone for neurodegeneration with brain iron accumulation. *Haematologica* **96,** 1708–1711 (2011).

78. Becker, E. M., Greer, J. M., Ponka, P. & Richardson, D. R. Erythroid differentiation and protoporphyrin IX down-regulate frataxin expression in Friend cells: Characterization of frataxin expression compared to molecules involved in iron metabolism and hemoglobinization. *Blood* **99,** 3813–3822 (2002).

79. Ponka, P. Tissue-specific regulation of iron metabolism and heme synthesis: distinct control mechanisms in erythroid cells. *Blood* **89,** 1–25 (1997).

80. Jauslin, M. L., Wirth, T., Meier, T. & Schoumacher, F. A cellular model for Friedreich Ataxia reveals small-molecule glutathione peroxidase mimetics as novel treatment strategy. *Hum. Mol. Genet.* **11,** 3055–3063 (2002).

81. Auchère, F., Santos, R., Planamente, S., Lesuisse, E. & Camadro, J. M. Glutathione-dependent redox status of frataxin-deficient cells in a yeast model of Friedreich's ataxia. *Hum. Mol. Genet.* **17,** 2790–2802 (2008).

82. Poburski, D. D., Boerner, J. B., Koenig, M., Ristow, M. & Thierbach, R. R. Time-resolved functional analysis of acute impairment of frataxin expression in an inducible cell model of Friedreich ataxia. *Biol. Open* **5,** 654–661 (2016).

83. D'Oria, V., Petrini, S., Travaglini, L., Priori, C., Piermarini, E., Petrillo, S., *et al.* Frataxin deficiency leads to reduced expression and impaired translocation of NF-E2-Related factor (Nrf2) in cultured motor neurons. *Int. J. Mol. Sci.* **14,** 7853–7865 (2013).

84. Abeti, R., Parkinson, M. H., Hargreaves, I. P., Angelova, P. R., Sandi, C., Pook, M. A., *et al.* 'Mitochondrial energy imbalance and lipid peroxidation cause cell death in Friedreich's ataxia'. *Cell Death Dis.* **7,** e2237 (2016).

85. Veatch, J. R., McMurray, M. A., Nelson, Z. W. & Gottschling, D. E. Mitochondrial Dysfunction Leads to Nuclear Genome Instability via an Iron-Sulfur Cluster Defect. *Cell* **137,** 1247–1258 (2009).

86. Karthikeyan, G., Santos, J. H., Graziewicz, M. A., Copeland, W. C., Isaya, G., Van Houten, B., *et al.* Reduction in frataxin causes progressive accumulation of mitochondrial damage. *Hum. Mol. Genet.* **12,** 3331–3342 (2003).

87. Koeppen, A. H., Morral, J. A., Davis, A. N., Qian, J., Petrocine, S. V, Knutson, M. D., *et al.* The dorsal root ganglion in Friedreich's ataxia. *Acta Neuropathol.* **118,** 763–776 (2009).

88. Corben, L. A., Georgiou-Karistianis, N., Bradshaw, J. L., Evans-Galea, M. V., Churchyard, A. J. & Delatycki, M. B. Characterising the neuropathology and neurobehavioural phenotype in friedreich ataxia a systematic review. *Advances in Experimental Medicine and Biology* **769,** 169–184 (2012).

89. Ramirez, R. L., Qian, J., Santambrogio, P., Levi, S. & Koeppen, A. H. Relation of cytosolic iron excess to cardiomyopathy of friedreich's ataxia. *Am. J. Cardiol.* **110,** 1820–1827 (2012).

90. Payne, R. M. & Wagner, G. R. Cardiomyopathy in Friedreich ataxia: Clinical findings and research. in *Journal of Child Neurology* **27,** 1179–1186 (2012).

91. Ramirez, R. L., Becker, A. B., Mazurkiewicz, J. E., Feustel, P. J., Gelman, B. B. & Koeppen, A. H. Pathology of Intercalated Discs in Friedreich Cardiomyopathy. *Journal of the American College of Cardiology* **66,** 1739–1740 (2015).

92. Pandolfo, M. in *Genetic Instabilities and Neurological Diseases* 277–296 (2006).

93. Friedreich ataxia. *Genetics home reference* Available at: https://ghr.nlm.nih.gov/condition/friedreich-ataxia. (Accessed: 25th December 2017)

94. Lecocq, C., Charles, P., Azulay, J. P., Meissner, W., Rai, M., N'Guyen, K., *et al.* Delayed-onset Friedreich's ataxia revisited. *Mov. Disord.* **31,** 62–69 (2016).

95. Dürr, A., Cossee, M., Agid, Y., Campuzano, V., Mignard, C., Penet, C., *et al.* Clinical and genetic abnormalities in patients with Friedreich's ataxia. *N. Engl. J. Med.* **335,** 1169–1175 (1996).

96. McDaniel, D. O., Keats, B., Vedanarayanan, V. V. & Subramony, S. H. Sequence variation in GAA repeat expansions may cause differential penotype display in friedreich's ataxia. *Mov. Disord.* **16,** 1153–1158 (2001).

97. Filla, A., De Michele, G., Cavalcanti, F., Pianese, L., Monticelli, A., Campanella, G., *et al.* The Relationship between Trinucleotide (GAA) Repeat Length and Clinical Features in Friedreich Ataxia. *Am. J. Hum. Genet* **59,** 554–560 (1996).

98. Mateo, I., Llorca, J., Volpini, V., Corral, J., Berciano, J. & Combarros, O. Expanded GAA repeats and clinical variation in Friedreich's ataxia. *Acta Neurol. Scand.* **109,** 75–78 (2004).

99. Ribaï, P., Pousset, F., Tanguy, M.-L., Rivaud-Pechoux, S., Le Ber, I., Gasparini, F., *et al.* Neurological, Cardiological, and Oculomotor Progression in 104 Patients With Friedreich Ataxia During Long-term Follow-up. *Arch. Neurol.* **64,** 558 (2007).

100. Santoro, L., Perretti, A., Lanzillo, B., Coppola, G., De Joanna, G., Manganelli, F., *et al.* Influence of GAA expansion size and disease duration on central nervous system impairment in Friedreich's ataxia: Contribution to the understanding of the pathophysiology of the disease. *Clin. Neurophysiol.* **111,** 1023–1030 (2000).

101. Pianese, L., Turano, M., Lo Casale, M. S., De Biase, I., Giacchetti, M., Monticelli, A., *et al.* Real time PCR quantification of frataxin mRNA in the peripheral blood leucocytes of Friedreich ataxia patients and carriers. *J. Neurol. Neurosurg. Psychiatry* **75,** 1061–1063 (2004).

102. Delatycki, M. B., Paris, D. B., Gardner, R. J., Nicholson, G. a, Nassif, N., Storey, E., *et al.* Clinical and genetic study of Friedreich ataxia in an Australian population. *Am. J. Med. Genet.* **87,** 168–174 (1999).

103. Bit-Avragim, N., Perrot, A., Schöls, L., Hardt, C., Kreuz, F. R., Zühlke, C., *et al.* The GAA repeat expansion in intron 1 of the frataxin gene is related to the severity of cardiac manifestation in patients with Friedreich's ataxia. *J. Mol. Med.* **78,** 626–632 (2000).

104. Pousset, F., Legrand, L., Monin, M.-L., Ewenczyk, C., Charles, P., Komajda, M., *et al.* A 22-Year Follow-up Study of Long-term Cardiac Outcome and Predictors of Survival in Friedreich Ataxia. *JAMA Neurol.* **72,** 1334–1341 (2015).

105. Alper, G. & Narayanan, V. Friedreich's ataxia. *Pediatric Neurology* **28,** 335–341 (2003).

106. Delatycki, M. B., Williamson, R. & Forrest, S. M. Friedreich ataxia: an overview. *J. Med. Genet.* **37,** 1–8 (2000).

107. Delatycki, M. B. & Corben, L. A. Clinical features of Friedreich ataxia. in *Journal of Child Neurology* **27,** 1133–1137 (2012).

108. Filla, A., DeMichele, G., Caruso, G., Marconi, R. & Campanella, G. Genetic data and natural history of Friedreich's disease: a study of 80 Italian patients. *J. Neurol.* **237,** 345–351 (1990).

109. McCabe, D. J. H., Ryan, F., Moore, D. P., McQuaid, S., King, M. D., Kelly, A., *et al.* Typical Friedreich's ataxia without GAA expansions and GAA expansions without typical Friedreich's ataxia. *J. Neurol.* **247,** 346–355 (2000).

110. Furman, J. M., Perlman, S. & Baloh, R. W. Eye movements in Friedreich's ataxia. *Arch. Neurol.* **40,** 343–6 (1983).

111. Fahey, M. C., Cremer, P. D., Aw, S. T., Millist, L., Todd, M. J., White, O. B., *et al.* Vestibular, saccadic and fixation abnormalities in genetically confirmed Friedreich ataxia. *Brain* **131,** 1035–1045 (2008).

112. Fortuna, F., Barboni, P., Liguori, R., Valentino, M. L., Savini, G., Gellera, C., *et al.* Visual system involvement in patients with Friedreich's ataxia. *Brain* **132,** 116–123 (2009).

113. Folker, J. E., Murdoch, B. E., Cahill, L. M., Delatycki, M. B., Corben, L. A. & Vogel, A. P. Kinematic analysis of lingual movements during consonant productions in dysarthric speakers with Friedreich's ataxia: A case-by-case analysis. *Clin. Linguist. Phon.* **25,** 66–79 (2011).

114. Folker, J. E., Murdoch, B. E., Rosen, K. M., Cahill, L. M., Delatycki, M. B., Corben, L. A., *et al.* Differentiating profiles of speech impairments in Friedreich's ataxia: a perceptual and instrumental approach. *Int. J. Lang. Commun. Disord.* **47,** 65–76 (2012).

115. Rance, G., Fava, R., Baldock, H., Chong, A., Barker, E., Corben, L., *et al.* Speech perception ability in individuals with Friedreich ataxia. *Brain* **131,** 2002–2012 (2008).

116. Satya-Murti, S., Cacace, A. & Hanson, P. Auditory dysfunction in Friedreich ataxia: Result of spiral ganglion degeneration. *Neurology* **30,** 1047–1047 (1980).

117. Lopez-Diaz-de-Leon, E., Silva-Rojas, A., Ysunza, A., Amavisca, R. & Rivera, R. Auditory neuropathy in Friedreich ataxia. A report of two cases. *Int. J. Pediatr. Otorhinolaryngol.* **67,** 641–648 (2003).

118. Rance, G., Corben, L. A., Du Bourg, E., King, A. & Delatycki, M. B. Successful treatment of auditory perceptual disorder in individuals with Friedreich ataxia. *Neuroscience* **171,** 552–555 (2010).

119. Rance, G., Ryan, M. M., Carew, P., Corben, L. A., Yiu, E., Tan, J., *et al.* Binaural speech processing in individuals with auditory neuropathy. *Neuroscience* **226,** 227–235 (2012).

120. Vezina, J. G., Bouchard, J. P. & Bouchard, R. Urodynamic Evaluation of Patients with Hereditary Ataxias. *Can. J. Neurol. Sci. / J. Can. des Sci. Neurol.* **9,** 127–129 (1982).

121. Nardulli, R., Monitillo, V., Losavio, E., Fiore, P., Nicolardi, G. & Megna, G. Urodynamic evaluation of 12 ataxic subjects: Neurophysiopathologic considerations. *Funct. Neurol.* **7,** 223–225 (1992).

122. Corben, L. A., Georgiou-Karistianis, N., Fahey, M. C., Storey, E., Churchyard, A., Horne, M., *et al.* Towards an understanding of cognitive function in Friedreich ataxia. *Brain Research Bulletin* **70,** 197–202 (2006).

123. Mantovan, M. C., Martinuzzi, A., Squarzanti, F., Bolla, A., Silvestri, I., Liessi, G., *et al.* Exploring mental status in Friedreich's ataxia: A combined neuropsychological, behavioral and neuroimaging study. *European Journal of Neurology* **13,** 827–835 (2006).

124. Nieto, A., Correia, R., de Nobrega, E., Monton, F., Hess, S. & Barroso, J. Cognition in Friedreich ataxia. *Cerebellum* **11,** 834–844 (2012).

125. Corben, L. A., Tai, G., Wilson, C., Collins, V., Churchyard, A. J. & Delatycki, M. B. A comparison of three measures of upper limb function in Friedreich ataxia. *J. Neurol.* **257,** 518–523 (2010).

126. Corben, L. A., Georgiou-Karistianis, N., Bradshaw, J. L., Hocking, D. R., Churchyard, A. J. & Delatycki, M. B. The Fitts task reveals impairments in planning and online control of movement in Friedreich ataxia: reduced cerebellar-cortico connectivity? *Neuroscience* **192,** 382–390 (2011).

127. Klopper, F., Delatycki, M. B., Corben, L. A., Bradshaw, J. L., Rance, G. & Georgiou-Karistianis, N. The test of everyday attention reveals significant sustained volitional attention and working memory deficits in friedreich ataxia. *J. Int. Neuropsychol. Soc.* **17,** 196–200 (2011).

128. Flood, M. K. & Perlman, S. L. The mental status of patients with Friedreich's ataxia. *J. Neurosci. Nurs.* **19,** 251–255 (1987).

129. Labelle, H., Tohmé, S., Duhaime, M. & Allard, P. Natural history of scoliosis in Friedreich's ataxia. *J. Bone Joint Surg. Am.* **68,** 564–572 (1986).

130. Milbrandt, T. A., Kunes, J. R. & Karol, L. A. Friedreich's ataxia and scoliosis: The experience at two institutions. *J. Pediatr. Orthop.* **28,** 234–238 (2008).

131. Koeppen, A. H., Becker, A. B., Qian, J. & Feustel, P. J. Friedreich Ataxia: Hypoplasia of Spinal Cord and

Dorsal Root Ganglia. *J. Neuropathol. Exp. Neurol.* **76,** 101–108 (2017).

132. Delatycki, M. B., Holian, A., Corben, L., Rawicki, H. B., Blackburn, C., Hoare, B., *et al.* Surgery for equinovarus deformity in Friedreich's ataxia improves mobility and independence. *Clin. Orthop. Relat. Res.* 138–141 (2005). doi:10.1097/01.blo.0000150339.74041.0e

133. Ran, S., Abeti, R. & Giunti, P. in *Diabetes Associated with Single Gene Defects and Chromosomal Abnormalities* **25,** 172–181 (2017).

134. Finocchiaro, G., Baio, G., Micossi, P., Pozza, G. & di Donato, S. Glucose metabolism alterations in Friedreich's ataxia. *Neurology* **38,** 1292–1296 (1988).

135. Schoenle, E. J., Boltshauser, E. J., Baekkeskov, S., Olsson, M. L., Torresani, T. & von Felten, A. Preclinical and manifest diabetes mellitus in young patients with friedreich's ataxia: no evidence of immune process behind the islet cell destruction. *Diabetologia* **32,** 378–381 (1989).

136. Weidemann, F., Störk, S., Liu, D., Hu, K., Herrmann, S., Ertl, G., *et al.* Cardiomyopathy of Friedreich ataxia. *Journal of Neurochemistry* **126,** 88–93 (2013).

137. Casazza, F. & Morpurgo, M. The varying evolution of Friedreich's ataxia cardiomyopathy. *Am. J. Cardiol.* **77,** 895–898 (1996).

138. Weidemann, F., Rummey, C., Bijnens, B., Störk, S., Jasaityte, R., Dhooge, J., *et al.* The heart in Friedreich ataxia: Definition of cardiomyopathy, disease severity, and correlation with neurological symptoms. *Circulation* **125,** 1626–1634 (2012).

139. Dutka, D. P., Donnelly, J. E., Nihoyannopoulos, P., Oakley, C. M. & Nunez, D. J. Marked variation in the cardiomyopathy associated with Friedreich's ataxia. *Heart* **81,** 141–147 (1999).

140. Schadt, K. A., Friedman, L. S., Regner, S. R., Mark, G. E., Lynch, D. R. & Lin, K. Y. Cross-sectional analysis of electrocardiograms in a large heterogeneous cohort of Friedreich ataxia subjects. in *Journal of Child Neurology* **27,** 1187–1192 (2012).

141. Lynch, D. R., Regner, S. R., Schadt, K. A., Friedman, L. S., Lin, K. Y. & St John Sutton, M. G. Management and therapy for cardiomyopathy in Friedreich's ataxia. *Expert Rev. Cardiovasc. Ther.* **10,** 767–777 (2012).

142. Bourke, T. & Keane, D. Friedreich's Ataxia: A review from a cardiology perspective. *Irish Journal of Medical Science* **180,** 799–805 (2011).

143. Kipps, A., Alexander, M., Colan, S. D., Gauvreau, K., Smoot, L., Crawford, L., *et al.* The longitudinal course of cardiomyopathy in Friedreich's ataxia during childhood. *Pediatr. Cardiol.* **30,** 306–310 (2009).

144. Rajagopalan, B., Francis, J. M., Cooke, F., Korlipara, L. V. P., Blamire, A. M., Schapira, A. H. V, *et al.* Analysis of the factors influencing the cardiac phenotype in Friedreich's ataxia. *Mov. Disord.* **25,** 846–852 (2010).

145. Schöls, L., Amoiridis, G., Przuntek, H., Frank, G., Epplen, J. T. & Epplen, C. Friedreich's ataxia. Revision of the phenotype according to molecular genetics. *Brain* **120,** 2131–2140 (1997).

146. De Michele, G., Perrone, F., Filla, A., Mirante, E., Giordano, M., De Placido, S., *et al.* Age of onset, sex, and cardiomyopathy as predictors of disability and survival in Friedreich's disease: A retrospective study on 119 patients. *Neurology* **47,** 1260–1264 (1996).

147. Fahey, M. C., Corben, L., Collins, V., Churchyard, A. J. & Delatycki, M. B. How is disease progress in Friedreich's ataxia best measured? A study of four rating scales. *J. Neurol. Neurosurg. Psychiatry* **78,** 411–413 (2007).

148. Burk, K., Malzig, U., Wolf, S., Heck, S., Dimitriadis, K., Schmitz-Hubsch, T., *et al.* Comparison of three clinical rating scales in Friedreich ataxia (FRDA). *Mov. Disord.* **24,** 1779–1784 (2009).

149. Friedman, L. S., Farmer, J. M., Perlman, S., Wilmot, G., Gomez, C. M., Bushara, K. O., *et al.* Measuring the rate of progression in Friedreich ataxia: implications for clinical trial design. *Mov. Disord.* **25,** 426–432 (2010).

150. Andermann, E., Remillard, G. M., Goyer, C., Blitzer, L., Andermann, F. & Barbeau, A. Genetic and Family Studies in Friedreich's Ataxia. *Can. J. Neurol. Sci. / J. Can. des Sci. Neurol.* **3,** 287–301 (1976).

151. Leone, M., Rocca, W. A., Rosso, M. G., Mantel, N., Schoenberg, B. S. & Schiffer, D. Friedreich's disease: survival analysis in an Italian population. *Neurology* **38,** 1433–8 (1988).

152. Tsou, A. Y., Paulsen, E. K., Lagedrost, S. J., Perlman, S. L., Mathews, K. D., Wilmot, G. R., *et al.* Mortality in Friedreich ataxia. *J. Neurol. Sci.* **307,** 46–49 (2011).

153. Abrahao, A., Pedroso, J. L., Braga-Neto, P., Bor-Seng-Shu, E., de Carvalho Aguiar, P. & Barsottini, O. G. P. Milestones in Friedreich ataxia: more than a century and still learning. *Neurogenetics* **16,** 151–160 (2015).

154. istituto Neurologico Carlo Besta, F., Biochimica Genetica, U., Schulz, J. B., Boesch, S., Bürk, K., Dürr, A., *et al.* Diagnosis and treatment of Friedreich ataxia: a European perspective. *Nat. Rev. Neurol* **5,** 222–234 (2009).

155. Sommerville, R. B., Vincenti, M. G., Winborn, K., Casey, A., Stitziel, N. O., Connolly, A. M., *et al.* Diagnosis and management of adult hereditary cardio-neuromuscular disorders: A model for the multidisciplinary care of complex genetic disorders. *Trends Cardiovasc. Med.* **27,** 51–58 (2017).

156. Corben, L. A., Lynch, D., Pandolfo, M., Schulz, J. B. & Delatycki, M. B. Consensus clinical management guidelines for Friedreich ataxia. *Orphanet J. Rare Dis.* **9,** 184 (2014).

157. Farmer, J. FRDA treatment pipeline. (2016). Available at: http://www.curefa.org/pipeline. (Accessed: 8th January 2018)

158. Strawser, C. J., Schadt, K. A. & Lynch, D. R. Therapeutic approaches for the treatment of Friedreich's ataxia. *Expert Review of Neurotherapeutics* **14,** 949–957 (2014).

159. Suno, M. & Nagaoka, A. Inhibition of mitochondrial swelling and lipid peroxidation by a novel compound,

idebenone (CV-2619). *Japanese Pharmacology and Therapeutics* **13,** 277–282 (1985).

160. Parkinson, M. H., Schulz, J. B. & Giunti, P. Co-enzyme Q10 and idebenone use in Friedreich's ataxia. *J. Neurochem.* **126,** 125–141 (2013).

161. Strawser, C., Schadt, K., Hauser, L., McCormick, A., Wells, M., Larkindale, J., *et al.* Pharmacological therapeutics in Friedreich ataxia: the present state. *Expert Rev. Neurother.* **17,** 895–907 (2017).

162. Myers, L., Farmer, J. M., Wilson, R. B., Friedman, L., Tsou, A., Perlman, S. L., *et al.* Antioxidant use in Friedreich ataxia. *J. Neurol. Sci.* **267,** 174–176 (2008).

163. Rustin, P., Von Kleist-Retzow, J. C., Chantrel-Groussard, K., Sidi, D., Munnich, A. & Rötig, A. Effect of idebenone on cardiomyopathy in Friedreich's ataxia: A preliminary study. *Lancet* **354,** 477–479 (1999).

164. Buyse, G., Mertens, L., Di Salvo, G., Matthijs, I., Weidemann, F., Eyskens, B., *et al.* Idebenone treatment in Friedreich's ataxia: neurological, cardiac, and biochemical monitoring. *Neurology* **60,** 1679–1681 (2003).

165. Lagedrost, S. J., Sutton, M. S. J., Cohen, M. S., Satou, G. M., Kaufman, B. D., Perlman, S. L., *et al.* Idebenone in Friedreich ataxia cardiomyopathy-results from a 6-month phase III study (IONIA). *Am. Heart J.* **161,** 639–645.e1 (2011).

166. Artuch, R., Aracil, A., Mas, A., Colomé, C., Rissech, M., Monrós, E., *et al.* Friedreich's ataxia: Idebenone treatment in early stage patients. *Neuropediatrics* **33,** 190–193 (2002).

167. Pineda, M., Arpa, J., Montero, R., Aracil, A., Domínguez, F., Galván, M., *et al.* Idebenone treatment in paediatric and adult patients with Friedreich ataxia: Long-term follow-up. *Eur. J. Paediatr. Neurol.* **12,** 470–475 (2008).

168. Lynch, D. R., Perlman, S. L. & Meier, T. A phase 3, double-blind, placebo-controlled trial of idebenone in friedreich ataxia. *Arch. Neurol.* **67,** 941–947 (2010).

169. Lodi, R., Hart, P. E., Rajagopalan, B., Taylor, D. J., Crilley, J. G., Bradley, J. L., *et al.* Antioxidant treatment improves in vivo cardiac and skeletal muscle bioenergetics in patients with Friedreich's ataxia. *Ann. Neurol.* **49,** 590–596 (2001).

170. Hart, P. E., Lodi, R., Rajagopalan, B., Bradley, J. L., Crilley, J. G., Turner, C., *et al.* Antioxidant treatment of patients with Friedreich ataxia: Four-year follow-up. *Arch. Neurol.* **62,** 621–626 (2005).

171. Lynch, D. R., Willi, S. M., Wilson, R. B., Cotticelli, M. G., Brigatti, K. W., Deutsch, E. C., *et al.* A0001 in Friedreich ataxia: biochemical characterization and effects in a clinical trial. *Mov. Disord.* **27,** 1026–1033 (2012).

172. Breuer, W., Ermers, M. J. J., Pootrakul, P., Abramov, A., Hershko, C. & Cabantchik, Z. I. Desferrioxamine-chelatable iron, a component of serum non-transferrin-bound iron, used for assessing chelation therapy. *Blood* **97,** 792–798 (2001).

173. Koeppen, A. H., Ramirez, R. L., Becker, A. B., Bjork, S. T., Levi, S., Santambrogio, P., *et al.* The pathogenesis of cardiomyopathy in Friedreich ataxia. *PLoS One* **10,** e0116396 (2015).

174. Pandolfo, M. & Hausmann, L. Deferiprone for the treatment of Friedreich's ataxia. *Journal of Neurochemistry* **126,** 142–146 (2013).

175. Al-Refaie, F. N., Sheppard, L. N., Nortey, P., Wonke, B. & Hoffbrand, A. V. Pharmacokinetics of the oral iron chelator deferiprone (L1) in patients with iron overload. *Br. J. Haematol.* **89,** 403–408 (1995).

176. Velasco-Sánchez, D., Aracil, A., Montero, R., Mas, A., Jiménez, L., O'Callaghan, M., *et al.* Combined therapy with idebenone and deferiprone in patients with Friedreich's ataxia. *Cerebellum* **10,** 1–8 (2011).

177. Arpa, J., Sanz-Gallego, I., Rodriguez-de-Rivera, F. J., Dominguez-Melcon, F. J., Prefasi, D., Oliva-Navarro, J., *et al.* Triple therapy with deferiprone, idebenone and riboflavin in Friedreich's ataxia - open-label trial. *Acta Neurol. Scand.* **129,** 32–40 (2014).

178. Coppola, G., Marmolino, D., Lu, D., Wang, Q., Cnop, M., Rai, M., *et al.* Functional genomic analysis of frataxin deficiency reveals tissue-specific alterations and identifies the PPARgamma pathway as a therapeutic target in Friedreich's ataxia. *Hum. Mol. Genet.* **18,** 2452–2461 (2009).

179. Marmolino, D., Manto, M., Acquaviva, F., Vergara, P., Ravella, A., Monticelli, A., *et al.* PGC-1alpha down-regulation affects the antioxidant response in Friedreich's ataxia. *PLoS One* **5,** e10025 (2010).

180. Holmström, K. M., Kostov, R. V. & Dinkova-Kostova, A. T. The multifaceted role of Nrf2 in mitochondrial function. *Current Opinion in Toxicology* **2,** 80–91 (2017).

181. Probst, B. L., Trevino, I., McCauley, L., Bumeister, R., Dulubova, I., Wigley, W. C., *et al.* RTA 408, a novel synthetic triterpenoid with broad anticancer and anti-inflammatory activity. *PLoS One* **10,** (2015).

182. Chen, P.-C., Vargas, M. R., Pani, A. K., Smeyne, R. J., Johnson, D. A., Kan, Y. W., *et al.* Nrf2-mediated neuroprotection in the MPTP mouse model of Parkinson's disease: Critical role for the astrocyte. *Proc. Natl. Acad. Sci. U. S. A.* **106,** 2933–8 (2009).

183. Reata Pharmaceuticals, Inc. Announces Positive Data From Part One of Moxie Trial of Omaveloxolone for Friedreich's Ataxia. (2017). Available at: http://investors.reatapharma.com/phoenix.zhtml?c=254306&p=irol-newsArticle&ID=2278245. (Accessed: 9th January 2018)

184. Yiu, E. M., Tai, G., Peverill, R. E., Lee, K. J., Croft, K. D., Mori, T. A., *et al.* An open-label trial in Friedreich ataxia suggests clinical benefit with high-dose resveratrol, without effect on frataxin levels. *J. Neurol.* **262,** 1344–1353 (2015).

185. Smoliga, J. M. & Blanchard, O. Enhancing the delivery of resveratrol in humans: If low bioavailability is the problem, what is the solution? *Molecules* **19,** 17154–17172 (2014).

186. Sturm, B., Stupphann, D., Kaun, C., Boesch, S., Schranzhofer, M., Wojta, J., *et al.* Recombinant human erythropoietin: Effects on frataxin expression in vitro. *Eur. J. Clin. Invest.* **35,** 711–717 (2005).

187. Boesch, S., Sturm, B., Hering, S., Scheiber-Mojdehkar, B., Steinkellner, H., Goldenberg, H., *et al.* Neurological effects of recombinant human erythropoietin in Friedreich's ataxia: a clinical pilot trial. *Mov. Disord.* **23,** 1940–1944 (2008).

188. Sacca, F., Piro, R., De Michele, G., Acquaviva, F., Antenora, A., Carlomagno, G., *et al.* Epoetin alfa increases frataxin production in Friedreich's ataxia without affecting hematocrit. *Mov. Disord.* **26,** 739–742 (2011).

189. Nachbauer, W., Hering, S., Seifert, M., Steinkellner, H., Sturm, B., Scheiber-Mojdehkar, B., *et al.* Effects of erythropoietin on frataxin levels and mitochondrial function in Friedreich ataxia--a dose-response trial. *Cerebellum* **10,** 763–769 (2011).

190. Mariotti, C., Nachbauer, W., Panzeri, M., Poewe, W., Taroni, F. & Boesch, S. Erythropoietin in Friedreich ataxia. *J. Neurochem.* **126,** 80–87 (2013).

191. Boesch, S., Nachbauer, W., Mariotti, C., Sacca, F., Filla, A., Klockgether, T., *et al.* Safety and tolerability of carbamylated erythropoietin in Friedreich's ataxia. *Mov. Disord.* **29,** 935–939 (2014).

192. Tomassini, B., Arcuri, G., Fortuni, S., Sandi, C., Ezzatizadeh, V., Casali, C., *et al.* Interferon gamma upregulates frataxin and corrects the functional deficits in a Friedreich ataxia model. *Hum. Mol. Genet.* **21,** 2855–2861 (2012).

193. Seyer, L., Greeley, N., Foerster, D., Strawser, C., Gelbard, S., Dong, Y., *et al.* Open-label pilot study of interferon gamma-1b in Friedreich ataxia. *Acta Neurol. Scand.* **132,** 7–15 (2015).

194. Wells, M., Seyer, L., Schadt, K. & Lynch, D. R. IFN-gamma for Friedreich ataxia: present evidence. *Neurodegener. Dis. Manag.* **5,** 497–504 (2015).

195. Marcotulli, C., Fortuni, S., Arcuri, G., Tomassini, B., Leonardi, L., Pierelli, F., *et al.* GIFT-1, a phase IIa clinical trial to test the safety and efficacy of IFNgamma administration in FRDA patients. *Neurol. Sci. Off. J. Ital. Neurol. Soc. Ital. Soc. Clin. Neurophysiol.* **37,** 361–364 (2016).

196. Safety, Tolerability and Efficacy of ACTIMMUNE® Dose Escalation in Friedreich's Ataxia (STEADFAST). Available at: https://www.clinicaltrials.gov/ct2/show/NCT02415127. (Accessed: 9th January 2017)

197. Horizon Pharma: Horizon Pharma plc Announces Topline Results from Phase 3 Study of ACTIMMUNE® (interferon gamma-1b) in Friedreich's Ataxia. Available at: http://ir.horizon-pharma.com/releasedetail.cfm?ReleaseID=1003338. (Accessed: 9th January 2018)

198. Koeppen, A. H., Ramirez, R. L., Becker, A. B. & Mazurkiewicz, J. E. Dorsal root ganglia in Friedreich ataxia: satellite cell proliferation and inflammation. *Acta Neuropathol. Commun.* **4,** 46 (2016).

199. Michael, S., Petrocine, S. V., Qian, J., Lamarche, J. B., Knutson, M. D., Garrick, M. D., *et al.* Iron and iron-responsive proteins in the cardiomyopathy of Friedreich's ataxia. *Cerebellum* **5,** 257–267 (2006).

200. Shinnick, J. E., Isaacs, C. J., Vivaldi, S., Schadt, K. & Lynch, D. R. Friedreich Ataxia and nephrotic syndrome: a series of two patients. *BMC Neurol.* **16,** 3 (2016).

201. Methylprednisolone Treatment of Friedreich Ataxia. Available at: https://clinicaltrials.gov/ct2/show/NCT02424435. (Accessed: 9th January 2018)

202. Sakamoto, N., Ohshima, K., Montermini, L., Pandolfo, M. & Wells, R. D. Sticky DNA, a Self-associated Complex Formed at Long GAA·TTC Repeats in Intron 1 of the Frataxin Gene, Inhibits Transcription. *J. Biol. Chem.* **276,** 27171–27177 (2001).

203. Savellev, A., Everett, C., Sharpe, T., Webster, Z. & Festenstein, R. DNA triplet repeats mediate heterochromatin-protein-1-sensitive variegated gene silencing. *Nature* **422,** 909–913 (2003).

204. Greene, E., Mahishi, L., Entezam, A., Kumari, D. & Usdin, K. Repeat-induced epigenetic changes in intron 1 of the frataxin gene and its consequences in Friedreich ataxia. *Nucleic Acids Res.* **35,** 3383–3390 (2007).

205. Rai, M., Soragni, E., Chou, C. J., Barnes, G., Jones, S., Rusche, J. R., *et al.* Two new pimelic diphenylamide HDAC inhibitors induce sustained frataxin upregulation in cells from Friedreich's ataxia patients and in a mouse model. *PLoS One* **5,** e8825 (2010).

206. Herman, D., Jenssen, K., Burnett, R., Soragni, E., Perlman, S. L. & Gottesfeld, J. M. Histone deacetylase inhibitors reverse gene silencing in Friedreich's ataxia. *Nat. Chem. Biol.* **2,** 551–558 (2006).

207. Rai, M., Soragni, E., Jenssen, K., Burnett, R., Herman, D., Coppola, G., *et al.* HDAC inihibitors correct frataxin deficiency in a Friedreich ataxia mouse model. *PLoS One* **3,** (2008).

208. Elgin, S. C. R. & Grewal, S. I. S. Heterochromatin: silence is golden. *Curr. Biol.* **13,** R895–R898 (2003).

209. Soragni, E. & Gottesfeld, J. M. Translating HDAC inhibitors in Friedreich's ataxia. *Expert Opin. orphan drugs* **4,** 961–970 (2016).

210. de Ruijter, A. J. M., van Gennip, A. H., Caron, H. N., Kemp, S. & van Kuilenburg, A. B. P. Histone deacetylases (HDACs): characterization of the classical HDAC family. *Biochem. J.* **370,** 737–49 (2003).

211. Denu, J. M. The Sir2 family of protein deacetylases. *Current Opinion in Chemical Biology* **9,** 431–440 (2005).

212. Sharma, S. & Taliyan, R. Targeting Histone Deacetylases: A Novel Approach in Parkinson's Disease. *Parkinsons. Dis.* **2015,** (2015).

213. Langley, B., Gensert, J. M., Beal, M. F. & Ratan, R. R. Remodeling chromatin and stress resistance in the central nervous system: histone deacetylase inhibitors as novel and broadly effective neuroprotective agents. *Curr. Drug Targets. CNS Neurol. Disord.* **4,** 41–50 (2005).

214. Mann, B. S., Johnson, J. R., Cohen, M. H., Justice, R. & Pazdur, R. FDA approval summary: vorinostat for treatment of advanced primary cutaneous T-cell lymphoma. *Oncologist* **12,** 1247–52 (2007).

215. Xu, C., Soragni, E., Chou, C. J., Herman, D., Plasterer, H. L., Rusche, J. R., *et al.* Chemical probes identify a role for histone deacetylase 3 in Friedreich's ataxia gene silencing. *Chem. Biol.* **16,** 980–989 (2009).

216. Sandi, C., Pinto, R. M., Al-Mahdawi, S., Ezzatizadeh, V., Barnes, G., Jones, S., *et al.* Prolonged treatment with pimelic o-aminobenzamide HDAC inhibitors ameliorates the disease phenotype of a Friedreich ataxia mouse model. *Neurobiol. Dis.* **42,** 496–505 (2011).

217. Marchetto, M. C., Brennand, K. J., Boyer, L. F. & Gage, F. H. Induced pluripotent stem cells (iPSCs) and neurological disease modeling: Progress and promises. *Hum. Mol. Genet.* **20,** 109–115 (2011).

218. Bellin, M., Marchetto, M. C., Gage, F. H. & Mummery, C. L. Induced pluripotent stem cells: The new patient? *Nature Reviews Molecular Cell Biology* **13,** 713–726 (2012).

219. Takahashi, K. & Yamanaka, S. Induction of Pluripotent Stem Cells from Mouse Embryonic and Adult Fibroblast Cultures by Defined Factors. *Cell* **126,** 663–676 (2006).

220. Park, I. H., Zhao, R., West, J. A., Yabuuchi, A., Huo, H., Ince, T. A., *et al.* Reprogramming of human somatic cells to pluripotency with defined factors. *Nature* **451,** 141–146 (2008).

221. Ku, S., Soragni, E., Campau, E., Thomas, E. A., Altun, G., Laurent, L. C., *et al.* Friedreich's ataxia induced pluripotent stem cells model intergenerational GAATTC triplet repeat instability. *Cell Stem Cell* **7,** 631–637 (2010).

222. Abràmoff, M. D., Magalhães, P. J. & Ram, S. J. Image processing with imageJ. *Biophotonics International* **11,** 36–41 (2004).

223. Plasterer, H. L., Deutsch, E. C., Belmonte, M., Egan, E., Lynch, D. R. & Rusche, J. R. Development of frataxin gene expression measures for the evaluation of experimental treatments in Friedreich's ataxia. *PLoS One* **8,** e63958 (2013).

224. Li, K., Besse, E. K., Ha, D., Kovtunovych, G. & Rouault, T. A. Iron-dependent regulation of frataxin expression: Implications for treatment of Friedreich ataxia. *Hum. Mol. Genet.* **17,** 2265–2273 (2008).

225. Hick, A., Wattenhofer-Donze, M., Chintawar, S., Tropel, P., Simard, J. P., Vaucamps, N., *et al.* Neurons and cardiomyocytes derived from induced pluripotent stem cells as a model for mitochondrial defects in Friedreich's ataxia. *Dis. Model. Mech.* **6,** 608–621 (2013).

226. Plasterer, H. L., Deutsch, E. C., Belmonte, M., Egan, E., Lynch, D. R. & Rusche, J. R. Development of Frataxin Gene Expression Measures for the Evaluation of Experimental Treatments in Friedreich's Ataxia. *PLoS One* **8,** (2013).

227. Jia, H., Pallos, J., Jacques, V., Lau, A., Tang, B., Cooper, A., *et al.* Histone deacetylase (HDAC) inhibitors targeting HDAC3 and HDAC1 ameliorate polyglutamine-elicited phenotypes in model systems of Huntington's disease. *Neurobiol. Dis.* **46,** 351–361 (2012).

228. Malvaez, M., McQuown, S. C., Rogge, G. A., Astarabadi, M., Jacques, V., Carreiro, S., *et al.* HDAC3-selective inhibitor enhances extinction of cocaine-seeking behavior in a persistent manner. *Proc. Natl. Acad. Sci.* **110,** 2647–2652 (2013).

229. Xu, C., Soragni, E., Chou, C. J., Herman, D., Plasterer, H. L., Rusche, J. R., *et al.* Chemical Probes Identify a Role for Histone Deacetylase 3 in Friedreich's Ataxia Gene Silencing. *Chem. Biol.* **16,** 980–989 (2009).

230. Lin, Y., Dion, V. & Wilson, J. H. Transcription promotes contraction of CAG repeat tracts in human cells. *Nat. Struct. Mol. Biol.* **13,** 179–180 (2006).

231. Ditch, S., Sammarco, M. C., Banerjee, A. & Grabczyk, E. Progressive GAA.TTC repeat expansion in human cell lines. *PLoS Genet.* **5,** e1000704 (2009).

232. Goula, A. V., Stys, A., Chan, J. P. K., Trottier, Y., Festenstein, R. & Merienne, K. Transcription Elongation and Tissue-Specific Somatic CAG Instability. *PLoS Genet.* **8,** (2012).

233. Ku, S., Soragni, E., Campau, E., Thomas, E. A., Altun, G., Laurent, L. C., *et al.* Friedreich's ataxia induced pluripotent stem cells model intergenerational GAATTC triplet repeat instability. *Cell Stem Cell* **7,** 631–637 (2010).

234. Orr, H. T. & Zoghbi, H. Y. Trinucleotide Repeat Disorders - annurev.neuro.29.051605.113042. *Annu. Rev. Neurosci.* **30,** 575–623 (2007).

235. Bidichandani, S. I., Ashizawa, T. & Patel, P. I. The GAA Triplet-Repeat Expansion in Friedreich Ataxia Interferes with Transcription and May Be Associated with an Unusual DNA Structure. *Am. J. Hum. Genet.* **62,** 111–121 (1998).

236. Menendez, L., Yatskievych, T. A., Antin, P. B. & Dalton, S. Wnt signaling and a Smad pathway blockade direct the differentiation of human pluripotent stem cells to multipotent neural crest cells. *Proc. Natl. Acad. Sci.* **108,** 19240–19245 (2011).

237. Chambers, S. M., Qi, Y., Mica, Y., Lee, G., Zhang, X. J., Niu, L., *et al.* Combined small-molecule inhibition accelerates developmental timing and converts human pluripotent stem cells into nociceptors. *Nat. Biotechnol.* **30,** 715–720 (2012).

238. Eigentler, A., Boesch, S., Schneider, R., Dechant, G. & Nat, R. Induced pluripotent stem cells from friedreich ataxia patients fail to upregulate frataxin during in vitro differentiation to peripheral sensory neurons. *Stem Cells Dev.* **22,** 3271–3282 (2013).

239. Chou, C. J., Herman, D. & Gottesfeld, J. M. Pimelic diphenylamide 106 is a slow, tight-binding inhibitor of class I histone deacetylases. *J. Biol. Chem.* **283,** 35402–35409 (2008).

240. Garcia-Arocena, D. & Hagerman, P. J. Advances in understanding the molecular basis of FXTAS. *Hum. Mol. Genet.* **19,** (2010).

241. Klein, A. F., Gasnier, E. & Furling, D. Gain of RNA function in pathological cases: Focus on myotonic dystrophy. *Biochimie* **93,** 2006–2012 (2011).

242. Soragni, E., Xu, C., Plasterer, H. L., Jacques, V., Rusche, J. R. & Gottesfeld, J. M. Rationale for the development of 2-aminobenzamide histone deacetylase inhibitors as therapeutics for Friedreich ataxia. *J. Child*

*Neurol.* **27,** 1164–1173 (2012).

243. Xu, C., Soragni, E., Jacques, V., Rusche, J. R. & Gottesfeld, J. M. Improved histone deacetylase inhibitors as therapeutics for the neurodegenerative disease Friedreich's ataxia: A new synthetic route. *Pharmaceuticals* **4,** 1578–1590 (2011).

244. Beconi, M., Aziz, O., Matthews, K., Moumne, L., O'Connell, C., Yates, D., *et al.* Oral administration of the pimelic diphenylamide HDAC inhibitor HDACi 4b is unsuitable for chronic inhibition of HDAC activity in the CNS in vivo. *PLoS One* **7,** e44498 (2012).

245. Yao, X., Anderson, D. L., Ross, S. A., Lang, D. G., Desai, B. Z., Cooper, D. C., *et al.* Predicting QT prolongation in humans during early drug development using hERG inhibition and an anaesthetized guinea-pig model. *Br. J. Pharmacol.* **154,** 1446–1456 (2008).

246. Libri, V., Yandim, C., Athanasopoulos, S., Loyse, N., Natisvili, T., Law, P. P., *et al.* Epigenetic and neurological effects and safety of high-dose nicotinamide in patients with Friedreich's ataxia: an exploratory, open-label, dose-escalation study. *Lancet (London, England)* **384,** 504–513 (2014).

247. Lynch, D. R. & Fischbeck, K. H. Nicotinamide in Friedreich's ataxia: useful or not? *Lancet (London, England)* **384,** 474–475 (2014).

248. Burk, K., Schulz, S. R. & Schulz, J. B. Monitoring progression in Friedreich ataxia (FRDA): the use of clinical scales. *J. Neurochem.* **126 Suppl,** 118–124 (2013).

249. Ebert, A. D., Yu, J., Rose, F. F., Mattis, V. B., Lorson, C. L., Thomson, J. A., *et al.* Induced pluripotent stem cells from a spinal muscular atrophy patient. *Nature* **457,** 277–280 (2009).

250. Egawa, N., Kitaoka, S., Tsukita, K., Naitoh, M., Takahashi, K., Yamamoto, T., *et al.* Drug screening for ALS using patient-specific induced pluripotent stem cells. *Sci. Transl. Med.* **4,** (2012).

251. Cooper, O., Seo, H., Andrabi, S., Guardia-Laguarta, C., Graziotto, J., Sundberg, M., *et al.* Pharmacological rescue of mitochondrial deficits in iPSC-derived neural cells from patients with familial Parkinson's disease. *Sci. Transl. Med.* **4,** (2012).

252. Lee, G., Ramirez, C. N., Kim, H., Zeltner, N., Liu, B., Radu, C., *et al.* Large-scale screening using familial dysautonomia induced pluripotent stem cells identifies compounds that rescue IKBKAP expression. *Nat. Biotechnol.* **30,** 1244–1248 (2012).

253. Xu, X., Lei, Y., Luo, J., Wang, J., Zhang, S., Yang, X. J., *et al.* Prevention of β-amyloid induced toxicity in human iPS cell-derived neurons by inhibition of Cyclin-dependent kinases and associated cell cycle events. *Stem Cell Res.* **10,** 213–227 (2013).